Investigation of Mechanical Heat Pump Systems for Heat Upgrading Applications

By

VISHAVDEEP SINGH

A Thesis Submitted in Partial Fulfilment

of the Requirements for the degree of

Master of Applied Science

in

Mechanical Engineering

Faculty of Engineering and Applied Science

University of Ontario Institute of Technology

Oshawa, Ontario, Canada

Abstract

Three high temperature heat pump systems based on vapor compression cycles are introduced and examined. Four fluids (water, cyclohexane, biphenyl and mercury) are selected and analysed thermodynamically as prospective working fluids for the high temperature heat pumps. These working fluids are used in cascaded cycles to upgrade the heat to a temperature of 600 °C. The equations of state used in performance analysis are Peng–Robinson, NRTL and IAPWS-95. A parametric analysis is carried out to study the effects of isentropic efficiency, sink temperature, source temperature, and ambient temperature on the system performance. Energetic and exergetic COPs of the overall and individual cycles are determined. The COP values obtained are found to range from 2.08 to 4.86, depending upon the cycle and temperature levels. The System 2 (energetic and exergetic COPs are 3.8 and 1.9 respectively) outperforms System 1 (energetic and exergetic COPs are 2.2 and 1.0 respectively) both energetically and exergetically, while operating under same conditions of source temperature 81°C and sink temperature 600 °C. The System 3 achieves maximum cycle temperature of 792 °C while operating under moderate pressure ratios. The high COP values in some instances make these systems promising alternatives to fossil fuel and electrical heating. As a possible sustainable scenario, these pumps can utilise low grade heat from geothermal, nuclear or thermal power plants and derive work from clean energy sources (solar, wind, nuclear) to deliver high grade heat. The high delivery temperatures make these heat pumps suitable for processes with corresponding needs, like high temperature endothermic reactions, metallurgical processes, distillation, and thermochemical water splitting.

Acknowledgement

I would like to express my deepest gratitude to my supervisor Professor Dr. Ibrahim Dincer and my co-supervisor Professor Dr. Marc A Rosen for their exemplary guidance, care and patience and for providing me with a remarkable atmosphere for research.

I would like to thank my colleagues at UOIT for their assistance during the preparation of this thesis, especially Farrukh Khalid, Mohammad Al Mehndi, Janette Hogerwaard, Monu Malik, and Calin Zamfirescu.

Last but not the least; I would like to express my gratitude to my parents for their limitless support, fortitude, inspiration and reassurance throughout my life. This thesis is dedicated to my mother, father, brother, and sister.

Furthermore, the financial support from the Natural Sciences and Engineering Research Council of Canada (NSERC) is greatly acknowledged.

Table of Contents

List of Figures

List of Tables

Nomenclature

C	cost ($)
COP	Coefficient of performance
ex	specific exergy (kJ/kg)
$\dot{E}x$	exergy rate (kW)
g	acceleration due to gravity (m/s^2)
h	specific enthalpy (kJ/kg)
$\dot{m}$	mass flow rate (kg/s)
P	pressure (kPa)
$\dot{Q}$	heat transfer rate (kW)
R	gas constant (J/molK)
s	specific entropy (kJ/kg K)
t	time (s)
T	temperature (^{0}C or K)
v	specific volume (m^3/kg)
V	velocity (m/s)
$\dot{W}$	work rate or power (kW)
Z	elevation (m)

Greek Letters

η	efficiency
ω	acentric factor

Subscripts

c	critical
ch	chemical
comp	compressor
cv	control volume
d	destruction
e	exit
en	energy
ev	expansion valve

ex	exergy
hp	heat pump
ht	heater
hx	heat exchanger
i	inlet
int	intermediate
isen	isentropic
ph	physical
s	source
0	dead state
1, 2,...	state numbers

Acronyms

BZT	Bethe-Zel'dovich-Thomson
CANDU	Canada Deuterium Uranium
CEPCI	Chemical Engineering Plant Cost Index
EES	Engineering Equation Solver
ELECNRTL	Electrolyte Non-Random Two-Liquid Model
Hg	Mercury
HP	Heat pump
HT	Heater
HX	Heat exchanger
IAPWS	International Association for the Properties of Water and Steam
NRTL	Non-Random Two-Liquid Model

Chapter 1: Introduction

1.1 Global Energy Scenario

The global energy outlook is complex and multi-dimensional, with each dimension holding a key for a sustainable future. Energy security has been a historical challenge for humanity and recent developments in technology, increasing population, and rising standards of living have contributed to a climbing global energy demand. Figure 1.1 shows global primary energy demand and the global CO_2 emissions for 2004 to 2013. It can be observed that during this period primary energy demand grew by 21.3 % and global CO_2 emissions by 22.4 %.

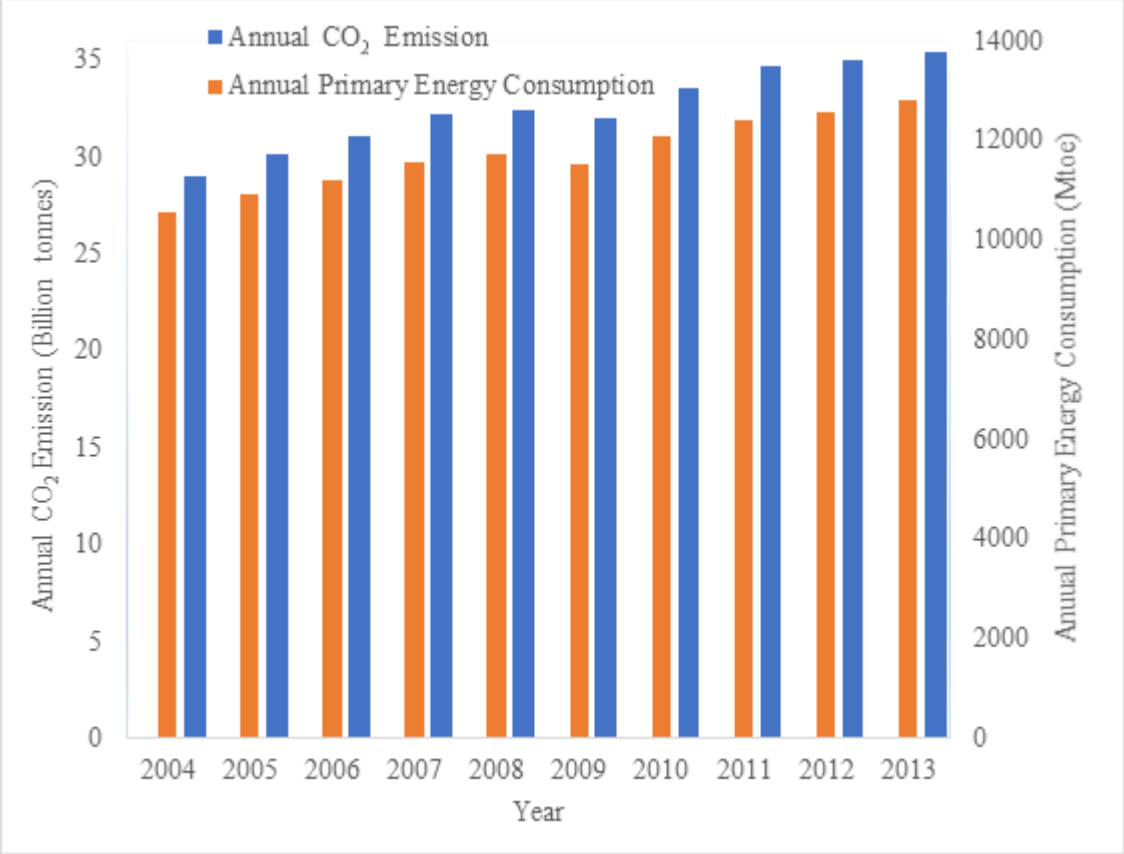

Figure 1.1 The trends in global primary energy demand and the global CO_2 emissions (data from BP SRWE 2015, Olivier et al. 2015).

The long-term growth in energy demand and emissions bring challenges relating to energy security, societal equity environmental stewardship and sustainability. Maintaining energy

security requires the effective policy formulation and execution to maintain, manage and explore new energy resources that can meet present and future demands (WEC, 2015). Energy equity speaks to having affordable and accessible energy supplies for all users. Environmental stewardship and sustainability involve of achievement of efficient resource utilisation and more environmentally benign energy systems. This triple energy challenge forms the "Energy Trilemma", as represented in Figure 1.2. This energy trilemma emphasize the balance required in these three dimensions to achieve wellbeing, abundance and competitiveness of individual countries and societies. The energy sector can deliver on development and climate goals and ensure sustainability provided it balance with other two dimensions.

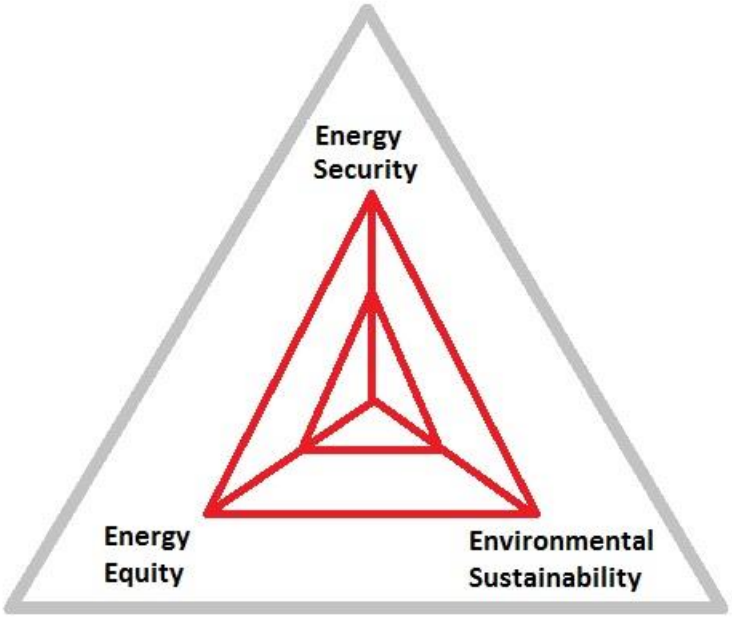

Figure 1.2 The energy trilemma (adapted from WEC, 2015).

One global energy scenarios report compares different policy strategies that lead to different energy scenarios in year 2050 (Biberacher and Gadocha, 2012). The report identifies the key technologies that can substantially reduce global emissions. The report points out the need for significant growth of renewable and nuclear energy systems. Other key technologies are carbon capture and storage, combined heat and power generation, and high efficiency end-use fuel and waste heat recovery. The future scenario involves significant growth of renewable energy supply as shown in Figure 3. Global renewable

energy supply has increased by 273.8 %, whereas global nuclear energy supply has declined by 9.7% over the same period. The growth of the nuclear energy sector in developing countries has offset the decline in nuclear energy supply in the developed world. The nuclear sector in China and India have grown by 121.9 % and 97.3% respectively, whereas in Japan it has declined by 94.8 %, over the same period of 10 years (BP SRWE 2015).

The reliability of renewable energy systems can be improved by integrating it with energy storage. Hydrogen provides an option of energy storage. Hydrogen can be used as an energy carrier that facilitates clean energy systems, and may prove particularly beneficial for the transportation sector. The integration of renewable energy with hydrogen production and utilization can help address the energy trilemma noted earlier. Grimes et al. (2007) describe hydrogen as an ideal solar energy carrier. Hydrogen production methods mainly linked to renewable energy are summarized by Dincer (2012). Hydrogen production from nuclear energy is expected by some to play significant role in future hydrogen economy (Marchetti, 2006). It is predicted that hydrogen production from thermochemical water decomposition can play an important role, and is likely to use nuclear and solar energy (Rosen, 2008).

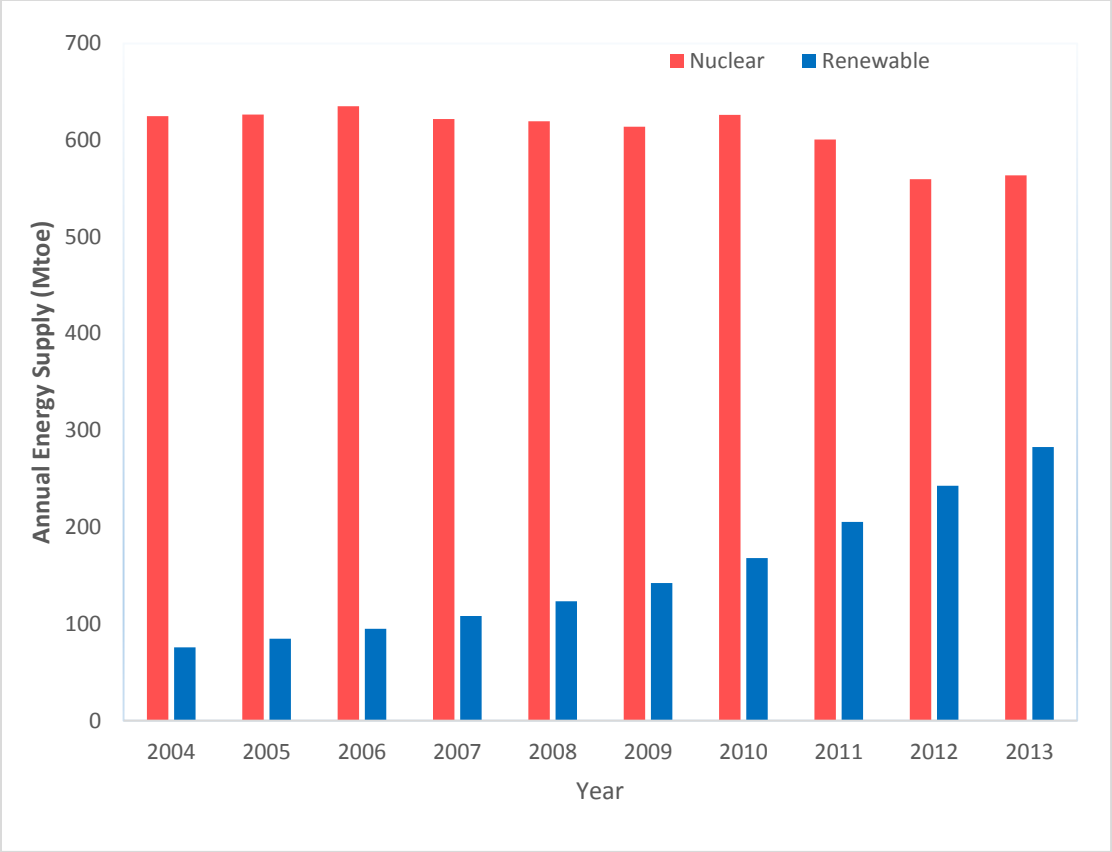

Figure 1.3 Trends in global energy supply from nuclear and renewable energy resources (data from BP SRWE 2015).

The study of Rosen (2008) also suggests that thermochemical hydrogen production can contribute to sustainability. Thermochemical decomposition of water has been extensively investigated by Abanades et al. (2006), who reviewed 280 thermochemical cycles and identified three that require lower temperatures. Of these three cycles the copper-chlorine cycle, which requires heat at a peak temperature of 550 °C, has been extensively investigated by Argonne National Laboratory and Atomic Energy of Canada Limited (Basco et al. 2003). The utilisation of waste heat from a CANDU nuclear reactor or any other high temperature industrial process for hydrogen production using the Cu-Cl cycle is possible, but the heat likely needs to be upgraded (i.e., have its temperature raised).

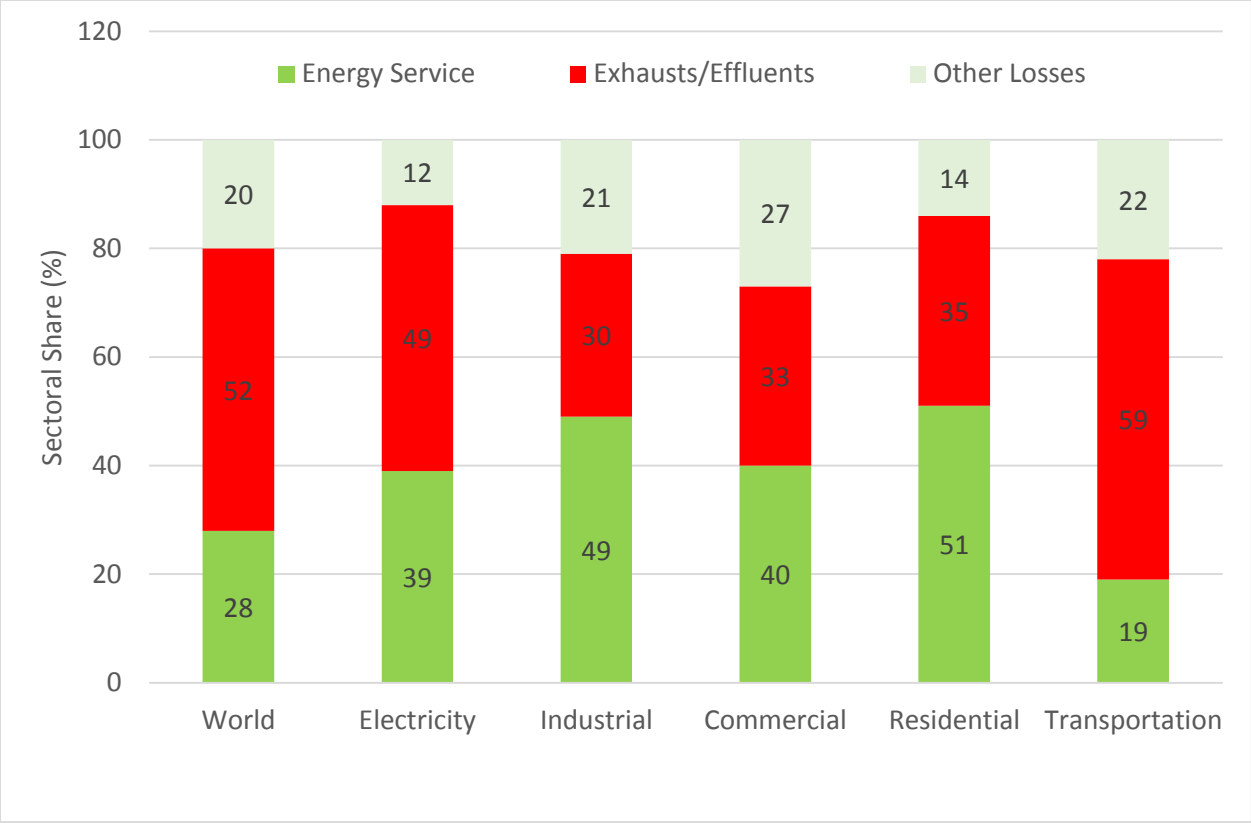

Figure 1.4 Sectoral shares of balance factors (Forman et al., 2016).

The heat upgradation makes a lot of sense when the energy conversion processes involve a large amount to affluent losses as shown in Figure 1.4. Globally more than 50 % of primary energy is lost as exhaust and effluents (Forman et al., 2016). The waste heat data analysis shows that 60 % of losses are in temperature range of below 100 °C as shown in Figure 1.5 (Forman et al., 2016).

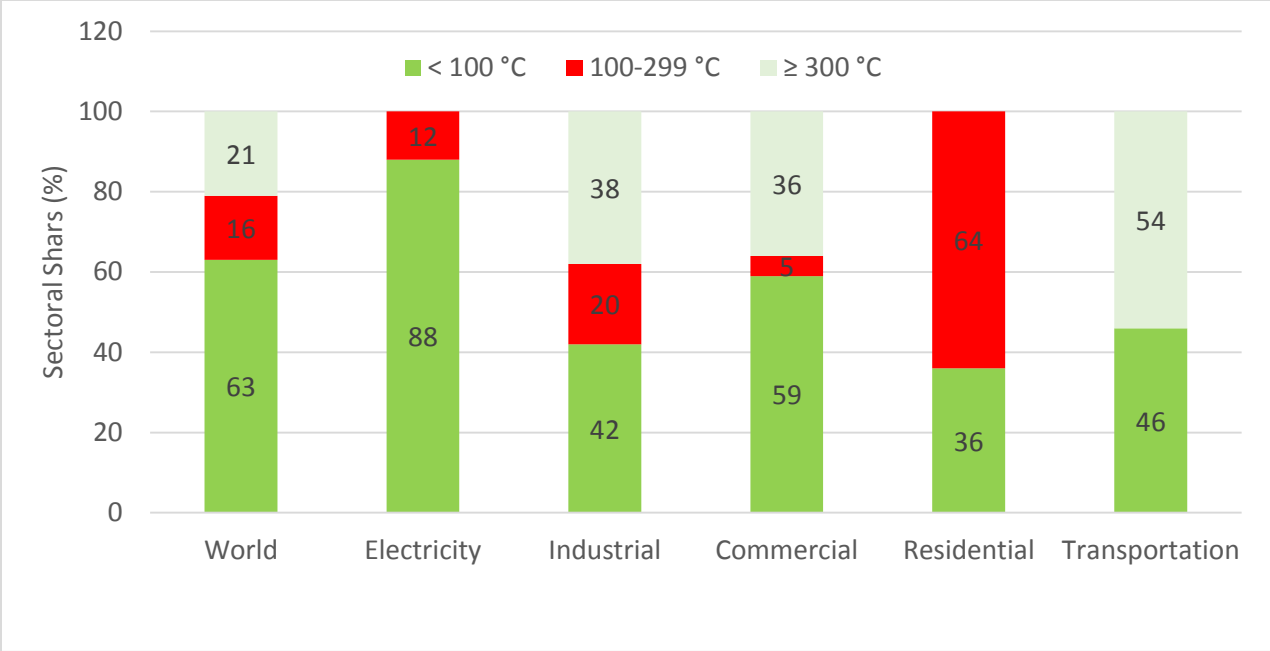

Figure 1.5 Sectoral shares of waste heat temperature distribution (Forman et al., 2016).

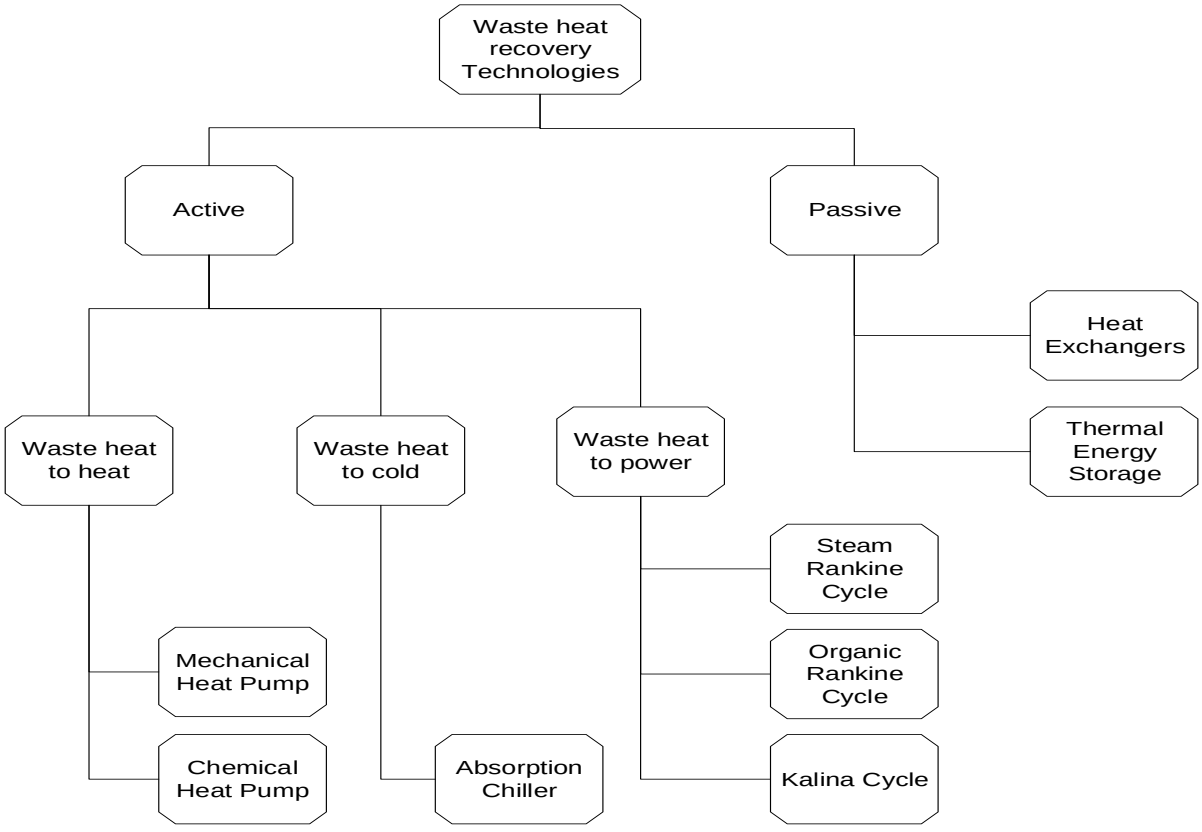

Figure 1.6 Low grade waste heat recovery technologies

This large amount of waste heat available needs to be recovered for sustainable utilisation of energy sources. The low grade waste heat recovery methods are shown in Figure 1.6. The active and passive methods integrated in the energy systems improves system performance, energy and exergy efficiencies. Actively waste heat recovered can be utilized in heating, cooling or power generation. The heat to heat recovery options upgrade the low temperature heat to high temperatures. The process heat temperature requirements of various sectors is shown in Figure 1.7.

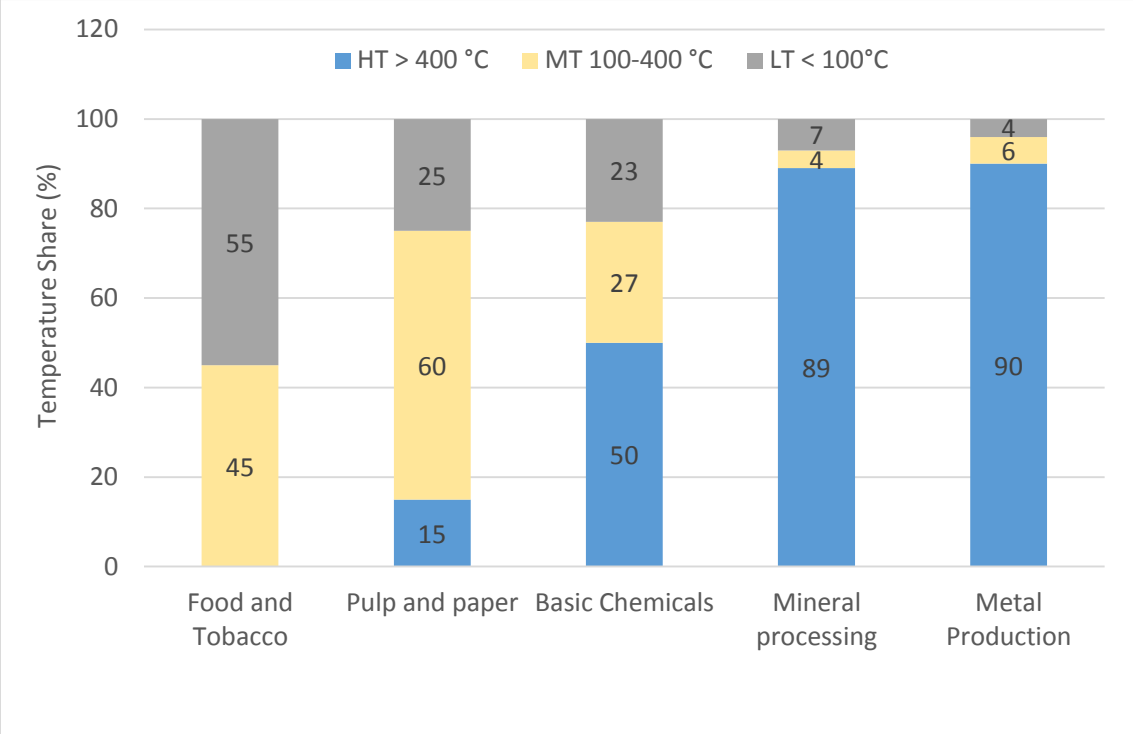

Figure 1.7 Process heat demand by temperature of different sectors (Bruckner et al.).

It is shown that majority of heavy industrial applications have requirement of high temperatures above 400 °C. The heat upgradation options available are heat pumps, fuel combustion or electrical heating. High temperature heat pumps provides an advantageous alternative to combustion for such a process. Luickx et al. (2008) report that heat pumps have better exergy efficiencies than combustion or electrical heating.

1.2 Motivation

The advantages of heat pumps over fossil fuel or electrical heating have been extensively reported for low temperature heat pumps. But reports of studies of the use of heat pumps

for high temperature applications have been limited. In particular, there appears to be clear lack of knowledge on high temperature heat pump systems, the working fluids used in such systems and their thermodynamic analyses. The utilisation of large amounts of industrial or utility waste heat, via upgraded for high temperature applications using mechanical heat pumps, can support energy sustainability. To help address these needs, the development of high temperature mechanical heat pump cycles and their thermodynamic analyses are the focus of this study.

1.3 Objectives

The objective of this study is to investigate heat upgrade options for high temperature applications using mechanical heat pumps. The heat pump systems are developed to upgrade CANDU reactor waste heat at ~80 °C for use by the Cu-Cl thermochemical cycle which requires heat at 550 °C. These heat pump systems also recover heat from Cu-Cl cycle to improve efficiency. The investigation begins with the identification of working fluids suitable for these operating conditions. Accurate equations of state are selected for modeling the systems. The modeling and simulation is performed using the ASPEN PLUS process simulation software. Balance equations are used for detailed analyses of each component of the system. The specific objectives and corresponding tasks required to achieve the objectives of the study are as follows:

1. To identify the working fluids that are suitable for the operating conditions, the identification is to be carried out based on their thermophysical properties and safety of use.
    - To search stable, economical and readily available working fluids that can operate under high temperature and pressures.
    - To identify the proper equations of state from literature that can determine the thermophysical properties of these fluids accurately.
2. To develop the heat pump systems using one or more working fluids that augment the available low grade heat to high temperatures (~ 600 °C).
    - To identify the suitable combination of working fluids that can be used in cascaded cycles to achieve high delivery temperatures.

- To develop different configuration of vapor compression cycles for the selected combination of fluids.

3. To develop the mathematical model of proposed systems.
    - To write the balance equations of each component used in the system.
    - To define energetic and exergetic performance of the individual cycle and overall system.
4. To perform the model validation of the developed systems in ASPEN PLUS.
    - To set up the model in ASPEN PLUS, building the process flowsheet, specifying properties.
    - To enter the components and feed specifications, run the simulation and examine simulation results.
5. To perform the energetic and exergetic performance analysis of the systems.
    - To evaluate the energetic and exergetic coefficients of performance.
    - To determine the exergy losses in each system and identify the components with maximum exergy destruction rate.
6. To carry out the parametric study of the proposed systems.
    - To perform a detailed parametric study and analyse the effect of operating parameters on the energetic and exergetic performance of system.
    - To analyse the effect of ambient conditions on the system performance.

Chapter 2: Literature Review

Mechanical heat pumps utilise the compression process to raise the temperature of a working fluid. Heat pumps based on numerous cycles have been studied in the past for various applications. This section covers studies performed on heat pump cycles, working fluids and their equations of state, thermodynamic analyses and the development of high temperature heat pumps.

2.1 Heat Pump Cycles

A few notable studies of heat pumps based on Stirling (Angelino and Invernizzi, 1996, Angelino and Invernizzi, 1993) and reversed Brayton cycles (Itard 1995, Ferreira, 2006).

Another type of heat pump used in high temperature applications is the chemical heat pump. Such a device adjusts operating pressures at which some exothermic or endothermic reactions take place to shift the reaction equilibrium in the desired direction. This process augments heat temperatures (Kato and Yoshizawa, 2001). Chan et al. (2013) reviewed low grade heat technologies and found chemical heat pumps with improved performance to be one of the key methods for heat upgrading. The authors summarize a number of techniques that improve heat transfer efficacy and reduce the intermittency of chemical heat pumps. Chua et al. (2010) review advances in heat pump technologies and conclude that the replacement of conventional boilers with heat pumps for residential heating can reduce the amount of CO_2 emissions by 50%. The authors highlight recent advances in heat pump technologies, which are focused on advanced cycle designs, improved cycle components and research on working fluids. De Boer et al. (2002) studied structural and thermodynamic properties of Na_2S-H_2O for application in chemical heat pumps. That study determined the vapor pressure-temperature equilibrium of sulphide hydrates and derived a set of thermodynamic functions associated with these compounds.

2.2 Working Fluids

The working fluids selected for heat pumps or power cycles need to be analyzed considering a number of parameters based on thermodynamic properties and safety of use. Göktun (1995) investigated the criteria for the selection of working fluids of high temperature heat pumps, comparing a number of selected fluids in terms of thermophysical and ecological properties. The maximum working temperature of these fluids is

approximately 150°C. Brown et al. (2015) investigated working fluids parametrically for five organic Rankine cycles, in order to find the ideal working fluid. The study concluded that the critical temperature and critical molar heat capacity of a working fluid has the largest influence on the efficiency and work output of the cycle. Shu et al. (2014) studied the suitability of alkanes for high temperature ORC cycles and demonstrated that the overall performance for cycles using cyclohexane and cyclopentane surpassed that for other linear alkanes and water.

Pan and Li (2006) investigated the difficulty of using non-azeotropic working fluids in high temperature heat pumps, the major issue being identified as incomplete condensation. Chen et al. (2010) and Quoilin and Lemort (2009) identified that three key properties of a working fluid affect the analysis, design and synthesis of a sub or supercritical Rankine cycle based system: (a) the density of liquid phase (b) the latent heat of vaporization and (c) the isobaric heat capacity of the vapor phase. Lai et al. (2011) investigated the suitability of alkanes, aromates and linear siloxanes as working fluids for high temperature organic Rankine cycles. The analysis considered two equations of state: BACK-ONE and PC-SAFT. The sub and supercritical ORC processes are modeled with maximum working temperature of 250 °C to 300 °C. Cyclopentane is found to be the most advantageous working fluid for all cases studied.

Fernandez et al. (2011) performed thermodynamic performance analyses of regenerative organic Rankine cycles utilizing linear and cyclic siloxanes. A novel adjustment of the Span-Wagnaer equation of state was used to determine the properties of the working fluids. The simple siloxanes hexamethyldisiloxane (MM) and octamethyltrisiloxane (MDM) were found to be the best performing among the examined working fluids.

2.3 High Temperature Mechanical Heat Pumps

Zamfirescu and Dincer (2009) reported the application of Bethe-Zel'dovich-Thomson (BZT) fluids for high temperature heat pumps. A total of 17 fluids from siloxanes and perfluorocarbons were studied as working fluids for very high temperature heat pumps. Energy and exergy analyses were carried out. The Martin-Hou, Span-Wagner and Peng-Robinson-Stryjek-Vera equations of state were used in the analyses.

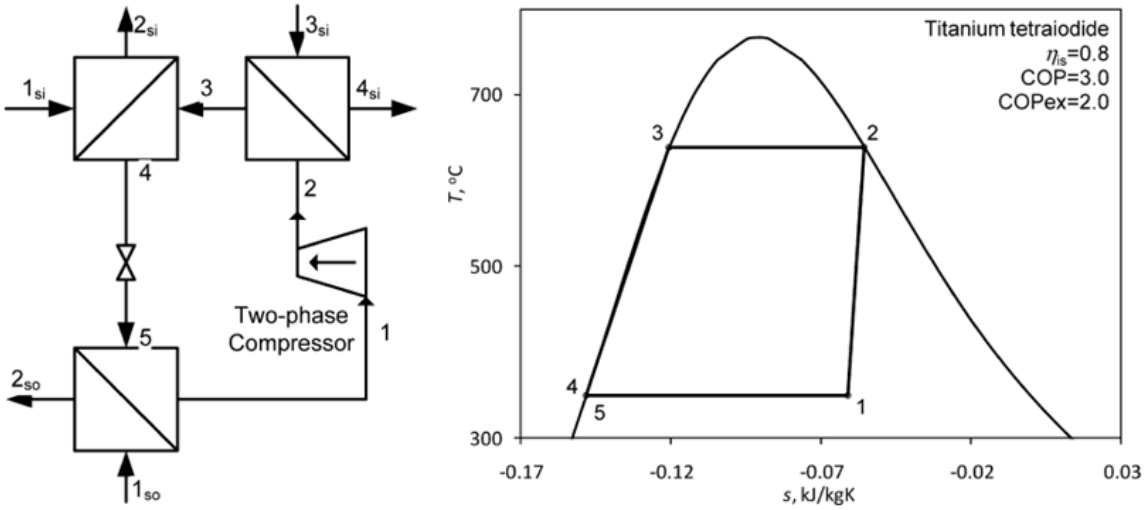

Figure 2.1 The schematic and T-s diagram of heat pump system that utilise the titanium based fluids (Zamfirescu et al. (2009))

Four types of heat pump configurations were studied with the 17 working fluids and siloxanes were found to exhibit the best performance. The maximum temperature reported in the study was in the range of 500 °C.

Zamfirescu et al. (2009) reported thermodynamic analyses of very high temperature heat pumps using organic and titanium based working fluids. Figure 4 shows the schematic and T-S diagram of the heat pump system that utilises titanium based fluids. From the T-S diagram it can be noted that these fluids undergo two phase compression. This study highlights the application of these heat pumps in hydrogen production or metallurgical processes. The organic fluids biphenyl methane and isoquinoline are found to be unsuitable for this application. The titanium-based fluids are reported to have COP values of 2.7 to 7.3. Titanium tetraiodide (TiI4) is reported to be a promising working fluid, achieving a maximum temperature of 650 °C and an energetic COP of 3.

Zamfirescu et al. (2010) studied a method to upgrade CANDU reactor waste heat and drive the Cu-Cl thermochemical cycle for hydrogen production. The study applied a mechanical heat pump with a cascaded cycle and used cyclohexane and biphenyl working fluids, with a maximum cycle temperature of 600 °C. The proposed heat pump utilised heat recovered from the Cu-Cl cycle. The integrated cycle reported to have 4% more efficient than the base system.

Chapter 3: Descriptions of Systems Developed

This study proposes three high temperature heat pump systems based on vapor compression cycles. Four fluids (water, cyclohexane, biphenyl and mercury) are selected and analysed thermodynamically as prospective working fluids for high temperature heat pumps. These working fluids are used in cascaded cycles to upgrade heat to 600 °C. Section 3.1 explains the properties relevant for the selection of working fluids, the thermophysical properties of selected fluids and their equations of state used in the thermodynamic analysis of system. Section 3.2 describes the detailed description of all three systems proposed in this study.

3.1 Selection of potential working fluids

The working fluids for high temperature heat pumps are selected on the basis of their thermodynamic behaviour and safety of use. The thermophysical properties relevant for these fluids are explained as follows:

3.1.1 Thermophysical Physical Properties

Now a days consistent efforts are made to develop environmentally benign working fluids used in energy conversion processes. These fluids are operated on Rankine cycles for heat-pump and heat to work cycles. The challenge in utilising these fluids is inadequate knowledge of thermodynamic properties. The thermodynamic data especially for fluids that can be potentially used in medium to high temperature applications is not sufficient or inaccurate. For example siloxanes or aromates are found to be suitable working fluids for high temperature applications, but experimental data is insufficient for applying multi-parameter equations of state. The critical properties of working fluids used in energy conversion processes are molecular mass, melting point, normal boiling point, critical temperature and critical pressure. This section explains the importance of each property on performance of fluid used in cycle.

- Molecular Mass: The complexity of a molecule can be related to their molecular mass. A heavy molecule is complex as it consists of a large number of atoms and can lead to chemical instability at higher temperatures (Zamfirescu et al. 2009). The past investigations observed that molecularly complex fluids are safe to use up to 100 °C higher than their critical temperature (Angelino and Invernizzi 1993).

- Melting Point: The melting point is another very important parameter related to fluids used in high temperature heat pump cycles. The majority of fluids exist in solid or highly viscous state at normal conditions, therefore these fluids needs special design considerations such as preheating.
- Normal Boiling Point: It is defined as the boiling point of fluid at atmospheric pressure. This parameter affects source temperature suitability. If normal boiling point is very high and source temperature is relatively low, the evaporator operates at vacuum conditions and there is possibility of contamination.
- Critical Temperature: The critical temperature is important parameters for vapor compression cycles, in case of high temperature heat pumps the working fluid critical temperature must be sufficiently high.
- Critical Pressure: It is one of the important parameter for heat pump design point of view, molecules with lower critical pressures can achieve large temperature elevation with relatively lower compression ratios, and it allows cheaper construction and safer working environment.

For the safe use of working fluid following properties need to be assessed:

- Flash point: It is defined as the lowest temperature a liquid forms sufficient vapors that can ignite in atmosphere in presence of a spark.
- Autoignition Temperature: It is the lowest temperature at which a substance self-ignites in atmosphere in absence of any spark.

The critical temperature can be used primarily to select the working fluid for a vapor compression cycle (Zamfirescu et al. 2009). Table 3.1 summarizes the properties of working fluids selected for the study. The critical temperature of cyclohexane and water are 280.65 °C and 373.94 °C respectively. Therefore these two fluids can be used in the bottoming cycles. The high critical temperatures of biphenyl (499.85 °C) and mercury (1461.85°C) are sufficiently high and these fluids can be used in the topping cycle.

Table 3.1 Thermophysical properties of selected working fluids (Rowley et al. 2004, Wagner and Prub 2002)

Thermophysical Properties	**Working Fluid**			
	Cyclohexane	**Biphenyl**	**Water**	**Mercury**
Chemical Formula	C_6H_{12}	$C_{12}H_{10}$	H_2O	Hg
Critical Temperature (°C)	280.65	499.85	373.946	1461.85
Critical Pressure (bar)	40.8	33.8	220.64	1608.03
Normal Boiling Point (°C)	80.72	255	100	356.69
Molecular Weight (kg/kmol)	84.16128	154.211	18.01528	200.59
Melting Point (°C)	0	69.05	6.54	-38.86
Flash Point (°C)	-20	113	Non flammable	Non flammable
Autoignition Temperature (°C)	245	540	Non flammable	Non flammable

3.1.2 Equations of State

In thermodynamic analysis the selection of the appropriate equations of state is very critical. Past studies (Zamfirescu et al. 2009, Zamfirescu et al, 2010) reported that Peng-Robinson equation of state is accurate for cyclohexane and biphenyl. The general form of Peng-Robinson equation is as follows (Peng and Robinson 1976):

$$P = \frac{RT}{v-b} - \frac{a\alpha(T)}{v(v+b)+b(v-b)} \tag{3.1}$$

$$a = 0.45724\frac{R^2T_c^2}{P_c} \tag{3.2}$$

$$b = 0.07780\frac{RT_c}{P_c} \tag{3.3}$$

$$\alpha(T) = [1 + k\left(1 - \sqrt{\frac{T}{T_c}}\right)]^2 \quad (3.4)$$

$$k = 0.37464 + 1.54226\ \omega - 0.26992\ \omega^2 \quad (3.5)$$

where R = 8.314 J/molK.

For thermodynamic analysis of water, IAPWS-95 formulation is used. It covers a wide range of temperatures and pressure (-21.8 °C at 2099 bar to 1000 °C at 10000 bar) quite accurately (Wagner and Prub 2002).

The NRTL equation of state is used for mercury. Thermophysical properties of mercury reported in literature (Sugawara et al. 1962) were compared with properties obtained by ASPEN software by applying the NRTL equation of state. For the operating range of temperatures (350 °C to 1100 °C) and pressures (1 bar to 15 bar), the data is in close match with maximum uncertainty of 5%.

3.2 Descriptions of the Present Systems

As pointed out earlier, there is a need for heat pump systems to upgrade heat at source temperatures of about 80 °C to 600 °C. The selected working fluids are used to develop three systems consisting of cascaded heat pump cycles. Systems 1 and 2 have two cascaded cycles and System 3 has three. System 1 uses water as the working fluid in a bottoming cycle and biphenyl in a topping cycle. For System 2, cyclohexane is used as the working fluid in a bottoming cycle and biphenyl in a topping cycle. System 3 uses cyclohexane and biphenyl working fluids in bottoming and intermediate cycles, respectively, and mercury in a topping cycle. The bottoming and intermediate cycles work under subcritical conditions, so the heat transfer between cycles is essentially through the condenser and the evaporator of the bottoming and topping cycles. The topping cycles of Systems 1 and 2 operate at supercritical conditions, so the sink of Systems 1 and 2 deliver sensible heat. The topping cycle of System 3 operates under subcritical conditions, so its sink delivers heat isothermally.

The conceptual development of the three heat pump systems, described below for each system separately, envision their integration with a waste heat source, namely condenser heat from a CANDU reactor at ~80 °C, and the Cu-Cl cycle for thermochemical water

splitting to produce hydrogen, which requires heat at a peak temperature of 550 °C. The heat pump cycles developed in the study also recover heat (available at temperatures between ~80 °C to ~485 °C) from the Cu-Cl cycle at various points.

3.2.1 System 1

The schematic of System 1 is shown in Figure 3.1. The water is in saturation condition with a temperature of ~81 °C at state point 1. It is evaporated with heat from the source and become saturated vapor at state point 2. This stream exchange heat with a hotter stream in an internal heat exchanger HX1 (HX1 is essentially an intercooler that reduce the temperature of same stream after being compressed down the line), and get superheated to reach a temperature of 101 °C at state point 3. This superheated vapor is compressed by a pressure ratio of 9.7 resulting a superheated state at discharge pressure 4.5 bar and temperature 448 °C. This hot stream exchange heat with the working fluid (biphenyl) of topping cycle in heat exchanger HX2 and exits at 281 °C at state point 5. The cold stream of heat exchanger HX2 enters at state point 11 with saturated condition at 256 °C and 1.04 bar pressure. It leaves the heat exchanger at 12 in superheated condition at 275.5 °C. The stream 5 enters heat exchanger HX1 and further cools down to 261 °C at state point 6, and again cooled down to state 7 with temperature 151 °C. This cooled stream is compressed again by same pressure ratio of 9.7 and reaches to 47 bar and 523 °C. This superheated water exchange heat with stream 12 in heat exchanger HX3 and cools down to 409 °C at state point 9. This stream supplies heat in HT2 and cooled down to a subcooled liquid at 102 °C and 47 bar at state point 10, the heat is delivered to Cu-Cl cycle for preheated the reactants.

This pressurized liquid is expanded in expansion valve to reach a saturated liquid at state point 1 and start the cycle again. The cold stream (biphenyl) entering HX3 is superheated to 404 °C at state point 13. This is further superheated to 470 °C at state 14 by heat recovered from Cu-Cl cycle. The superheated biphenyl is compressed to a supercritical state at point 15 with pressure of 67 bar and temperature 600 °C. This supercritical fluid deliver the high temperature heat through HT5 and cools down to 256 °C at state point 16. The high-pressure liquid is expanded in expansion valve EXP2 and reach saturation state at point 11. These two cascaded cycles working in tandem upgrade the heat by consuming compressor work.

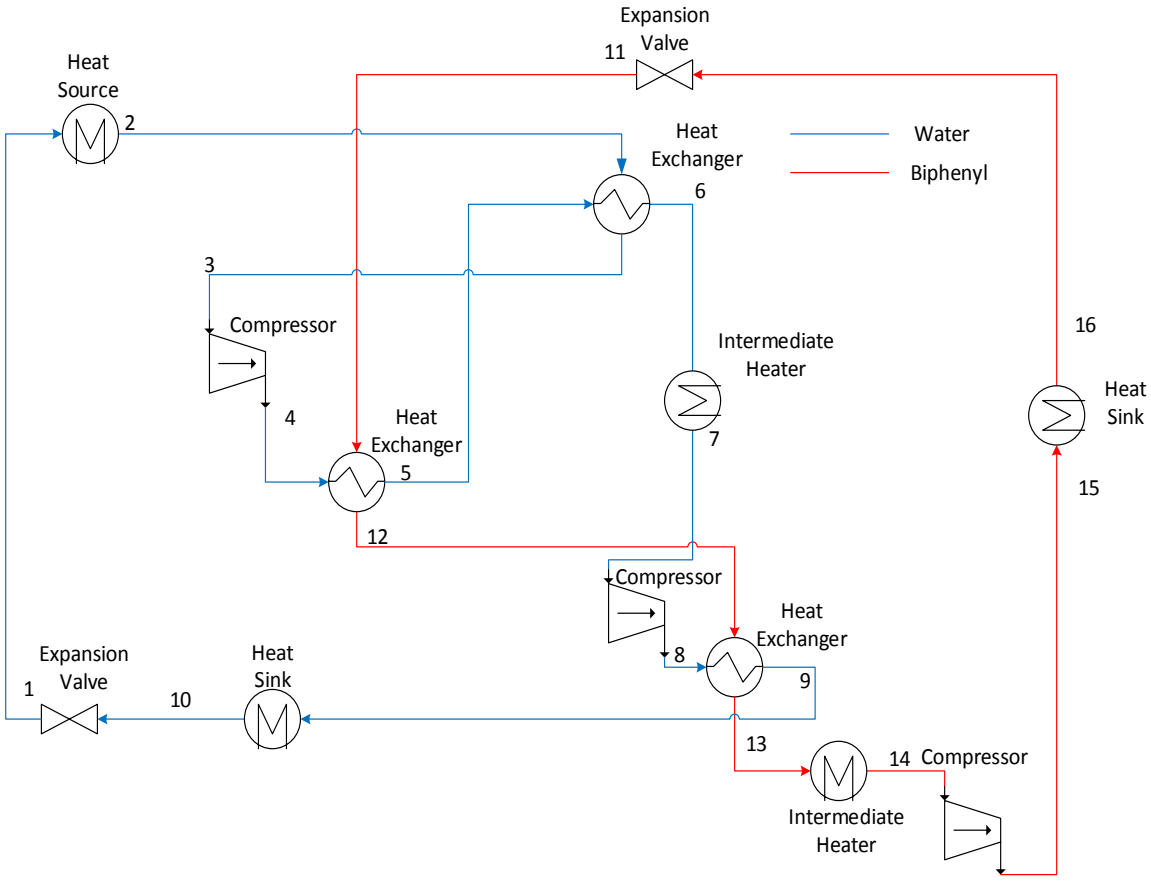

Figure 3.1 The schematic diagram of System 1 (operates on water and biphenyl as working fluids)3.2.2 System 2

The schematic of System 2 is shown in Figure 3.2. The saturated vapor of cyclohexane with a temperature of ~81 °C at state point 1 enters HT1. It is superheated with heat recovered from Cu-Cl cycle to reach a temperature of 160 °C at state point 2. This superheated vapor is compressed by a compressor COMP1 with a discharge pressure of 30 bar and temperature 275 °C at state point 3. This hot stream exchange heat with the working fluid (biphenyl) of topping cycle in heat exchanger HX1 and exits at 257 °C at state point 4. This stream cools down in HT2 to a subcooled liquid at 80 °C and 30 bar at state point 5, the heat is delivered to Cu-Cl cycle for preheating the reactants. This pressurized liquid is expanded in expansion valve EXP1 to reach a saturated liquid at state point 6. It is evaporated with heat from the source HT2 and become saturated vapor at state point 2 and starts the cycle again.

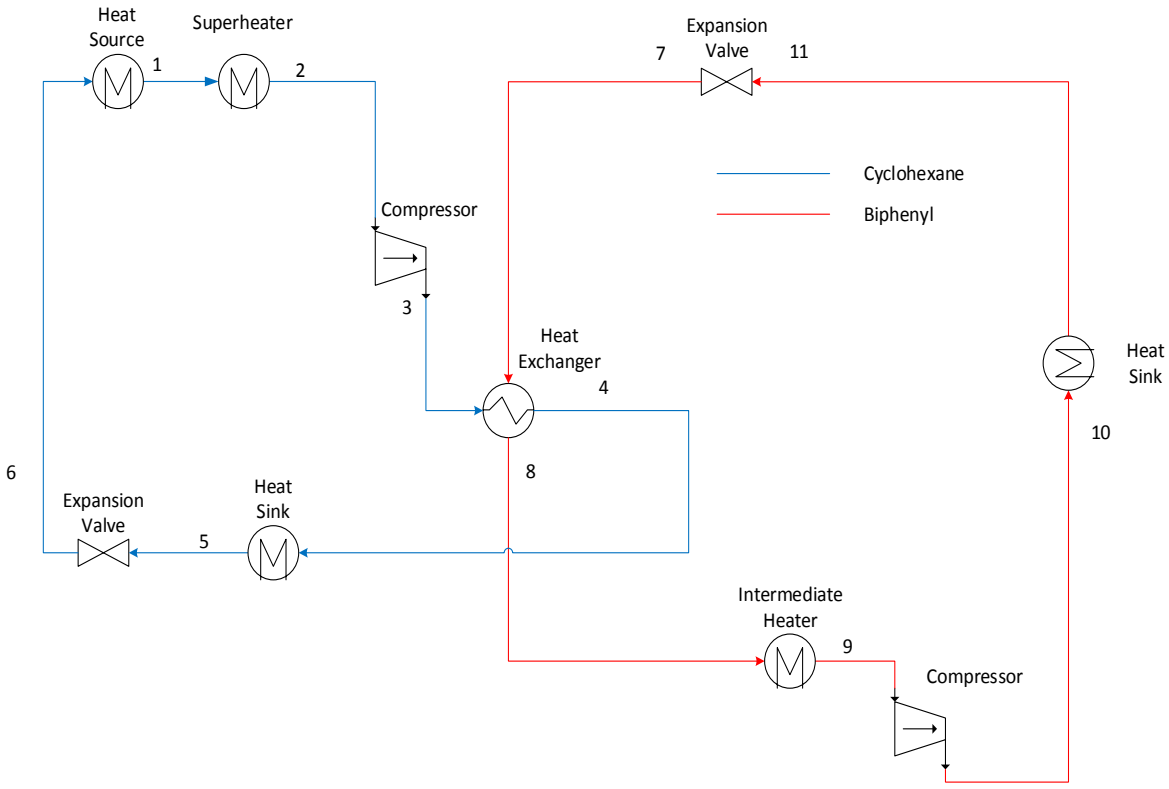

Figure 3.2 The schematic diagram of System 2 (operates on cyclohexane and biphenyl as working fluids)

The cold stream (biphenyl) of heat exchanger HX1 enters at state point 7 with saturated liquid condition at 256 °C and 1.00 bar pressure. It is evaporated and leaves the heat exchanger at 8 with vapor fraction of 0.64. This is further superheated to 470 °C at state 9 by heat recovered from Cu-Cl cycle.

The superheated biphenyl is compressed to a supercritical state at point 10 with pressure of 67 bar and temperature 600 °C. This supercritical fluid deliver the high temperature heat through HT5 and cools down to 256 °C at state point 11. The high-pressure liquid is expanded in expansion valve EXP2 and reach saturation state at point 7. These two cascaded cycles working in tandem to upgrade the heat by consuming compressor work.

3.2.3 System 3

The schematic of System 3 is shown in Figure 3.3.The saturated vapor of cyclohexane with a temperature of ~81 °C at state point 1 enters HT1. It is superheated with heat recovered from Cu-Cl cycle to reach a temperature of 160 °C at state point 2. This superheated vapor is compressed by a compressor comp1 with a discharge pressure of 30 bar and 275 °C at state point 3. This hot stream exchange heat with the working fluid (biphenyl) of topping

cycle in heat exchanger HX1 and exits at 257 °C at state point 4. This stream cools down in HT2 to a subcooled liquid at 80 °C and 30 bar at state point 5, the heat is delivered to Cu-Cl cycle for preheating the reactants. This pressurized liquid is expanded in expansion valve EXP1 to reach a saturated liquid at state point 6. It is evaporated with heat from the source HT2 and become saturated vapor at state point 2 and start the cycle again. The cold stream (biphenyl) of heat exchanger HX1 enters at state point 7 with saturated liquid condition at 256 °C and 1.04 bar pressure. It is evaporated and leaves the heat exchanger at 8 with vapor fraction of 0.64.

This stream enters heat exchanger HX2 and exchange heat internally with hot stream at 11 (biphenyl) and leaves at state point 9 with temperature 376 °C. The superheated stream is compressed in compressor COMP2 to a pressure of 10.07 bar and reaches a temperature of 430.75 °C at state point 10. This high temperature and pressure stream enters heat exchanger HX3 and exchange heat with topping cycle fluid (mercury) that enters HX3 as saturated liquid at state point 14 with temperature of 387 °C and pressure 1.7 bar. The biphenyl stream leaves the heat exchanger at 392 °C and vapor fraction of 0.12. The stream enters HX2 and leaves at state point 12 with temperature 260 °C and pressure 10.07 bar. The stream loose heat in HT4 to reach a temperature of 256 °C at state point 13, this high-pressure liquid is expanded in expansion valve EXP2 and reach saturation state at point 7 starting point of this intermediate cycle.

The mercury stream leaves the HX3 at state point 15 as saturated vapor, the stream is slightly superheated HT5 by heat recovered from Cu-Cl cycle to avoid liquid phase during compression, it enters the compressor at state point 16 and leaves at 17 with pressure 4 bar and temperature 746 °C. This extremely hot stream is cooled down before further compression in HT6 (an intercooler) and leaves at state point 17 at 443.84 °C. The compressor COMP4 compresses the stream further and at state point 19 it has temperature of 749.28 and pressure 8 bar.

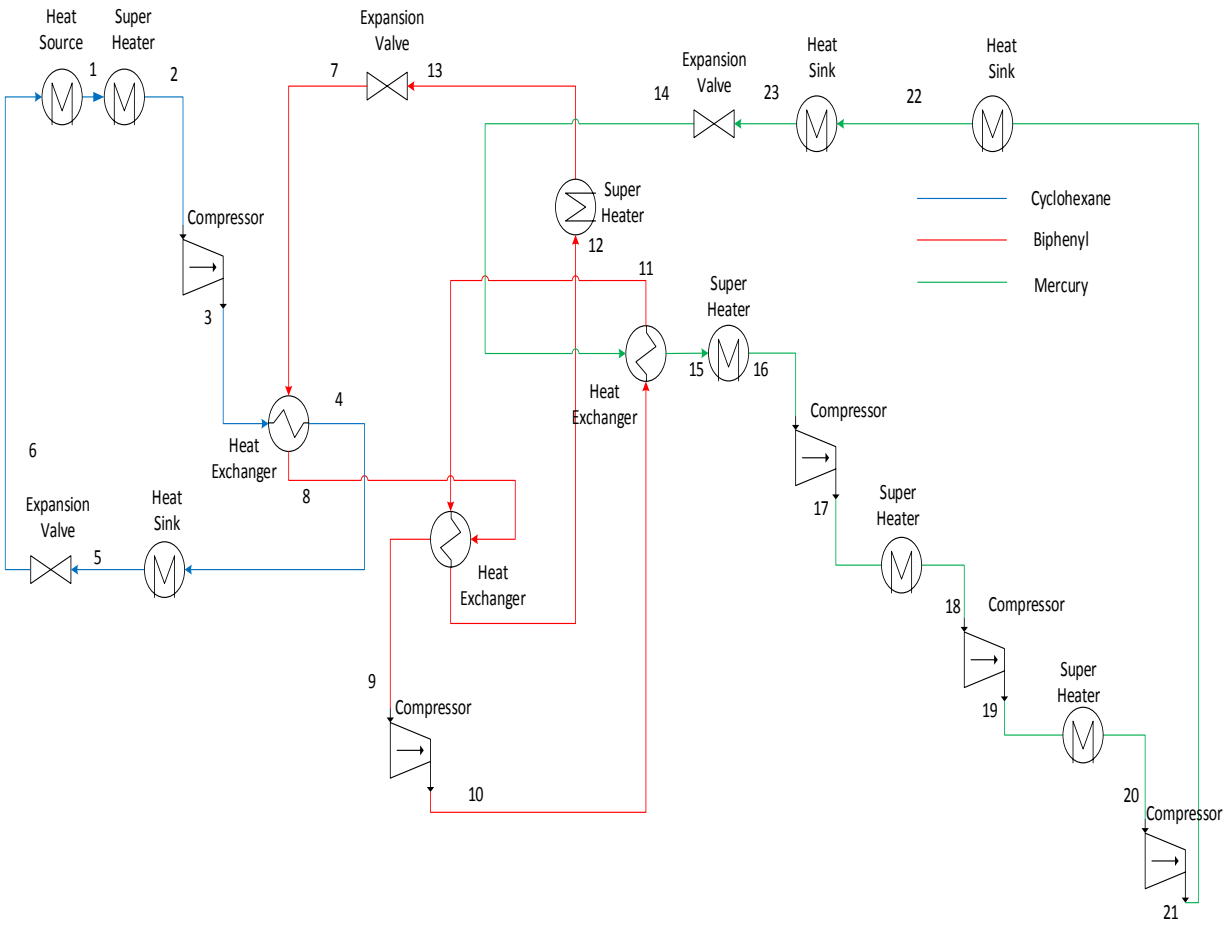

Figure 3.3 The schematic diagram of System 3 (operates on cyclohexane, biphenyl and mercury as working fluids)

Stream is cooled again in HT7 (intercooler) at state point 20 with temperature of 497.8 °C. The stream is further compressed in COMP5 and leaves at state point at 21 with pressure 15 bar and temperature 791.68 °C. The superheated mercury is condensed in HT8 and leaves as saturated liquid at state point 22 with temperature 554.38 °C. The saturated liquid is cooled sensibly in HT9 to reach state point 23 with temperature 387 °C. The high-pressure liquid is expanded in expansion valve EXP3 and reach saturation state at point 14. These three cascaded cycles working in tandem upgrade the heat by consuming compressor work. The section 5.3 elaborates the thermodynamic results of this System and Table 5.3 summarizes the base case state points.

Chapter 4: Model Development and Analyses

This chapter presents the thermodynamic analyses of systems developed in the present study. The subsections explain the energetic and exergetic principles used to analyse the performance of. The general mass, energy, entropy, and exergy balance equations are presented in section 4.1. In following sections the balance equations for all major components of the systems are provided. The energetic and exergetic COPs of system are defined at the end of each section.

4.1 Thermodynamic Analysis

The heat upgrade systems developed in this study are essentially the vapor compression cycle that utilise the mechanical power to upgrade the heat quality. Every system utilise the combination of components like heat exchangers, expansion valves, and compressors to achieve the desired state of working fluids. The thermodynamic performance of every component is aggregated to assess the overall performance of the system. The following sub sections presents a general form of balance equations.

4.1.1 Mass Balance Equation

The mass balance equation applies the conservation of mass for a control volume and can be written as:

$$\sum_i \dot{m}_i - \sum_e \dot{m}_e = \frac{dm_{cv}}{dt} \tag{4.1}$$

where m and ṁ are the mass and mass flow rate, the subscripts i and e represents the inlet and exit, cv refers to control volume.

4.1.2 Energy Balance Equation

The energy balance equation is written according to first law of thermodynamics applied to a control volume, which is written as:

$$\dot{Q} - \dot{W} + \sum_i \dot{m}_i\left(h_i + \frac{V_i^2}{2} + gZ_i\right) - \sum_e \dot{m}_e\left(h_e + \frac{V_e^2}{2} + gZ_e\right) = \frac{dE_{cv}}{dt} \tag{4.2}$$

where $\dot{Q}$ and $\dot{W}$ are heat transfer rate and work rate, E is the energy, t stands for time. The symbols h, V, g and Z represents the specific enthalpy, velocity, acceleration of gravity and elevation, respectively.

4.1.3 Entropy Balance Equation

The entropy balance equation accounts for the entropy enters, exits and generated in the control volume. The entropy balance equations can be written as follows (Bejan 2002):

$$\sum_i \dot{m}_i s_i - \sum_i \dot{m}_e s_e + \sum_k \frac{\dot{Q}_k}{T_k} + \dot{S}_{gen} = \frac{dS_{cv}}{dt} \tag{4.3}$$

4.1.4 Exergy Balance Equation

The exergy analysis is powerful tool to assess the thermodynamic performance of system. It accounts both first and second law, and gives the detailed insights of system performance. It identifies the key or potential areas of improvement. The exergy destruction assessment is useful to form the strategies for efficient and effective utilisation of energy. The major improvements in the thermodynamic performance of power generation or refrigeration units can be attributed to the guidelines provided by exergy analysis.

From thermodynamic analysis point of view, a component's performance can be assessed by physical and chemical exergy of the entering and exiting the control volume. The kinetic and elevation terms are assumed to remains constant, due to negligible change in velocity and elevation (Dincer and Rosen, 2012). The physical exergy is the maximum work that can be done when system interacts with surroundings before achieving thermal and mechanical equilibrium. The chemical exergy comes into play when chemical change takes place before system achieves chemical equilibrium with environment, e.g. combustion chamber (Bejan et al., 1995). The exergy balance of a control volume is written as follows:

$$\dot{E}x^Q + \sum_i \dot{m}_i ex_i = \sum_e \dot{m}_e ex_e + \dot{E}x_W + \dot{E}x_d \tag{4.4}$$

$$\dot{E}x^Q = \dot{Q}\left(1 - \frac{T_0}{T}\right) \tag{4.5}$$

$$\dot{E}x_W = \dot{W} \tag{4.6}$$

$$ex = ex_{ph} + ex_{ch} \tag{4.7}$$

The physical exergy, ex_{ph} can be calculated as follows:

$$ex_{ph} = h - h_0 - T_0(s - s_0) \quad (4.8)$$

Here, $\dot{E}x^{Q}$ and $\dot{E}x_{W}$ denote the rate of exergy associated with work and heat transfer respectively, $\dot{E}x_{d}$ denotes the rate of exergy destruction in control volume, and ex denotes the specific exergy of the stream.

4.2 Thermodynamic analyses of System 1

The energy and exergy analysis of System 1 is presented in this section. The energetic and exergetic COPs of individual cycles and overall COPs of the system are defined. These models are used to produce the results and perform parametric studies to assess the effect of operating parameters on system performance. The reference state of surrounding is defined as at temperature $T_0 = 25$ ℃ and a pressure $P_0 = 1$ bar.

Following assumptions are used in the analyses of the system:

- There is negligible change in the kinetic and potential energy.
- There is no heat loss in the compressor and expansion valves.
- The heat exchangers incur no heat loss to environment.
- The isentropic efficiency value of the compressor is 0.75 (Zamfirescu et al. 2010)
- The pressure drop in pipelines and heat exchangers is negligible.

4.2.1 Balance Equations

The mass, energy, entropy and exergy balance equations are written for System 1 as shown in Fig. 3.1.

- Heater 1(Heat Source of Bottoming Cycle)

The mass balance for Heater 1 can be written as follows:

$$\dot{m}_1 = \dot{m}_2 \quad (4.9)$$

The energy balance for Heater 1 can be written as follows:

$$\dot{m}_1 h_1 + \dot{Q}_{ht1} = \dot{m}_2 h_2 \quad (4.10)$$

The entropy balance for Heater 1 can be written as follows:

$$\dot{m}_1 s_1 + \frac{\dot{Q}_{ht1}}{T_0} + \dot{S}_{gen,ht1} = \dot{m}_2 s_2 \quad (4.11)$$

The exergy balance for Heater 1 can be written as follows:

$$\dot{m}_1 ex_1 + \dot{Q}_{ht1}\left(1 - \frac{T_0}{T_s}\right) = \dot{m}_2 ex_2 + \dot{E}x_{d,ht1} \quad (4.12)$$

- Heater 2 (Heat Sink of Bottoming Cycle)

The mass balance equation for Heater 2 can be written as follows:

$$\dot{m}_9 = \dot{m}_{10} \quad (4.13)$$

The energy balance for Heater 2 can be written as follows:

$$\dot{m}_9 h_9 + \dot{Q}_{ht2} = \dot{m}_{10} h_{10} \quad (4.14)$$

The entropy balance for Heater 2 can be written as follows:

$$\dot{m}_9 s_9 + \frac{\dot{Q}_{ht2}}{T_0} + \dot{S}_{gen,ht2} = \dot{m}_{10} s_{10} \quad (4.15)$$

The exergy balance for Heater 2 can be written as follows:

$$\dot{m}_9 ex_9 + \dot{Q}_{ht2}\left(1 - \frac{T_0}{T_s}\right) = \dot{m}_{10} ex_{10} + \dot{E}x_{d,ht2} \quad (4.16)$$

Here, $\dot{Q}_{ht2}$ represents the heat rejected by sink.

- Compressor 1

The mass balance equation for Compressor 1 can be written as follows:

$$\dot{m}_3 = \dot{m}_4 \quad (4.17)$$

The energy balance equation for Compressor 1 can be written as follows:

$$\dot{m}_3 h_3 + \dot{W}_{comp1} = \dot{m}_4 h_4 \quad (4.18)$$

The entropy balance equation for Compressor 1 can be written as follows:

$$\dot{m}_3 s_3 + \dot{W}_{comp1} + \dot{S}_{gen,comp1} = \dot{m}_4 s_4 \quad (4.19)$$

The exergy balance equation for Compressor 1 can be written as follows:

$$\dot{m}_3 ex_3 + \dot{W}_{comp1} = \dot{m}_4 ex_4 + \dot{E}x_{d,comp1} \quad (4.20)$$

- Heat Exchanger 1

The Heat Exchanger 1 is used for internally transfer heat from hot stream of water to cold stream, the mass balance can be written as:

For cold stream (water): $\dot{m}_2 = \dot{m}_3$ (4.21)

For hot stream (water): $\dot{m}_5 = \dot{m}_6$ (4.22)

The energy balance equation for Heat Exchanger 1 can be written as:

$$\dot{m}_2 h_2 + \dot{m}_5 h_5 = \dot{m}_4 h_4 + \dot{m}_6 h_6 \quad (4.23)$$

The entropy balance equation for Heat Exchanger 1 can be written as:

$$\dot{m}_2 s_2 + \dot{m}_5 s_5 + \dot{S}_{gen,hx1} = \dot{m}_4 s_4 + \dot{m}_6 s_6 \quad (4.24)$$

The exergy balance equation for Heat Exchanger 1 can be written as

$$\dot{m}_2 ex_2 + \dot{m}_5 ex_5 = \dot{m}_4 ex_4 + \dot{m}_6 ex_6 + \dot{E}x_{d,hx1} \quad (4.25)$$

- Heater 3

The mass balance equation for Heater 3 can be written as follows:

$$\dot{m}_6 = \dot{m}_7 \quad (4.26)$$

The energy balance for Heater 3 can be written as follows:

$$\dot{m}_6 h_6 + \dot{Q}_{ht3} = \dot{m}_7 h_7 \quad (4.27)$$

The entropy balance for Heater 3 can be written as follows:

$$\dot{m}_6 s_6 + \frac{\dot{Q}_{ht3}}{T_0} + \dot{S}_{gen,ht3} = \dot{m}_7 s_7 \quad (4.28)$$

The exergy balance for Heater 3 can be written as follows:

$$\dot{m}_6 ex_6 + \dot{Q}_{ht3}\left(1 - \frac{T_0}{T_s}\right) = \dot{m}_7 ex_7 + \dot{E}x_{d,ht3} \quad (4.29)$$

- Compressor 2

The mass balance equation for Compressor 2 can be written as follows:

$$\dot{m}_7 = \dot{m}_8 \quad (4.30)$$

The energy balance equation for Compressor 2 can be written as follows:

$$\dot{m}_7 h_7 + \dot{W}_{comp2} = \dot{m}_8 h_8 \quad (4.31)$$

The entropy balance equation for Compressor 2 can be written as follows:

$$\dot{m}_7 s_7 + \dot{W}_{comp2} + \dot{S}_{gen,comp2} = \dot{m}_8 s_8 \quad (4.32)$$

The exergy balance equation for Compressor 2 can be written as follows:

$$\dot{m}_7 ex_7 + \dot{W}_{comp2} = \dot{m}_8 ex_8 + \dot{E}x_{d,comp2} \quad (4.33)$$

- Heat Exchanger 2

The mass balance for Heat Exchanger 2 can be written as:

For water: $\dot{m}_4 = \dot{m}_5$ (4.34)

For biphenyl: $\dot{m}_{11} = \dot{m}_{12}$ (4.35)

The energy balance equation for Heat Exchanger 2 can be written as:

$$\dot{m}_3 h_3 + \dot{m}_{11} h_{11} = \dot{m}_{12} h_{12} + \dot{m}_4 h_4 \quad (4.36)$$

The entropy balance equation for Heat Exchanger 2 can be written as:

$$\dot{m}_3 s_3 + \dot{m}_{11} s_{11} + \dot{S}_{gen,hx2} = \dot{m}_{12} s_{12} + \dot{m}_4 s_4 \quad (4.37)$$

The exergy balance equation for Heat Exchanger 2 can be written as

$$\dot{m}_3 ex_3 + \dot{m}_{11} ex_{11} = \dot{m}_{12} ex_{12} + \dot{m}_4 ex_4 + \dot{E}x_{d,hx2} \quad (4.38)$$

- Heater 4

The mass balance equation for Heater 4 can be written as follows:

$$\dot{m}_{13} = \dot{m}_{14} \tag{4.39}$$

The energy balance for Heater 4 can be written as follows:

$$\dot{m}_{13} h_{13} + \dot{Q}_{ht4} = \dot{m}_{14} h_{14} \tag{4.40}$$

The entropy balance for Heater 4 can be written as follows:

$$\dot{m}_{13} s_{13} + \frac{\dot{Q}_{ht4}}{T_0} + \dot{S}_{gen,ht4} = \dot{m}_{14} s_{14} \tag{4.41}$$

The exergy balance for Heater 4 can be written as follows:

$$\dot{m}_{13} ex_{13} + \dot{Q}_{ht4} \left(1 - \frac{T_0}{T_s}\right) = \dot{m}_{14} ex_{14} + \dot{E}x_{d,ht4} \tag{4.42}$$

- Expansion Valve 1

The mass balance equation for the expansion valve 1 can be written as follows:

$$\dot{m}_{10} = \dot{m}_1 \tag{4.43}$$

The energy balance equation for the expansion valve 1 can be written as follows:

$$\dot{m}_{10} h_{10} = \dot{m}_1 h_1 \tag{4.44}$$

The entropy balance equation for the expansion valve 1 can be written as follows:

$$\dot{m}_{10} s_{10} + \dot{S}_{gen,ev1} = \dot{m}_1 s_1 \tag{4.45}$$

The exergy balance equation for the expansion valve 1 can be written as follows:

$$\dot{m}_{10} ex_{10} = \dot{m}_1 ex_1 + \dot{E}x_{d,ev1} \tag{4.46}$$

- Expansion Valve 2

The mass balance equation for the expansion valve 2 can be written as follows:

$$\dot{m}_{16} = \dot{m}_{11} \tag{4.47}$$

The energy balance equation for the expansion valve 2 can be written as follows:

$$\dot{m}_{16}h_{16} = \dot{m}_{11}h_{11} \tag{4.48}$$

The entropy balance equation for the expansion valve 2 can be written as follows:

$$\dot{m}_{16}s_{16} + \dot{S}_{gen,ev2} = \dot{m}_{11}s_{11} \tag{4.49}$$

The exergy balance equation for the expansion valve 2 can be written as follows:

$$\dot{m}_{16}ex_{16} = \dot{m}_{11}ex_{11} + \dot{E}x_{d,ev2} \tag{4.50}$$

- Heater 5 (Heat Sink of Topping Cycle)

The mass balance equation for Heater 5 can be written as follows:

$$\dot{m}_{15} = \dot{m}_{16} \tag{4.51}$$

The energy balance for Heater 5 can be written as follows:

$$\dot{m}_{15}h_{15} = \dot{Q}_{ht5} + \dot{m}_{16}h_{16} \tag{4.52}$$

The entropy balance for Heater 5 can be written as follows:

$$\dot{m}_{15}s_{15} + \dot{S}_{gen,ht5} = \dot{m}_{16}s_{16} + \frac{\dot{Q}_{ht5}}{T_0} \tag{4.53}$$

The exergy balance for Heater 5 can be written as follows:

$$\dot{m}_{15}ex_{15} = \dot{m}_{16}ex_{16} + \dot{E}x_{d,ht5} + \dot{Q}_{ht5}\left(1 - \frac{T_0}{T_s}\right) \tag{4.54}$$

$\dot{Q}_{ht5}$ - represents the heat rejected by sink.

- Compressor 3

The mass balance equation for Compressor 3 can be written as follows:

$$\dot{m}_{14} = \dot{m}_{15} \tag{4.55}$$

The energy balance equation for Compressor 3 can be written as follows:

$$\dot{m}_{14}h_{14} + \dot{W}_{comp3} = \dot{m}_{15}h_{15} \quad (4.56)$$

The entropy balance equation for Compressor 3 can be written as follows:

$$\dot{m}_{14}s_{14} + \dot{W}_{comp3} + \dot{S}_{gen,comp3} = \dot{m}_{15}s_{15} \quad (4.57)$$

The exergy balance equation for Compressor 3 can be written as follows:

$$\dot{m}_{14}ex_{14} + \dot{W}_{comp3} = \dot{m}_{15}ex_{15} + \dot{E}x_{d,comp3} \quad (4.58)$$

4.2.1 Energetic COP

For the heat pump, a coefficient of performance can be used to express energetic performance. The energetic COP of the bottoming cycle, topping cycle and overall system can be written as:

$$COP_{en,1} = \frac{(\dot{m}_9h_9 - \dot{m}_{10}h_{10})}{\dot{W}_{comp1} + \dot{W}_{comp2}} \quad (4.59)$$

$$COP_{en,2} = \frac{(\dot{m}_{15}h_{15} - \dot{m}_{16}h_{16})}{\dot{W}_{comp3}} \quad (4.60)$$

$$COP_{en} = \frac{(\dot{m}_9h_9 - \dot{m}_{10}h_{10}) + (\dot{m}_{15}h_{15} - \dot{m}_{16}h_{16})}{\dot{W}_{comp,net}} \quad (4.61)$$

4.2.3 Exergetic COP

The exergetic COP of the bottoming cycle, topping cycle and overall system can be written as:

$$COP_{ex,1} = \frac{(\dot{m}_9ex_9 - \dot{m}_{10}ex_{10})}{\dot{W}_{comp1} + \dot{W}_{comp2}} \quad (4.62)$$

$$COP_{ex,2} = \frac{(\dot{m}_{15}ex_{15} - \dot{m}_{16}ex_{16})}{\dot{W}_{comp3}} \quad (4.63)$$

$$COP_{ex} = \frac{(\dot{m}_9ex_9 - \dot{m}_{10}ex_{10}) + (\dot{m}_{15}ex_{15} - \dot{m}_{16}ex_{16})}{\dot{W}_{comp,net}} \quad (4.64)$$

4.3 Thermodynamic analyses of System 2

The energy and exergy analysis of System 2 is presented in this section. The energetic and exergetic COPs of individual cycles and overall COPs of the system are defined. These models are used to produce the results and perform parametric studies to assess the effect of operating parameters on system performance. The reference state of surrounding is defined as at Temperature $T_0 = 25$ ℃ and a pressure $P_0 = 1$ bar.

Following assumptions are used in the analyses of the system:

- There is negligible change in the kinetic and potential energy.
- There is no heat loss in the compressor and expansion valves.
- The heat exchangers incur no heat loss to environment.
- The isentropic efficiency value of the compressor is 0.75 (Zamfirescu et al. 2010)
- The pressure drop in pipelines and heat exchangers is negligible.

4.3.1 Balance Equations

The mass, energy, entropy and exergy balance are written for System 2 as shown in Fig. 3.2.

- Heater 1(Heat Source of Bottoming Cycle)

The mass balance for Heater 1 can be written as follows:

$$\dot{m}_1 = \dot{m}_2 \tag{4.65}$$

The energy balance for Heater 1 can be written as follows:

$$\dot{m}_1 h_1 + \dot{Q}_{ht1} = \dot{m}_2 h_2 \tag{4.66}$$

The entropy balance for Heater 1 can be written as follows:

$$\dot{m}_1 s_1 + \frac{\dot{Q}_{ht1}}{T_0} + \dot{S}_{gen,ht1} = \dot{m}_2 s_2 \tag{4.67}$$

The exergy balance for Heater 1 can be written as follows:

$$\dot{m}_1 ex_1 + \dot{Q}_{ht1}\left(1 - \frac{T_0}{T_s}\right) = \dot{m}_2 ex_2 + \dot{E}x_{d,ht1} \tag{4.68}$$

- Compressor 1

The mass balance equation for Compressor 1 can be written as follows:

$$\dot{m}_2 = \dot{m}_3 \tag{4.69}$$

The energy balance equation for Compressor 1 can be written as follows:

$$\dot{m}_2 h_2 + \dot{W}_{comp1} = \dot{m}_3 h_3 \tag{4.70}$$

The entropy balance equation for Compressor 1 can be written as follows:

$$\dot{m}_2 s_2 + \dot{W}_{comp1} + \dot{S}_{gen,comp1} = \dot{m}_3 s_3 \tag{4.71}$$

The exergy balance equation for Compressor 1 can be written as follows:

$$\dot{m}_2 ex_2 + \dot{W}_{comp1} = \dot{m}_3 ex_3 + \dot{E}x_{d,comp1} \tag{4.72}$$

- Heat Exchanger 1

The mass balance for Heat Exchanger 1 can be written as:

For cyclohexane: $\dot{m}_3 = \dot{m}_4$ (4.73)

For biphenyl: $\dot{m}_7 = \dot{m}_8$ (4.74)

The energy balance equation for Heat Exchanger 1 can be written as:

$$\dot{m}_3 h_3 + \dot{m}_7 h_7 = \dot{m}_4 h_4 + \dot{m}_8 h_8 \tag{4.75}$$

The entropy balance equation for Heat Exchanger 1 can be written as:

$$\dot{m}_3 s_3 + \dot{m}_7 s_7 + \dot{S}_{gen,hx1} = \dot{m}_4 s_4 + \dot{m}_8 s_8 \tag{4.76}$$

The exergy balance equation for Heat Exchanger 1 can be written as

$$\dot{m}_3 ex_3 + \dot{m}_7 ex_7 = \dot{m}_4 ex_4 + \dot{m}_8 ex_8 + \dot{E}x_{d,hx1} \tag{4.77}$$

- Heater 2 (Heat Sink of Bottoming Cycle)

The mass balance equation for Heater 2 can be written as follows:

$$\dot{m}_4 = \dot{m}_5 \tag{4.78}$$

The energy balance for Heater 2 can be written as follows:

$$\dot{m}_4 h_4 = \dot{Q}_{ht2} + \dot{m}_5 h_5 \tag{4.79}$$

The entropy balance for Heater 2 can be written as follows:

$$\dot{m}_4 s_4 + \dot{S}_{gen,ht2} = \frac{\dot{Q}_{ht2}}{T_0} + \dot{m}_5 s_5 \tag{4.80}$$

The exergy balance for Heater 2 can be written as follows:

$$\dot{m}_4 ex_4 = \dot{Q}_{ht2}\left(1 - \frac{T_0}{T_s}\right) + \dot{m}_5 ex_5 + \dot{E}x_{d,ht2} \tag{4.81}$$

- Expansion Valve 1

The mass balance equation for the expansion valve 1 can be written as follows:

$$\dot{m}_5 = \dot{m}_6 \tag{4.82}$$

The energy balance equation for the expansion valve 1 can be written as follows:

$$\dot{m}_5 h_5 = \dot{m}_6 h_6 \tag{4.83}$$

The entropy balance equation for the expansion valve 1 can be written as follows:

$$\dot{m}_5 s_5 + \dot{S}_{gen,ev1} = \dot{m}_6 s_6 \tag{4.84}$$

The exergy balance equation for the expansion valve 1 can be written as follows:

$$\dot{m}_5 ex_5 = \dot{m}_6 ex_6 + \dot{E}x_{d,ev1} \tag{4.85}$$

- Heater 3

The mass balance equation for Heater 3 can be written as follows:

$$\dot{m}_6 = \dot{m}_1 \tag{4.86}$$

The energy balance for Heater 3 can be written as follows:

$$\dot{m}_6 h_6 + \dot{Q}_{ht3} = \dot{m}_1 h_1 \quad (4.87)$$

The entropy balance for Heater 3 can be written as follows:

$$\dot{m}_6 s_6 + \frac{\dot{Q}_{ht3}}{T_0} + \dot{S}_{gen,ht3} = \dot{m}_1 s_1 \quad (4.88)$$

The exergy balance for Heater 3 can be written as follows:

$$\dot{m}_6 ex_6 + \dot{Q}_{ht3}\left(1 - \frac{T_0}{T_s}\right) = \dot{m}_1 ex_1 + \dot{E}x_{d,ht3} \quad (4.89)$$

- Heater 4

The mass balance equation for Heater 4 can be written as follows:

$$\dot{m}_8 = \dot{m}_9 \quad (4.90)$$

The energy balance for Heater 4 can be written as follows:

$$\dot{m}_8 h_8 + \dot{Q}_{ht4} = \dot{m}_9 h_9 \quad (4.91)$$

The entropy balance for Heater 4 can be written as follows:

$$\dot{m}_8 s_8 + \frac{\dot{Q}_{ht4}}{T_0} + \dot{S}_{gen,ht4} = \dot{m}_9 s_9 \quad (4.92)$$

The exergy balance for Heater 4 can be written as follows:

$$\dot{m}_8 ex_8 + \dot{Q}_{ht4}\left(1 - \frac{T_0}{T_s}\right) = \dot{m}_9 ex_9 + \dot{E}x_{d,ht4} \quad (4.93)$$

- Compressor 2

The mass balance equation for Compressor 2 can be written as follows:

$$\dot{m}_9 = \dot{m}_{10} \quad (4.94)$$

The energy balance equation for Compressor 2 can be written as follows:

$$\dot{m}_9 h_9 + \dot{W}_{comp2} = \dot{m}_{10} h_{10} \quad (4.95)$$

The entropy balance equation for Compressor 2 can be written as follows:

$$\dot{m}_9 s_9 + \dot{W}_{comp2} + \dot{S}_{gen,comp2} = \dot{m}_{10} s_{10} \quad (4.96)$$

The exergy balance equation for Compressor 2 can be written as follows:

$$\dot{m}_9 ex_9 + \dot{W}_{comp2} = \dot{m}_{10} ex_{10} + \dot{E}x_{d,comp2} \quad (4.97)$$

- Heater 5 (Heat Sink of Topping Cycle)

The mass balance equation for Heater 5 can be written as follows:

$$\dot{m}_{10} = \dot{m}_{11} \quad (4.98)$$

The energy balance for Heater 5 can be written as follows:

$$\dot{m}_{10} h_{10} = \dot{Q}_{ht5} + \dot{m}_{11} h_{11} \quad (4.99)$$

The entropy balance for Heater 5 can be written as follows:

$$\dot{m}_{10} s_{10} + \dot{S}_{gen,ht5} = \frac{\dot{Q}_{ht5}}{T_0} + \dot{m}_{11} s_{11} \quad (4.100)$$

The exergy balance for Heater 5 can be written as follows:

$$\dot{m}_{10} ex_{10} = \dot{Q}_{ht5} \left(1 - \frac{T_0}{T_s}\right) + \dot{m}_{11} ex_{11} + \dot{E}x_{d,ht5} \quad (4.101)$$

- Expansion Valve 2

The mass balance equation for the expansion valve 2 can be written as follows:

$$\dot{m}_{11} = \dot{m}_7 \quad (4.102)$$

The energy balance equation for the expansion valve 2 can be written as follows:

$$\dot{m}_{11} h_{11} = \dot{m}_7 h_7 \quad (4.103)$$

The entropy balance equation for the expansion valve 2 can be written as follows:

$$\dot{m}_{11} s_{11} + \dot{S}_{gen,ev2} = \dot{m}_7 s_7 \quad (4.104)$$

The exergy balance equation for the expansion valve 2 can be written as follows:

$$\dot{m}_{11} ex_{11} = \dot{m}_7 ex_7 + \dot{E}x_{d,ev2} \quad (4.105)$$

4.3.2 Energetic COP

For the heat pump, a coefficient of performance can be used to express energetic performance. The energetic COP of the bottoming cycle, topping cycle and overall system can be written as:

$$COP_{en,1} = \frac{(\dot{m}_4 h_4 - \dot{m}_5 h_5)}{\dot{W}_{comp1}} \quad (4.106)$$

$$COP_{en,2} = \frac{(\dot{m}_{10} h_{10} - \dot{m}_{11} h_{11})}{\dot{W}_{comp2}} \quad (4.107)$$

$$COP_{en} = \frac{(\dot{m}_{10} h_{10} - \dot{m}_{11} h_{11}) + (\dot{m}_4 h_4 - \dot{m}_5 h_5)}{\dot{W}_{comp,net}} \quad (4.108)$$

4.3.3 Exergetic COP

The exergetic COP of the bottoming cycle, topping cycle and overall system can be written as:

$$COP_{ex,1} = \frac{(\dot{m}_4 ex_4 - \dot{m}_5 ex_5)}{\dot{W}_{comp1}} \quad (4.109)$$

$$COP_{ex,2} = \frac{(\dot{m}_{10} ex_{10} - \dot{m}_{11} ex_{11})}{\dot{W}_{comp2}} \quad (4.110)$$

$$COP_{ex} = \frac{(\dot{m}_{10} ex_{10} - \dot{m}_{11} ex_{11}) + (\dot{m}_4 ex_4 - \dot{m}_5 ex_5)}{\dot{W}_{comp,net}} \quad (4.111)$$

4.4 Thermodynamic analyses of System 3

The energy and exergy analysis of System 3 is presented in this section. The energetic and exergetic COPs of individual cycles and overall COPs of the system are defined. These models are used to produce the results and perform parametric studies to assess the effect of operating parameters on system performance. The reference state of surrounding is defined as at temperature $T_0 = 25$ ℃ and a pressure $P_0 = 1$ bar.

Following assumptions are used in the analyses of the system:

- There is negligible change in the kinetic and potential energy.

- There is no heat loss in the compressor and expansion valves.
- The heat exchangers incur no heat loss to environment.
- The isentropic efficiency value of the compressor is 0.75 (Zamfirescu et al. 2010)
- The pressure drop in pipelines and heat exchangers is negligible.

4.4.1 Balance Equations

The mass, energy, entropy and exergy balance are written for System 3 as shown in Fig. 3.3.

- Heater 1 (Heat Source of Bottoming Cycle)

The mass balance for Heater 1 can be written as follows:

$$\dot{m}_1 = \dot{m}_2 \tag{4.112}$$

The energy balance for Heater 1 can be written as follows:

$$\dot{m}_1 h_1 + \dot{Q}_{ht1} = \dot{m}_2 h_2 \tag{4.113}$$

The entropy balance for Heater 1 can be written as follows:

$$\dot{m}_1 s_1 + \frac{\dot{Q}_{ht1}}{T_0} + \dot{S}_{gen,ht1} = \dot{m}_2 s_2 \tag{4.114}$$

The exergy balance for Heater 1 can be written as follows:

$$\dot{m}_1 ex_1 + \dot{Q}_{ht1}\left(1 - \frac{T_0}{T_s}\right) = \dot{m}_2 ex_2 + \dot{E}x_{d,ht1} \tag{4.115}$$

- Compressor 1

The mass balance equation for Compressor 1 can be written as follows:

$$\dot{m}_2 = \dot{m}_3 \tag{4.116}$$

The energy balance equation for Compressor 1 can be written as follows:

$$\dot{m}_2 h_2 + \dot{W}_{comp1} = \dot{m}_3 h_3 \tag{4.117}$$

The entropy balance equation for Compressor 1 can be written as follows:

$$\dot{m}_2 s_2 + \dot{W}_{comp1} + \dot{S}_{gen,comp1} = \dot{m}_3 s_3 \quad (4.118)$$

The exergy balance equation for Compressor 1 can be written as follows:

$$\dot{m}_2 ex_2 + \dot{W}_{comp1} = \dot{m}_3 ex_3 + \dot{E}x_{d,comp1} \quad (4.119)$$

- Heat Exchanger 1

The mass balance for Heat Exchanger 1 can be written as:

For cyclohexane: $\dot{m}_3 = \dot{m}_4$ (4.120)

For biphenyl: $\dot{m}_7 = \dot{m}_8$ (4.121)

The energy balance equation for Heat Exchanger 1 can be written as:

$$\dot{m}_3 h_3 + \dot{m}_7 h_7 = \dot{m}_4 h_4 + \dot{m}_8 h_8 \quad (4.122)$$

The entropy balance equation for Heat Exchanger 1 can be written as:

$$\dot{m}_3 s_3 + \dot{m}_7 s_7 + \dot{S}_{gen,hx1} = \dot{m}_4 s_4 + \dot{m}_8 s_8 \quad (4.123)$$

The exergy balance equation for Heat Exchanger 1 can be written as

$$\dot{m}_3 ex_3 + \dot{m}_7 ex_7 = \dot{m}_4 ex_4 + \dot{m}_8 ex_8 + \dot{E}x_{d,hx1} \quad (4.124)$$

- Heater 2 (Heat Sink of Bottoming Cycle)

The mass balance equation for Heater 2 can be written as follows:

$$\dot{m}_4 = \dot{m}_5 \quad (4.125)$$

The energy balance for Heater 2 can be written as follows:

$$\dot{m}_4 h_4 = \dot{m}_5 h_5 + \dot{Q}_{ht2} \quad (4.126)$$

The entropy balance for Heater 2 can be written as follows:

$$\dot{m}_4 s_4 + \dot{S}_{gen,ht2} = \dot{m}_5 s_5 + \frac{\dot{Q}_{ht2}}{T_0} \quad (4.127)$$

The exergy balance for Heater 2 can be written as follows:

$$\dot{m}_4 ex_4 = \dot{m}_5 ex_5 + \dot{Q}_{ht2}\left(1 - \frac{T_0}{T_s}\right) + \dot{E}x_{d,ht2} \quad (4.128)$$

- Expansion Valve 1

The mass balance equation for the expansion valve 1 can be written as follows:

$$\dot{m}_5 = \dot{m}_6 \quad (4.129)$$

The energy balance equation for the expansion valve 1 can be written as follows:

$$\dot{m}_5 h_5 = \dot{m}_6 h_6 \quad (4.130)$$

The entropy balance equation for the expansion valve 1 can be written as follows:

$$\dot{m}_5 s_5 + \dot{S}_{gen,ev1} = \dot{m}_6 s_6 \quad (4.131)$$

The exergy balance equation for the expansion valve 1 can be written as follows:

$$\dot{m}_5 ex_5 = \dot{m}_6 ex_6 + \dot{E}x_{d,ev1} \quad (4.132)$$

- Heater 3

The mass balance equation for Heater 3 can be written as follows:

$$\dot{m}_6 = \dot{m}_1 \quad (4.133)$$

The energy balance for Heater 3 can be written as follows:

$$\dot{m}_6 h_6 + \dot{Q}_{ht3} = \dot{m}_1 h_1 \quad (4.134)$$

The entropy balance for Heater 3 can be written as follows:

$$\dot{m}_6 s_6 + \frac{\dot{Q}_{ht3}}{T_0} + \dot{S}_{gen,ht3} = \dot{m}_1 s_1 \quad (4.135)$$

The exergy balance for Heater 3 can be written as follows:

$$\dot{m}_6 ex_6 + \dot{Q}_{ht3}\left(1 - \frac{T_0}{T_s}\right) = \dot{m}_1 ex_1 + \dot{E}x_{d,ht3} \quad (4.136)$$

- Heat Exchanger 2

The Heat Exchanger 2 is used for internally transfer heat from hot stream of biphenyl to cold stream, the mass balance can be written as:

For biphenyl: $\dot{m}_8 = \dot{m}_9$ (4.137)

For biphenyl: $\dot{m}_{11} = \dot{m}_{12}$ (4.138)

The energy balance equation for Heat Exchanger 2 can be written as:

$$\dot{m}_{11}h_{11} + \dot{m}_8 h_8 = \dot{m}_9 h_9 + \dot{m}_{12}h_{12} \quad (4.139)$$

The entropy balance equation for Heat Exchanger 2 can be written as:

$$\dot{m}_{11}s_{11} + \dot{m}_8 s_8 + \dot{S}_{gen,hx2} = \dot{m}_9 s_9 + \dot{m}_{12}s_{12} \quad (4.140)$$

The exergy balance equation for Heat Exchanger 2 can be written as

$$\dot{m}_{11}ex_{11} + \dot{m}_8 ex_8 = \dot{m}_9 ex_9 + \dot{m}_{12}ex_{12} + \dot{E}x_{d,hx2} \quad (4.141)$$

- Compressor 2

The mass balance equation for Compressor 2 can be written as follows:

$$\dot{m}_9 = \dot{m}_{10} \quad (4.142)$$

The energy balance equation for Compressor 2 can be written as follows:

$$\dot{m}_9 h_9 + \dot{W}_{comp2} = \dot{m}_{10}h_{10} \quad (4.143)$$

The entropy balance equation for Compressor 2 can be written as follows:

$$\dot{m}_9 s_9 + \dot{S}_{gen,comp2} = \dot{m}_{10}s_{10} \quad (4.144)$$

The exergy balance equation for Compressor 2 can be written as follows:

$$\dot{m}_9 ex_9 + \dot{W}_{comp2} = \dot{m}_{10}ex_{10} + \dot{E}x_{d,comp2} \quad (4.145)$$

- Heat Exchanger 3

The mass balance for Heat Exchanger 3 can be written as:

For mercury: $\dot{m}_{14} = \dot{m}_{15}$ (4.146)

For biphenyl: $\dot{m}_{10} = \dot{m}_{11}$ (4.147)

The energy balance equation for Heat Exchanger 3 can be written as:

$$\dot{m}_{14}h_{14} + \dot{m}_{10}h_{10} = \dot{m}_{11}h_{11} + \dot{m}_{15}h_{15} \quad (4.148)$$

The entropy balance equation for Heat Exchanger 3 can be written as:

$$\dot{m}_{14}s_{14} + \dot{m}_{10}s_{10} + \dot{S}_{gen,hx3} = \dot{m}_{11}s_{11} + \dot{m}_{15}s_{15} \quad (4.149)$$

The exergy balance equation for Heat Exchanger 3 can be written as

$$\dot{m}_{14}ex_{14} + \dot{m}_{10}ex_{10} = \dot{m}_{11}ex_{11} + \dot{m}_{15}ex_{15} + \dot{E}x_{d,hx3} \quad (4.150)$$

- Heater 4

The mass balance equation for Heater 4 can be written as follows:

$$\dot{m}_{12} = \dot{m}_{13} \quad (4.151)$$

The energy balance for Heater 4 can be written as follows:

$$\dot{m}_{12}h_{12} + \dot{Q}_{ht4} = \dot{m}_{13}h_{13} \quad (4.152)$$

The entropy balance for Heater 4 can be written as follows:

$$\dot{m}_{12}s_{12} + \frac{\dot{Q}_{ht4}}{T_0} + \dot{S}_{gen,ht4} = \dot{m}_{13}s_{13} \quad (4.153)$$

The exergy balance for Heater 4 can be written as follows:

$$\dot{m}_{12}ex_{12} + \dot{Q}_{ht4}\left(1 - \frac{T_0}{T_s}\right) = \dot{m}_{13}ex_{13} + \dot{E}x_{d,ht4} \quad (4.154)$$

- Expansion Valve 2

The mass balance equation for the expansion valve 2 can be written as follows:

$$\dot{m}_{13} = \dot{m}_{7} \quad (4.155)$$

The energy balance equation for the expansion valve 2 can be written as follows:

$$\dot{m}_{13}h_{13} = \dot{m}_7 h_7 \quad (4.156)$$

The entropy balance equation for the expansion valve 2 can be written as follows:

$$\dot{m}_{13}s_{13} + \dot{S}_{gen,ev2} = \dot{m}_7 s_7 \quad (4.157)$$

The exergy balance equation for the expansion valve 2 can be written as follows:

$$\dot{m}_{13}ex_{13} = \dot{m}_7 ex_7 + \dot{E}x_{d,ev2} \quad (4.158)$$

- Heater 5

The mass balance equation for Heater 5 can be written as follows:

$$\dot{m}_{15} = \dot{m}_{16} \quad (4.159)$$

The energy balance for Heater 5 can be written as follows:

$$\dot{m}_{15}h_{15} + \dot{Q}_{ht5} = \dot{m}_{16}h_{16} \quad (4.160)$$

The entropy balance for Heater 5 can be written as follows:

$$\dot{m}_{15}s_{15} + \frac{\dot{Q}_{ht5}}{T_0} + \dot{S}_{gen,ht5} = \dot{m}_{16}s_{16} \quad (4.161)$$

The exergy balance for Heater 5 can be written as follows:

$$\dot{m}_{15}ex_{15} + \dot{Q}_{ht5}\left(1 - \frac{T_0}{T_s}\right) = \dot{m}_{16}ex_{16} + \dot{E}x_{d,ht5} \quad (4.162)$$

- Compressor 3

The mass balance equation for Compressor 3 can be written as follows:

$$\dot{m}_{16} = \dot{m}_{17} \quad (4.163)$$

The energy balance equation for Compressor 3 can be written as follows:

$$\dot{m}_{16}h_{16} + \dot{W}_{comp3} = \dot{m}_{17}h_{17} \quad (4.164)$$

The entropy balance equation for Compressor 3 can be written as follows:

$$\dot{m}_{16}s_{16} + \dot{S}_{gen,comp3} = \dot{m}_{17}s_{17} \quad (4.165)$$

The exergy balance equation for Compressor 3 can be written as follows:

$$\dot{m}_{16} ex_{16} + \dot{W}_{comp3} = \dot{m}_{17} ex_{17} + \dot{E}x_{d,comp3} \quad (4.166)$$

- Heater 6 (Intercooler)

The mass balance equation for Heater 6 can be written as follows:

$$\dot{m}_{17} = \dot{m}_{18} \quad (4.167)$$

The energy balance for Heater 6 can be written as follows:

$$\dot{m}_{17} h_{17} = \dot{Q}_{ht6} + \dot{m}_{18} h_{18} \quad (4.168)$$

The entropy balance for Heater 6 can be written as follows:

$$\dot{m}_{17} s_{17} + \dot{S}_{gen,ht6} = \frac{\dot{Q}_{ht6}}{T_0} + \dot{m}_{18} s_{18} \quad (4.169)$$

The exergy balance for Heater 6 can be written as follows:

$$\dot{m}_{17} ex_{17} = \dot{Q}_{ht6} \left(1 - \frac{T_0}{T_s}\right) + \dot{m}_{18} ex_{18} + \dot{E}x_{d,ht6} \quad (4.170)$$

- Compressor 4

The mass balance equation for Compressor 4 can be written as follows:

$$\dot{m}_{18} = \dot{m}_{19} \quad (4.171)$$

The energy balance equation for Compressor 4 can be written as follows:

$$\dot{m}_{18} h_{18} + \dot{W}_{comp4} = \dot{m}_{19} h_{19} \quad (4.172)$$

The entropy balance equation for Compressor 4 can be written as follows:

$$\dot{m}_{18} s_{18} + \dot{S}_{gen,comp4} = \dot{m}_{19} s_{19} \quad (4.173)$$

The exergy balance equation for Compressor 4 can be written as follows:

$$\dot{m}_{18} ex_{18} + \dot{W}_{comp4} = \dot{m}_{19} ex_{19} + \dot{E}x_{d,comp4} \quad (4.174)$$

- Heater 7(Intercooler)

The mass balance equation for Heater 7 can be written as follows:

$$\dot{m}_{19} = \dot{m}_{20} \tag{4.175}$$

The energy balance for Heater 7 can be written as follows:

$$\dot{m}_{19} h_{19} = \dot{Q}_{ht7} + \dot{m}_{20} h_{20} \tag{4.176}$$

The entropy balance for Heater 7 can be written as follows:

$$\dot{m}_{19} s_{19} + \dot{S}_{gen,ht7} = \frac{\dot{Q}_{ht7}}{T_0} + \dot{m}_{20} s_{20} \tag{4.177}$$

The exergy balance for Heater 7 can be written as follows:

$$\dot{m}_{19} ex_{19} = \dot{Q}_{ht7} \left(1 - \frac{T_0}{T_s}\right) + \dot{m}_{20} ex_{20} + \dot{E}x_{d,ht7} \tag{4.178}$$

- Compressor 5

The mass balance equation for Compressor 5 can be written as follows:

$$\dot{m}_{20} = \dot{m}_{21} \tag{4.179}$$

The energy balance equation for Compressor 5 can be written as follows:

$$\dot{m}_{20} h_{20} + \dot{W}_{comp5} = \dot{m}_{21} h_{21} \tag{4.180}$$

The entropy balance equation for Compressor 5 can be written as follows:

$$\dot{m}_{20} s_{20} + \dot{S}_{gen,comp5} = \dot{m}_{21} s_{21} \tag{4.181}$$

The exergy balance equation for Compressor 5 can be written as follows:

$$\dot{m}_{20} ex_{20} + \dot{W}_{comp5} = \dot{m}_{21} ex_{21} + \dot{E}x_{d,comp5} \tag{4.182}$$

- Heater 8 (Heat Sink of Topping Cycle)

The mass balance equation for Heater 8 can be written as follows:

$$\dot{m}_{21} = \dot{m}_{22} \tag{4.183}$$

The energy balance for Heater 8 can be written as follows:

$$\dot{m}_{21}h_{21} = \dot{Q}_{ht8} + \dot{m}_{22}h_{22} \quad (4.184)$$

The entropy balance for Heater 8 can be written as follows:

$$\dot{m}_{21}s_{21} + \dot{S}_{gen,ht8} = \frac{\dot{Q}_{ht8}}{T_0} + \dot{m}_{22}s_{22} \quad (4.185)$$

The exergy balance for Heater 8 can be written as follows:

$$\dot{m}_{21}ex_{21} = \dot{Q}_{ht8}\left(1 - \frac{T_0}{T_s}\right) + \dot{m}_{22}ex_{22} + \dot{E}x_{d,ht8} \quad (4.186)$$

- Heater 9

The mass balance equation for Heater 9 can be written as follows:

$$\dot{m}_{22} = \dot{m}_{23} \quad (4.187)$$

The energy balance for Heater 9 can be written as follows:

$$\dot{m}_{22}h_{22} = \dot{Q}_{ht9} + \dot{m}_{23}h_{23} \quad (4.188)$$

The entropy balance for Heater 9 can be written as follows:

$$\dot{m}_{22}s_{22} + \dot{S}_{gen,ht9} = \frac{\dot{Q}_{ht9}}{T_0} + \dot{m}_{23}s_{23} \quad (4.189)$$

The exergy balance for Heater 9 can be written as follows:

$$\dot{m}_{22}ex_{22} = \dot{Q}_{ht9}\left(1 - \frac{T_0}{T_s}\right) + \dot{m}_{23}ex_{23} + \dot{E}x_{d,ht9} \quad (4.190)$$

- Expansion Valve 3

The mass balance equation for the expansion valve 3 can be written as follows:

$$\dot{m}_{23} = \dot{m}_{14} \quad (4.191)$$

The energy balance equation for the expansion valve 3 can be written as follows:

$$\dot{m}_{23}h_{23} = \dot{m}_{14}h_{14} \quad (4.192)$$

The entropy balance equation for the expansion valve 3 can be written as follows:

$$\dot{m}_{23}s_{23} + \dot{S}_{gen,ev3} = \dot{m}_{14}s_{14} \quad (4.193)$$

The exergy balance equation for the expansion valve 3 can be written as follows:

$$\dot{m}_{23}ex_{23} = \dot{m}_{14}ex_{14} + \dot{E}x_{d,ev3} \quad (4.194)$$

4.4.2 Energetic COP

For the heat pump, a coefficient of performance can be used to express energetic performance. The energetic COP of the bottoming cycle, topping cycle and overall system can be written as:

$$COP_{en,1} = \frac{(\dot{m}_4h_4 - \dot{m}_5h_5)}{\dot{W}_{comp1}} \quad (4.195)$$

$$COP_{en,2} = \frac{(\dot{m}_{10}h_{10} - \dot{m}_{11}h_{11})}{\dot{W}_{comp2}} \quad (4.196)$$

$$COP_{en,3} = \frac{(\dot{m}_{21}h_{21} - \dot{m}_{22}h_{22})}{\dot{W}_{comp3} + \dot{W}_{comp4} + \dot{W}_{comp5}} \quad (4.197)$$

$$COP_{en} = \frac{(\dot{m}_{21}h_{21} - \dot{m}_{22}h_{22}) + (\dot{m}_4h_4 - \dot{m}_5h_5)}{\dot{W}_{comp,net}} \quad (4.198)$$

4.4.3 Exergetic COP

The exergetic COP of the bottoming cycle, topping cycle and overall system can be written as:

$$COP_{ex,1} = \frac{(\dot{m}_4ex_4 - \dot{m}_5ex_5)}{\dot{W}_{comp1}} \quad (4.199)$$

$$COP_{ex,2} = \frac{(\dot{m}_{10}ex_{10} - \dot{m}_{11}ex_{11})}{\dot{W}_{comp2}} \quad (4.200)$$

$$COP_{ex,3} = \frac{(\dot{m}_{21}ex_{21} - \dot{m}_{22}ex_{22})}{\dot{W}_{comp3} + \dot{W}_{comp4} + \dot{W}_{comp5}} \quad (4.201)$$

$$COP_{ex} = \frac{(\dot{m}_{21}ex_{21} - \dot{m}_{22}ex_{22}) + (\dot{m}_4ex_4 - \dot{m}_5ex_5)}{\dot{W}_{comp,net}} \quad (4.202)$$

4.5 Cost Analysis

The cost analysis provides an estimation of the cost of whole system based on the aggregated costs of individual components. The cost analysis integrated with exergy provides a holistic picture of system performance that includes both thermodynamic and economic aspects (Dincer and Rosen, 2007). The capital cost of an engineering system is estimated for a base year and chemical engineering plant cost index (CEPCI) is used for the cost adjustments.

4.5.1 Purchase Cost Estimation

The first step of economic analysis of a system is estimating the cost of each individual component. The analysis in this thesis is performed using an equipment capacity-based estimation equation (Turton, 2009). The coefficients depend on the type of equipment. It can stated as follows:

$$\log Z = K_1 + K_2 \log(A) + K_3[\log(A)]^2 \tag{4.203}$$

Where Z is the estimated procurement cost of equipment, based on the prices in year 2001. The coefficients K_i are defined by Turton (2009), the factor A is based on the capacity of the equipment, in terms of power, volume flow rate or heat transfer area. The values of coefficients used in equation 4.203 are provided in Table 4.1. The cost of expansion valve is directly estimated from the valves available in market and compared with the cost estimated in equation 4.204

$$Z_{ev} = 12.36\ \dot{m} \tag{4.204}$$

where $\dot{m}$ represents the mass flow rate.

The cost reflected in equations 4.1 and 4.2 corresponds to year 2001 and 2012. The updated costs of the equipment are obtained by adjusting these equations to current year, using Chemical Engineering Plant Cost Index CEPCI given by

$$C_1 = C_2 \frac{\text{CEPCI 1}}{\text{CEPCI 2}} \tag{4.205}$$

where C_1 represents the cost of equipment in year of interest, C_2 represents the cost of equipment in base year. $CEPCI_1$ and $CEPCI_2$ represents the chemical engineering plant cost

index for the year of interest and year of cost data availability respectively. The CEPCI values corresponding to years 2001, 2010, 2012, and 2015 are 394, 551, 571 (Norwegian University of Science and Technology, 2011), and 560.7 (Chemical engineering online, 2015).

Table 4.1 Coefficients of different equipment's cost estimation equation (data from Turton, 2009)

Coefficients\Components	Heat exchangers	Compressor	Heater
A	Area (m^2)	Power (kW)	Duty (kW)
$\mathbf{K_1}$	4.3247	2.2897	2.2628
$\mathbf{K_2}$	-0.303	1.3604	0.8581
$\mathbf{K_3}$	0.1634	-0.1027	0.0003

Chapter 5: Aspen Plus Simulation Framework

The three high temperature heat pumps are modelled in Aspen Plus software in order to analyze energetically and exergetically. This thermodynamic analysis is carried out based on the energetic and exergetic inputs and outputs of the cascaded cycles. The Aspen Plus software simulates the processes based on the thermodynamic principles of mass, energy, entropy and exergy balances applied to the engineering components or units. The simultaneous linear equations are solved in background, by incorporating the appropriate property sets, standard equations of states, operating conditions and thermodynamic models. The mathematical models are used to predict the performance of individual units and overall systems or plants. Following steps are required for implementing Aspen Plus simulation and analysis. (Chukwu, 2008; Orhan, 2011):

- Choose and define the units or components for the simulation and connecting these units in logical manner on the Aspen Plus flowsheet. This step also involves labeling the blocks, selecting parameters and joining with appropriate streams.
- Defining the global variable sets, which includes the unit system, type of run, input conditions and mode etc.
- Describing all the components of the system. The components are defined by user specified values of parameters linked to each component. These values are saved in project database and can be varied to see the performance variation with each parameter.
- Specifying the flow rates, fluid, and mass or mole fraction for all feed streams.
- Defining the operating parameters for all the units.
- Running the simulation for partial or complete system.
- Execute the model analyses, sensitivity or parametric analysis of the system.

The modeling is performed at component and system level. The initial step is component modeling, which involves a detailed modeling of each component of the system. The parameters are user defined inputs that are required for each component. These parameters

are provided based on the acceptable and reliable values given in literature. Three configuration of high temperature heat pump systems are developed using Aspen Plus.

Each system is analyzed energetically and exergetically. The exergy destruction rates of all major components are calculated based on the simulation results data of each stream. The operating parameters are identified and sensitivity analysis is performed to observe the effect on performance and determine the key parameters. The systems are analyzed and compare to determine the most suitable configuration. The simulation results provides the insights of system performance and emphasize the need to develop more configurations.

5.1 Simulation Procedure

In this section the simulation of the heat pump configuration is explained in details. The operation models and component property methods that are used in development of the systems are explained. The Aspen Plus terms are defined in this section.

5.1.1 Unit Operation Models

The Aspen Plus software used components or unit operation models as a representation of actual equipment e.g., compressors, heat exchangers. The unit operation models ideally match the behavior of corresponding actual component, and governed by the stream input, operating conditions and input parameters. Some of the blocks that are used in the modeling and simulation of systems are described in following subsection.

5.1.1.1 Heat Exchangers

The heat exchangers are the equipment that allows exchange of thermal energy between two or more streams. The Aspen Plus has separate categories for simple heaters. The heat exchanger analysis finds the thermal or phase of output streams that exchange heat. Different types of blocks are used to represent some of the broad categories of heat exchangers e.g. Heater (heat up or cool down stream), HeatX (a heat exchanger with two streams), MHeatX (heat exchanger has more than two streams).The heater represents the heating or cooling process, disregards of source. This block defines the outlet condition in

terms of temperature, vapor fractions and the duty is calculated based on the amount of heating or cooling required to achieve the set conditions.

The heat exchangers has two or more streams exchanging heat, the parameters defined in terms of stream exit conditions and pressure drops. The temperature of approach is also need to be defined.

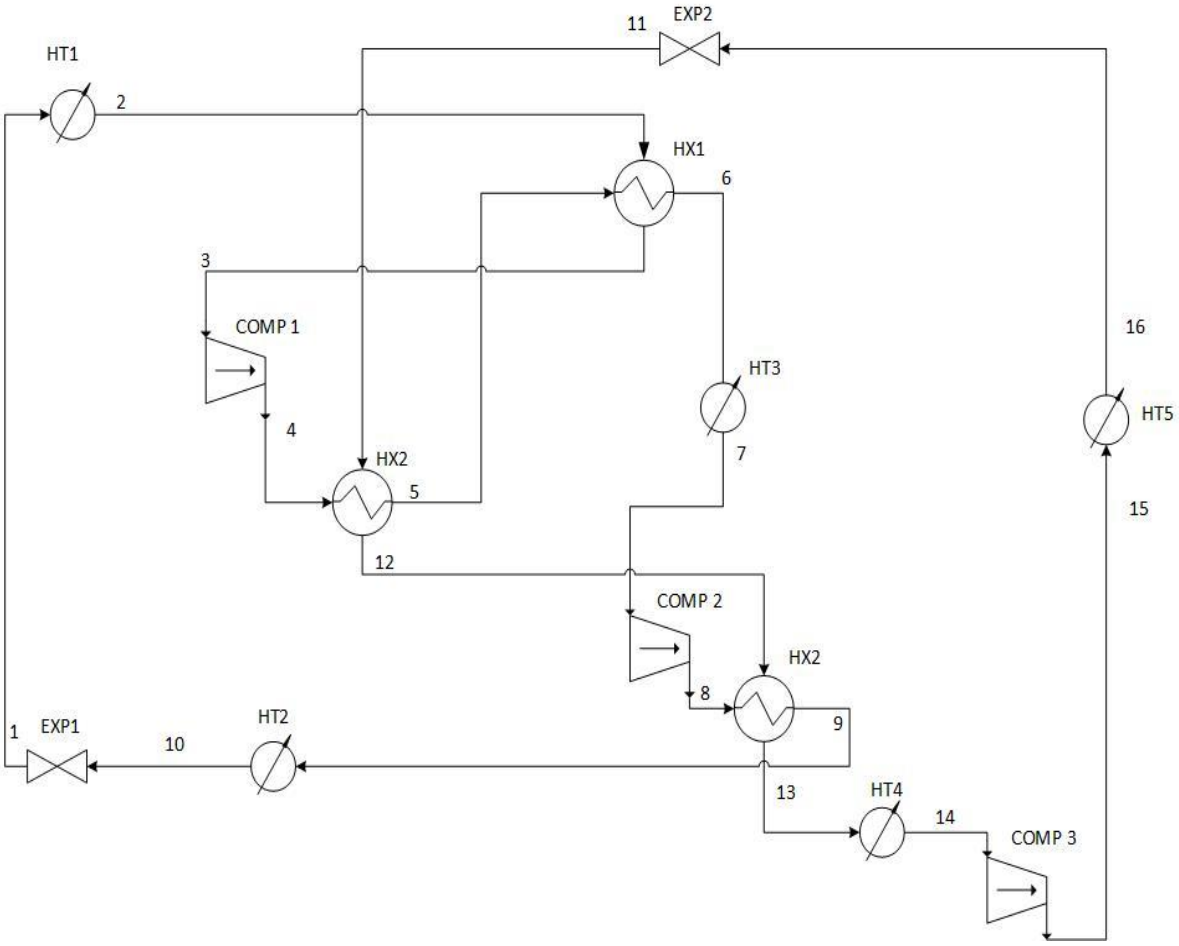

Figure 5.1 The Aspen Plus flowsheet System1 (water and biphenyl as working fluids)

5.1.1.2 Pressure Changers

The pressure changers operation models are used to vary the stream pressures. These models may represent compressors, pumps, turbines or expansion valves. The important blocks available are Pump (a hydraulic turbine or pump), Compr (a turbine or compressor), MCompr (a multistage turbine or compressor), Valve (control valve) etc.

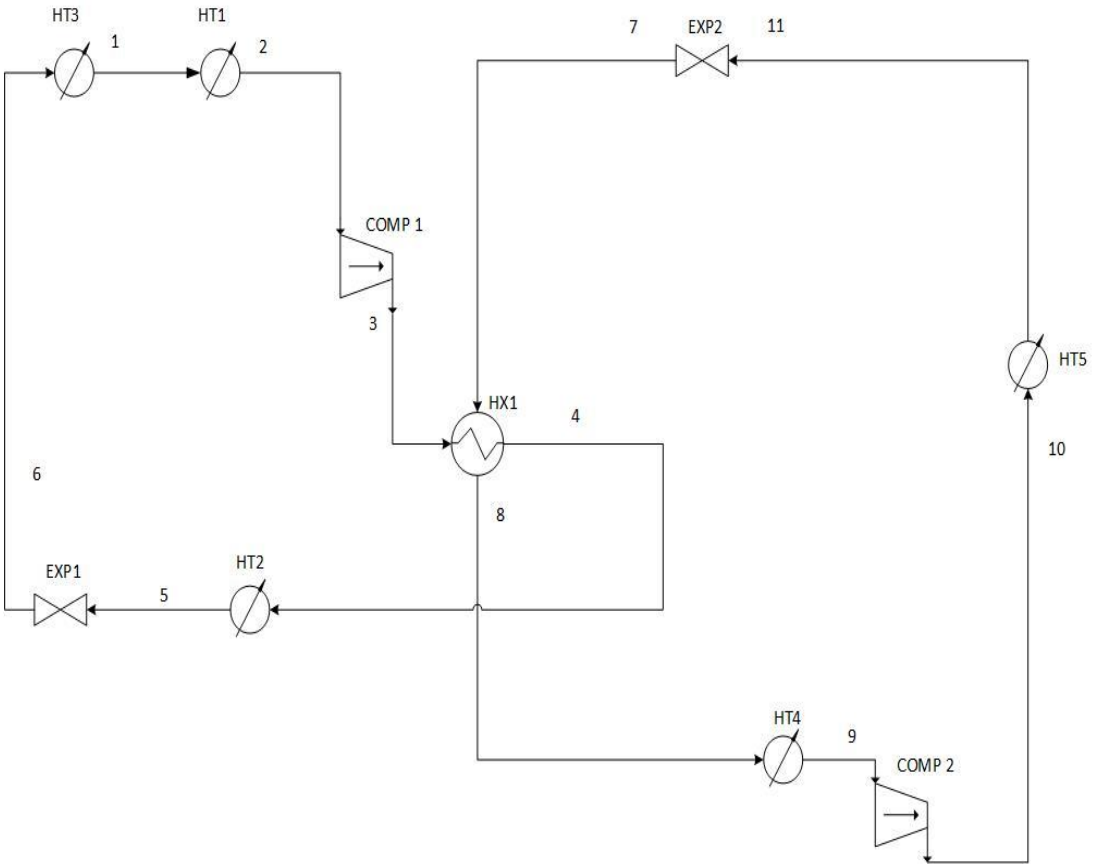

Figure 5.2 The Aspen Plus flowsheet of System 2 (cyclohexane and biphenyl as working fluids)

The Pump simulates the hydraulic turbines or pumps. The pumps handle the liquid phase and input parameters are isentropic efficiencies, pressure ratios, exit pressures etc. The power input required either provided or calculated in simulation. Similarly a Compr model simulates either a turbine or compressor. It may represent an isentropic turbine or compressor, a polytropic turbine or compressor, positive displacement devices. The input parameters are isentropic efficiencies, pressure ratios, or exit pressure. The input or output power is either provided or calculated in simulation.

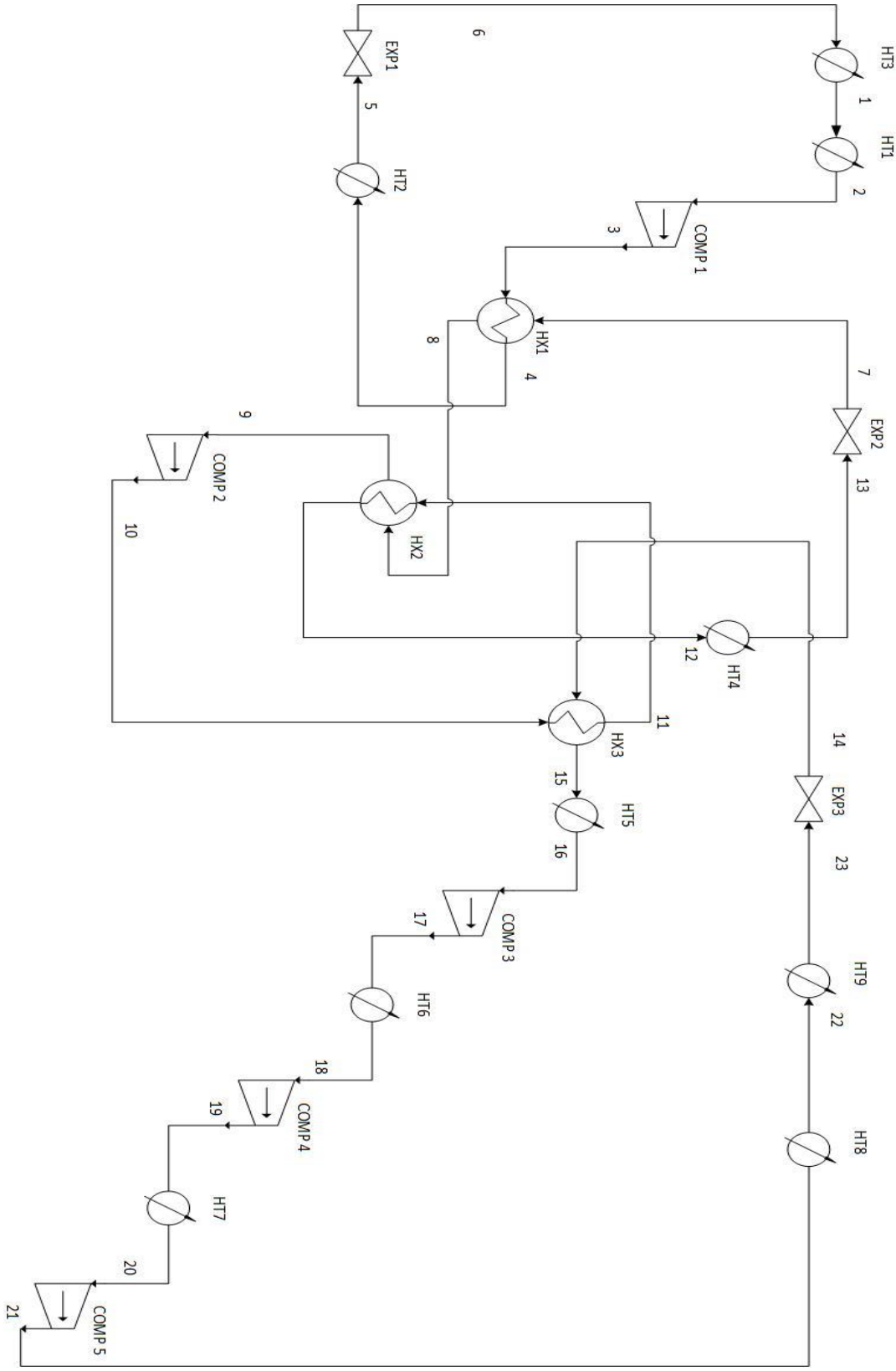

Figure 5.3 Aspen Plus flowsheet of System 3 (cyclohexane, biphenyl and mercury as working fluids)

5.1.2 Property Methods

The Aspen plus allows the user to select the thermodynamic models predefined in the library or allows the user to use custom methods. It classify the property methods as follows:

- Equation of state
- Activity coefficient models
- Special methods

5.1.2.1 Equation of State

Equations of state describe a relationship between pressure, volume, and temperature of pure components and/or mixtures.

The relationship between volume, pressure and temperature of pure substances or certain mixtures can be represented in terms of mathematical formula. These equations models the behavior of substance on fairly wide range of temperatures and pressures. The models are developed for numerous substances and reported in literature. Aspen Plus allows the user to select the equation of state to model the material or fluid selected. A large number of equations of state available in its library. These equations of state holds good for gas or vapor phase modeling or low polarity liquids. Ideal gas, Peng–Robinson-Stryjek-Vera, Elliott, Suresh, Donohue equations of state are some of the examples available in Aspen Plus.

5.1.2.2 Activity Coefficient Method

These methods mainly used in modeling the liquid phase of a substance, these methods has been reported to approximate a large number of substances. These methods are not consistent around critical region. Some examples of the activity coefficient methods are Wilson, NRTL and ELECNRTL.

The ELECNRTL model method a flexible electrolyte equation of state. It successfully models the thermodynamic behavior of electrolyte solutions. The ELECNRTL and NRTL are consistent in modeling the liquid phase and apply the Redlich Kwong equation of state for vapor phase property calculations.

5.1.2.3 Special Methods

Aspen Plus also provides some special methods provided in literature for the modeling of pure substances of mixtures. Some of these methods provided in library are STEAM-TA (ASME steam table correlations), STEAMNBS, and IAPWS-95 etc.

5.1.3 Property Method Selection for the Simulation

The selection of property method is very critical for the accurate modeling of these heat pump systems. The selected property methods should represent the thermodynamic behavior of certain components and must be applicable for the entire working range of operating conditions. The improper selection of these methods leads to erroneous results. The working fluids selected for this study are cyclohexane, biphenyl, water and mercury. The equations of state for these fluids has been selected from the literature and reported in chapter 3. In case multiple working fluids are used in a single Aspen project, the property method corresponding to the working fluids can provided before simulation. The Figure 5.1, 5.2 and 5.3 represents the Aspen plus flowsheets of System 1, 2 and 3 respectively.

\

Chapter 6: Results and Discussion

This chapter presents the results of energetic and exergetic analysis discussed in preceding chapter. The individual systems results are presented in sections 6.1, 6.2 and 6.3. The section 6.4 presents further discussion and comparison of the systems. Each system is analyzed energetically and exergetically, the base case state points are tabulated for each system. The parametric studies are performed to determine the effect of operating parameters and determine the best performance scenarios. The performance of systems is assessed based on the energetic and exergetic COP values. The heat pump systems developed for the present study are cascaded and use different working fluid for each cycle, therefore the performance analysis of overall system and each cycle provides the insights of system behaviour. The relevant parameters that affect the performance of heat pumps are source temperature, sink temperature, the intermediate temperature of cascaded systems and isentropic efficiencies of the compressors. The pressures are also included in the study to assess the effect of minimum, intermediate and maximum pressures on system performance. The last section compares the performance of each system for similar sink and source conditions.

6.1 System 1 Results

6.1.1 Energy and Exergy Analysis Results of System 1

The analysis of System 1 is presented in this section. The table 6.1 tabulates the inputs and calculated thermodynamic data of the streams in System 1for base case. The System 2 is a cascaded system, which utilises water in bottoming cycle and biphenyl in the topping cycle.

The heat delivered by source at 81.3 ℃ and at a corresponding pressure of 0.5 bar. The system sink delivers heat at an elevated temperature of 600 ℃ and condenser pressure is 67 bar. The energetic and exergetic COP values overall system are found to be 2.29 and 1.065 respectively. The net work input for System 1 is 1630 kW. The intermediate temperature and pressure of topping cycle fluid is 256 ℃ and 1.04 bar.

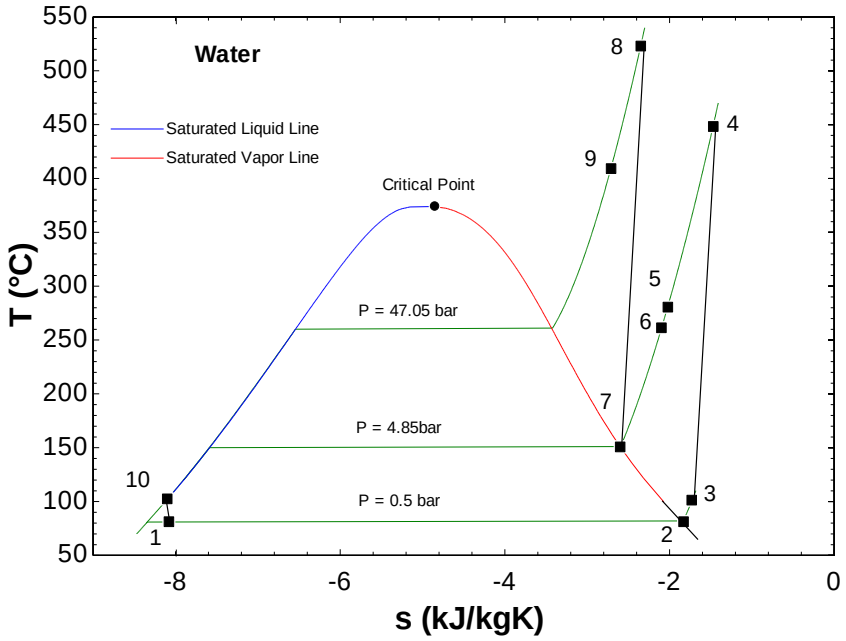

Figure 6.1 The T-s diagram of the bottoming cycle of System 1(working fluid is water)

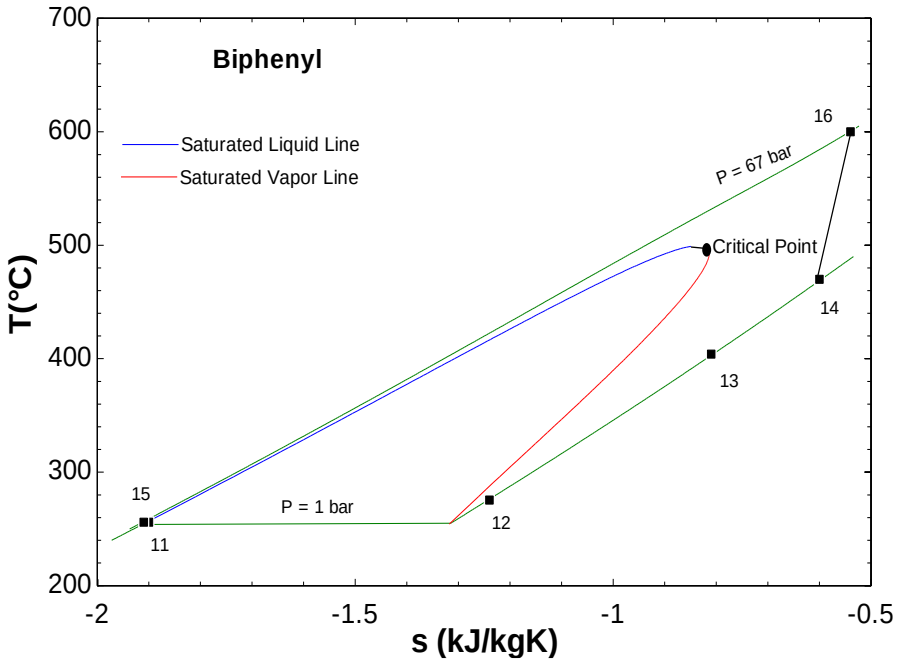

Figure 6.2 The T-s diagram of the topping cycle of System 1 (working fluid is biphenyl)

Table 6.1 Input and calculated thermodynamic data of System 1.

State Point	Mole Flow Rate (kmol/s)	Mass Flow Rate (kg/s)	Temperature (°C)	Pressure (bar)	Specific Enthalpy (kJ/kg)	Specific Entropy (kJ/kgK)	Specific Exergy (kJ/kg)
1	0.0555	1	81.3	0.5	-15538	-8.08	34.41
2	0.0555	1	81.3	0.5	-13326	-1.83	385.92
3	0.0555	1	101.3	0.5	-13286	-1.73	393.15
4	0.0555	1	448.3	4.85	-12597	-1.47	1006.86
5	0.0555	1	280.5	4.85	-12946	-2.02	821.59
6	0.0555	1	261.3	4.85	-12986	-2.1	803.61
7	0.0555	1	150.7	4.85	-13224	-2.6	714.68
8	0.0555	1	523	47.05	-12480	-2.35	1385.68
9	0.0555	1	409.1	47.05	-12747	-2.71	1226.57
10	0.0555	1	102.5	47.05	-15538	-8.1	40.64
11	0.0065	1	256	1.04	1181.2	-1.9	116.35
12	0.0065	1	275.5	1.04	1530.8	-1.24	269.36
13	0.0065	1	404.1	1.04	1798	-0.81	406.38
14	0.0065	1	470	1.04	1947	-0.6	492.81
15	0.0065	1	600	67	2143.6	-0.54	672.51
16	0.0065	1	256	67	1184.9	-1.91	122.45

The rate of exergy destruction for the key components of System 1 corresponding to base case are presented in Figure 6.3. The exergy destruction rate is highest for compressor 1, closely followed by compressor 2. The heat exchanger 2 is also quite high. The exergy destruction data clearly marks that the performance of compressors 1, compressor 2 and heat exchanger 2 is critical for the efficiency of system. Any system performance improvement strategies must involve focus on these components.

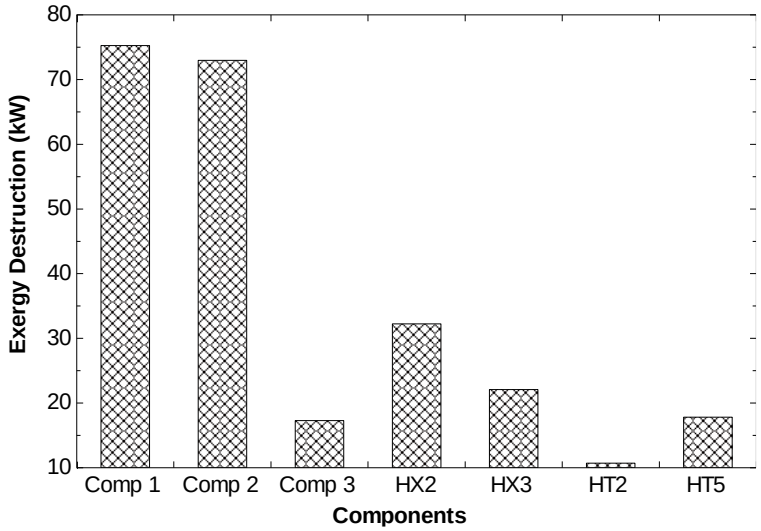

Figure 6.3 Exergy destruction rates of components of System 1.

The effect of the variation of ambient temperature on the rate of exergy destruction of selected units is shown in Figure 6.4. As the ambient temperature is varied from 15 °C to 45 °C, the exergy destruction rate for all the components increases. It is observed that over the range of 30 °C the exergy destruction rate of the selected components increase in the range of 10 to 11%.

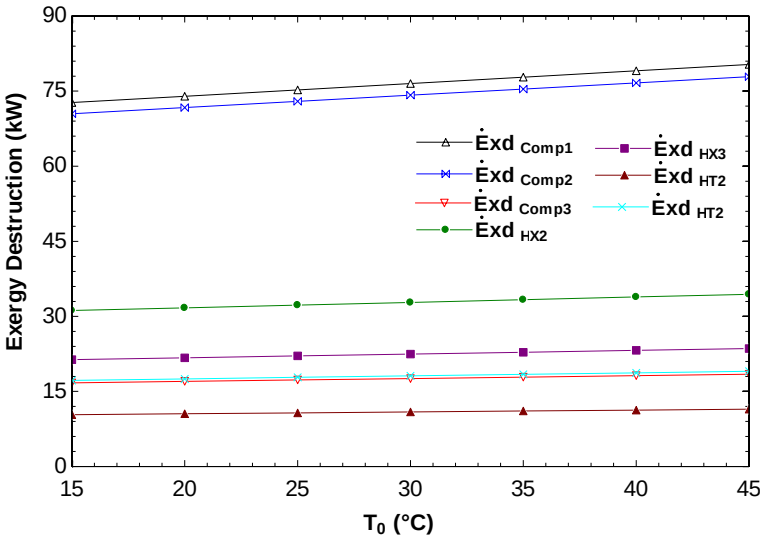

Figure 6.4 Effect of ambient temperature on the rate of exergy destruction of selected components of System 1.

Figure 6.5 shows the influence of source temperature on the energetic and exergetic COP of the system. The source temperature is varied from 80 °C to 120 °C, it is observed that the energetic COP decreases by 5% whereas the exergetic COP increase by 2.8%. The decrease in energetic COP is attributed to the fact that higher source temperature increases the specific volume of fluid at compressor inlet and increases work done by the compressor 1 operating at same pressure ratio.

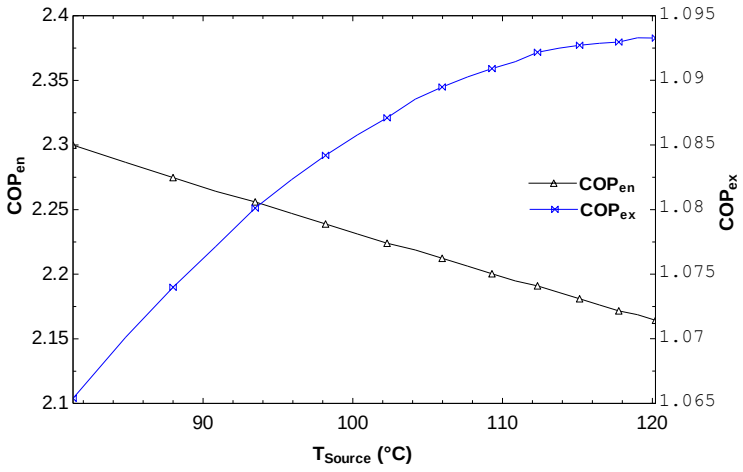

Figure 6.5 Influence of source temperature on the energetic and exergetic COPs.

The increase in exergetic COP is due to the fact the increased inlet exergy counters the increased work required and improves the overall exergetic performance of the system.

The vapor compression cycles utilise the evaporation and condensation processes for heat input and delivery. The operating pressure controls the temperature of these processes. The effect of pressure variation at source is shown in Figure 6.6. The variation is very similar to the effect of source temperature, the energetic COP decreases and exergetic COP increases with increase in evaporation pressure. The cascaded system utilise multiple fluids operating respective vapor compression cycles to achieve required the heat delivery temperature. This system utilise water and biphenyl in bottoming and topping cycle respectively. The system development starts with determination of ideal temperature for the condenser-evaporator, called as intermediate temperature. The suitable temperature is restricted by working fluid properties.

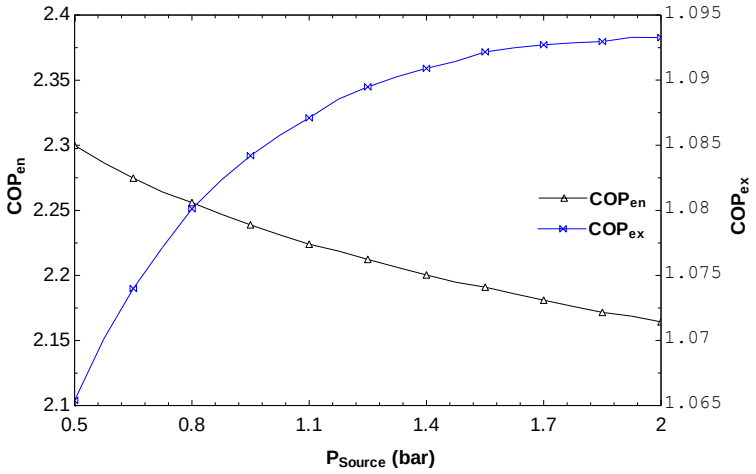

Figure 6.6 Influence of evaporation pressure on energetic and exergetic COPs.

The intermediate temperature for System 1 is determined around 255 °C. Figure 6.7 illustrates the influence of evaporation temperature of biphenyl on the energetic and exergetic COPs of the overall system. This Figure shows that the performance of system improves with increase in intermediate temperature. The temperature cannot be increased invariably as it increases the maximum pressure required for the bottoming cycle which use water. For water the upper most limit is well below its critical temperature 373 °C, unless bottoming cycle is operated under supercritical conditions.

Figure 6.8 indicates the effect of corresponding intermediate pressures on the performance of system. The energetic and exergetic COPs of the overall system increase with increase in operating evaporator pressure.

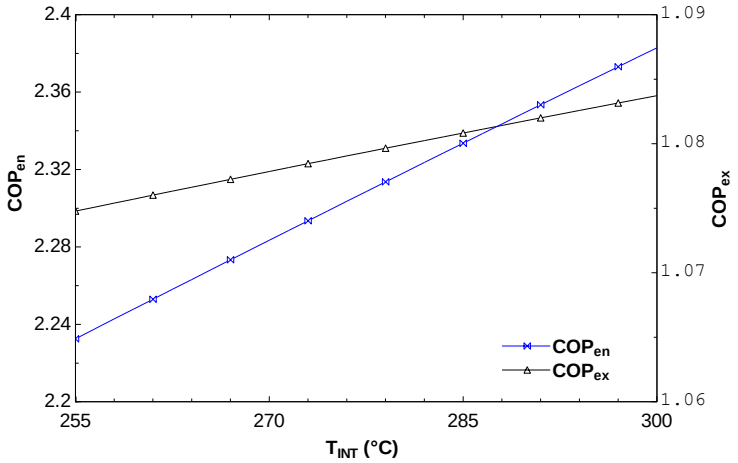

Figure 6.7 Influence of intermediate temperature on energetic and exergetic COPs.

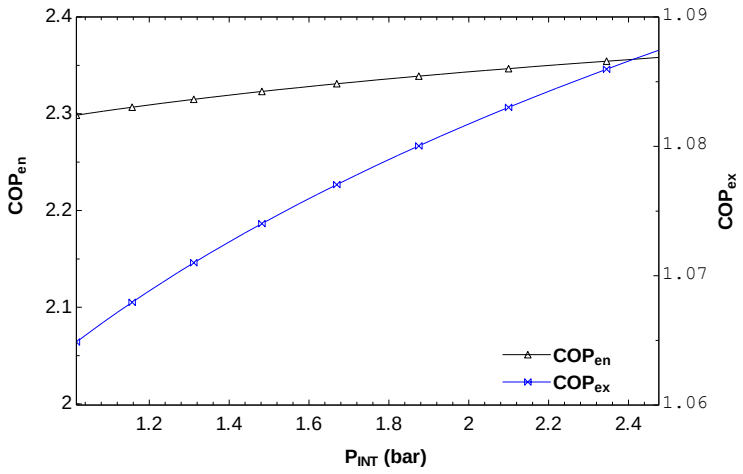

Figure 6.8 Influence of intermediate pressure on energetic and exergetic COPs.

The sink temperature represents the maximum temperature of heat delivery, which is achieved by vapor compression.

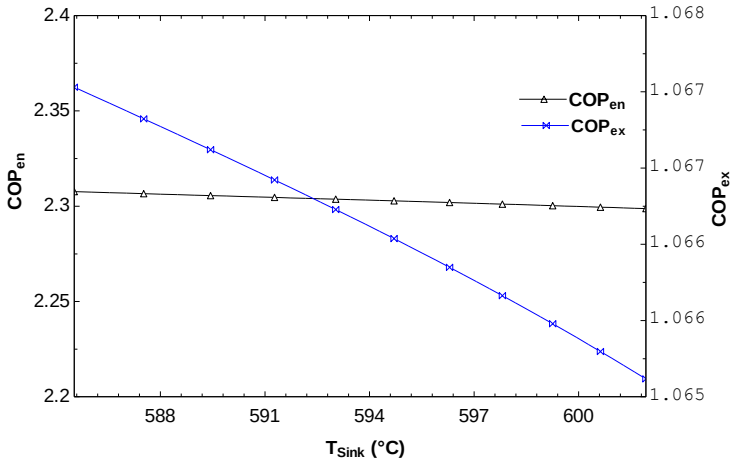

Figure 6.9 Influence of sink temperature on energetic and exergetic COPs.

Figure 6.9 presents the effect of sink temperature on the energetic and exergetic COPs of the overall system. Both COPs decrease with increase in maximum temperature. This attributed to the fact that the high temperature corresponds to high pressure, in other words the increase in sink temperatures increase the required compressor work, which affects the performance of system negatively. The Figure 6.10 presents the effect of sink pressures on the performance, where the energetic and exergetic COPs of the overall system decrease with increase in sink pressures.

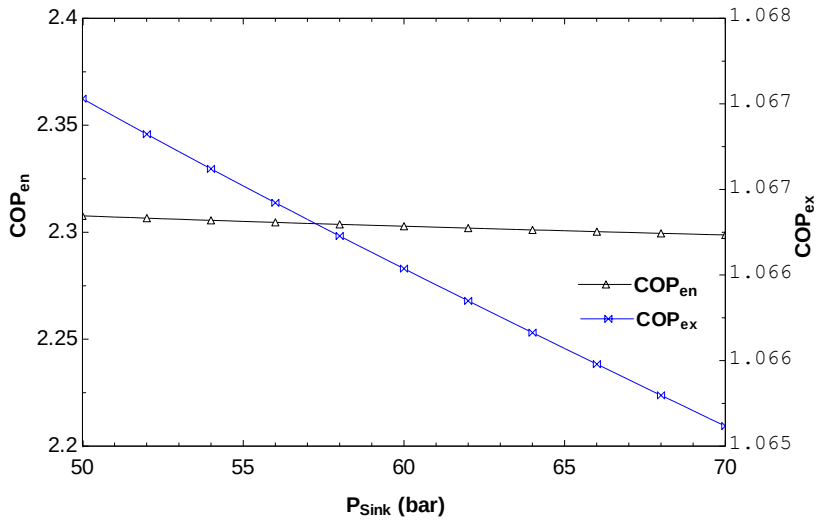

Figure 6.10 Influence of sink pressure on energetic and exergetic COPs.

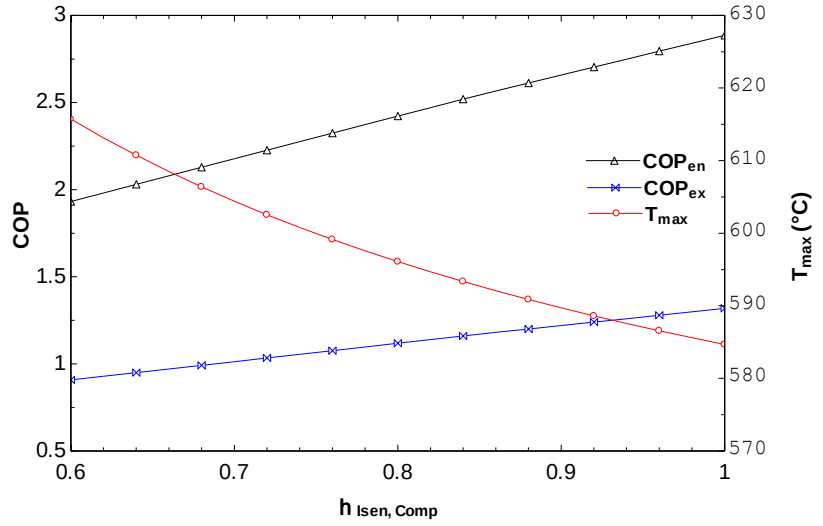

Figure 6.11 Influence of isentropic efficiency on the performance of System 1.

The influence of compressor isentropic efficiency on the performance of the system is shown in Figure 6.11. The isentropic efficiencies of modern machines typically vary from 0.7 to 0.85 (Zamfirescu et al. 2010). The parametric study is performed for a range of 0.6-1, to cover a large spectrum of situations. The isentropic efficiency, of each compressor is varied simultaneously, to assess the effect on the energetic and exergetic COPs of the overall system. The Figure 6.11 shows that with increase in isentropic efficiency energetic COP increase from 1.93 to 2.29 and exergetic COP increase from 0.907 to 1.06. The higher efficiencies reduce the total work input required for the same compression ratio and positively affect the performance of system. The sink temperature also decreases from 615

°C to 584 °C, which indicates the compressor exit temperatures are low for higher isentropic efficiencies. The lower exit temperatures allows lesser energy loss in intercooling and improves the overall performance of the system.

Figure 6.12 shows the influence of ambient temperature on the overall energetic and exergetic COP of system. The energetic COP remains constant over the range of 15-45 °C, whereas the exergetic COP decrease by 11.23%.

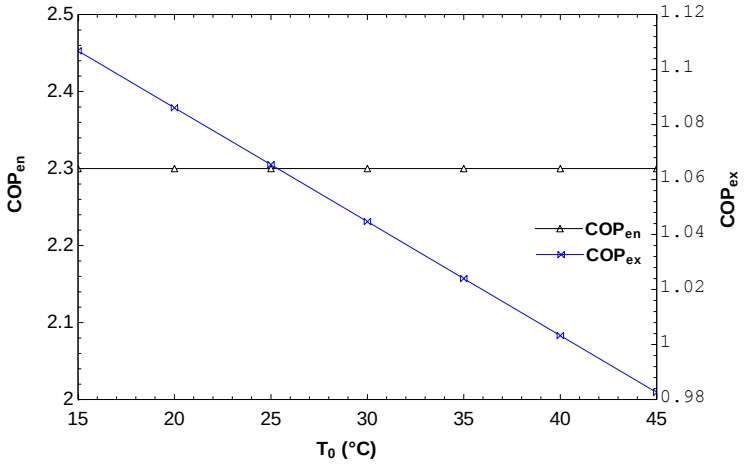

Figure 6.12 Influence of ambient temperature on the energetic and exergetic COPs of System 1.

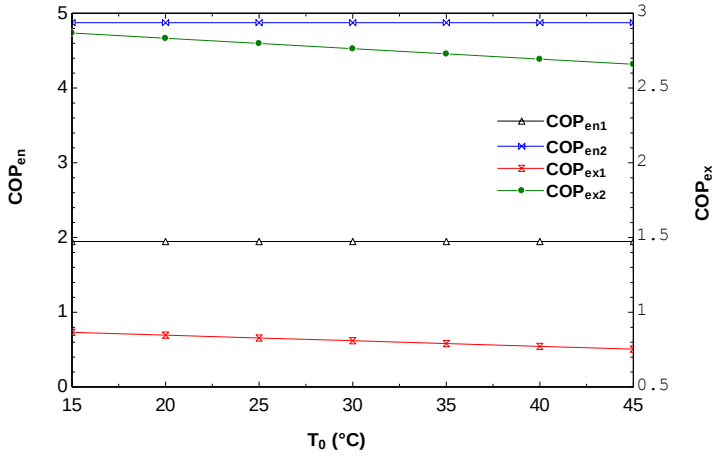

Figure 6.13 Influence of ambient temperature on the energetic and exergetic COPs of the topping and bottoming cycles of System 1.

Figure 6.13 shows the effect of ambient temperature on the energetic and exergetic COPs of topping and bottoming cycles of System1. The energetic COP remains unchanged over the range of 15-45 °C, whereas the exergetic COP of bottoming cycle and topping cycle

reduced by 13.01% and 7.29 % respectively. This analysis of energetic and exergetic COPs clearly indicates that, the exergetic performance analysis gives better information, about the influence on system performance when external conditions vary.

6.2 System 2 Results

6.2.1 Energy and Exergy Analysis results of System 2

The analysis of System 2 is presented in this section. The table 6.2 tabulates the inputs and calculated thermodynamic data of the streams in System 2 for base case. The System 2 is a cascaded system, which utilises cyclohexane in bottoming cycle and biphenyl in the topping cycle. The heat delivered by source at 81.3 °C and at a corresponding pressure of 1.0014 bar. The system sink delivers heat at an elevated temperature of 600C and condenser pressure is 67 bar. The energetic and exergetic COPs of the overall system values 3.76 and 1.85 respectively. The net work input for System 2 is 382 kW. The intermediate temperature and pressure of topping cycle fluid is 256 °C and 1.04 bar.

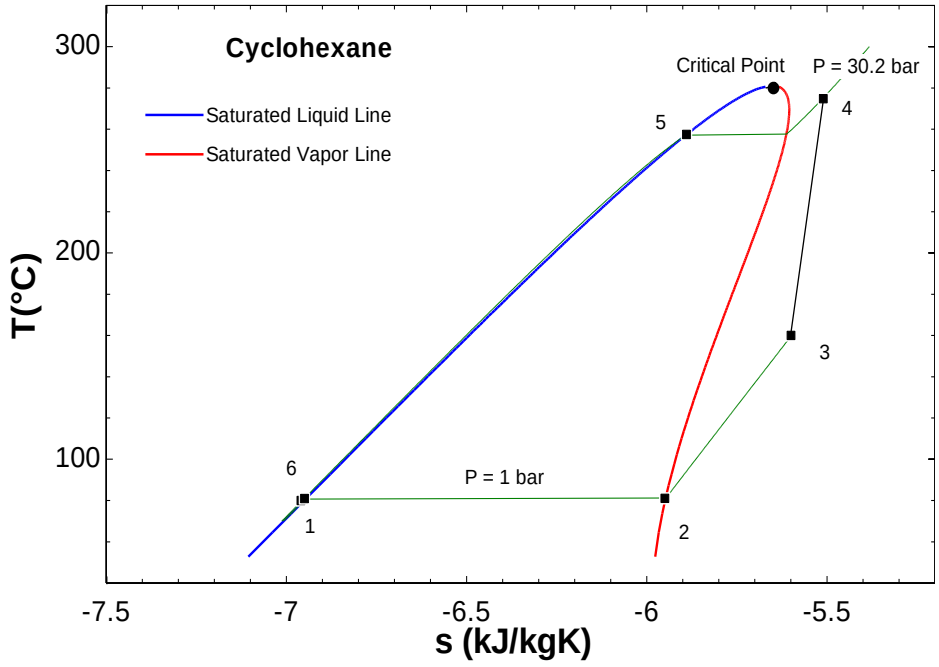

Figure 6.14 The T-s diagram of the bottoming cycle of System 2(working fluid is Cyclohexane)

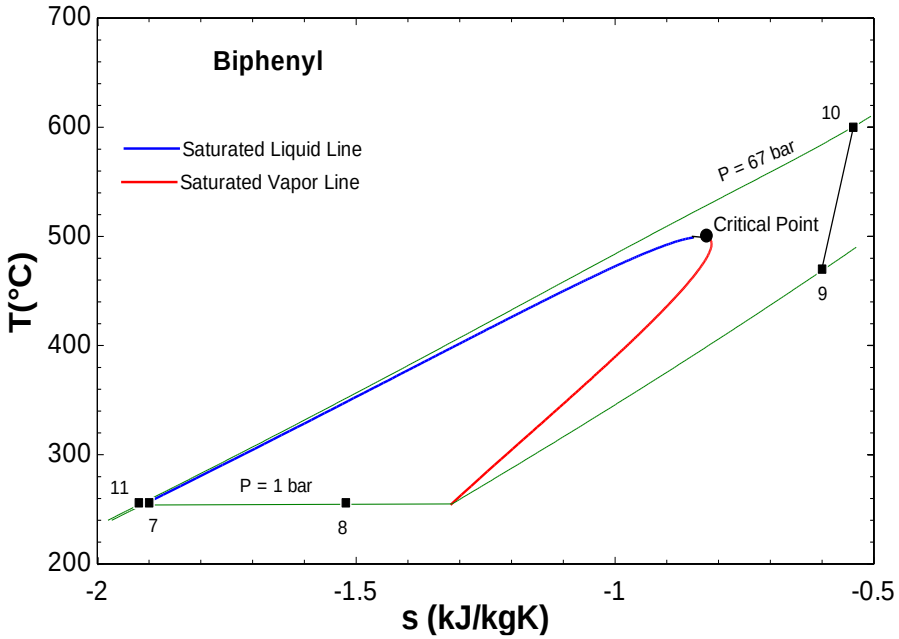

Figure 6.15 The T-s diagram of the bottoming cycle of System 2 (working fluid is Biphenyl)

Table 6.2 Input and calculated thermodynamic data of System 2

State Point	Mass Flow Rate (kg/s)	Mole Flow Rate (kmol/s)	Temperature (°C)	Pressure (bar)	Specific Enthalpy (kJ/kg)	Specific Entropy (kJ/kgK)	Specific Exergy (kJ/kg)
1	1	0.01188	81.01	1	-1389.2	-5.95	64.8
2	1	0.01188	160	1	-1251.6	-5.6	98.22
3	1	0.01188	274.72	30.2	-1066.5	-5.51	257.73
4	1	0.01188	257.44	30.2	-1267.1	-5.89	169.37
5	1	0.01188	80	30.2	-1742.5	-6.96	12.18
6	1	0.01188	81	1	-1742.5	-6.95	8.93
7	1	0.00648	256	1	1181.23	-1.9	116.35
8	1	0.00648	256	1	1381.83	-1.52	203.93
9	1	0.00648	470	1	1946.98	-0.6	492.81
10	1	0.00648	599.95	67	2143.62	-0.54	672.51
11	1	0.00648	256	67	1181.26	-1.92	120.86

The rate of exergy destruction for the key components of System 2 corresponding to base case are presented in Figure 6.16. The exergy destruction rate is highest for compressor 1, closely followed by compressor 2. The exergy destruction rate for heater 5 is also quite

high. The exergy destruction data clearly marks that the performance of compressors 1, compressor 2 and heater 5 is critical for the efficiency of system. Any system performance improvement strategies must involve focus on these components.

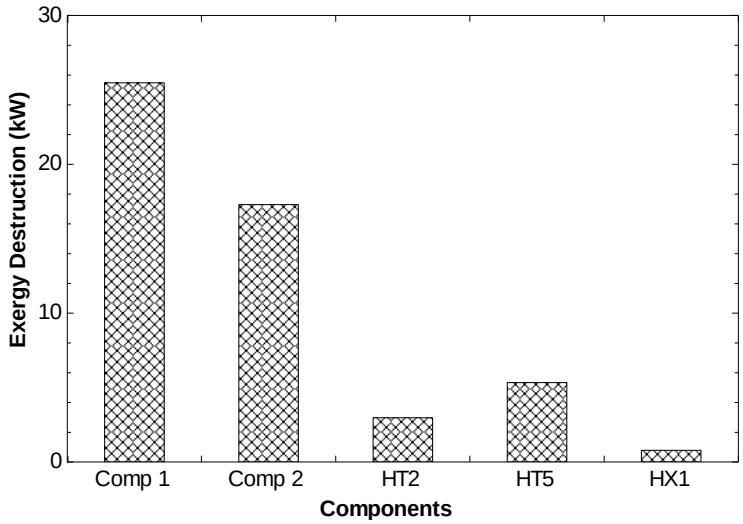

Figure 6.16 Exergy destruction rates of components of System 2.

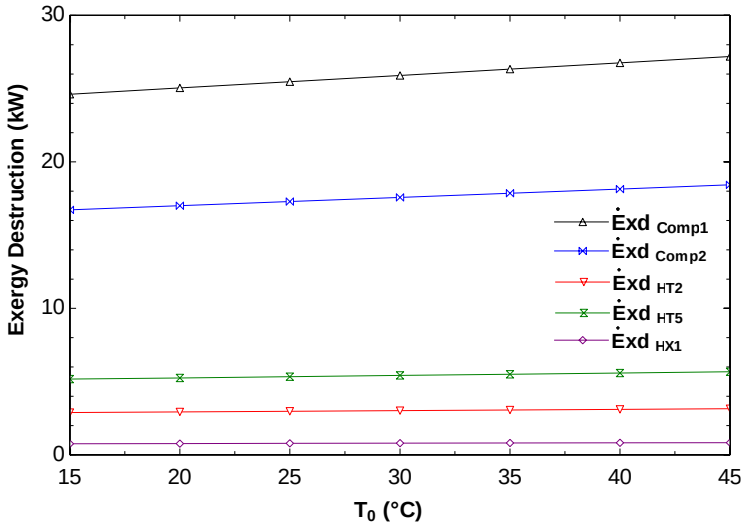

Figure 6.17 Effect of ambient temperature on the rate of exergy destruction of selected components of System 2.

The effect of the variation of ambient temperature on the rate of exergy destruction of selected units is shown in Figure 6.17.

As the ambient temperature is varied from 15 °C to 45 °C (288K-318K), the exergy destruction rate for all the components increases. It is observed that over the range of 30

°C the exergy destruction rate of the selected components increases by 9.07% to 10.43%. Exergy destruction rate increase is highest for Compressor 1 and Heat exchanger 1 and lowest for heater 2.

Figure 6.18 shows the influence of source temperature on the energetic and exergetic COP of the system. The source temperature is varied from 59 °C to 85 °C, and it is observed that both energetic COP and exergetic COP increases by 15.9% and 15.85% respectively. The change energetic COP of overall system 2 is opposed to change observed in System1. The cyclohexane is a retrograde fluid and behaviour depicted is different as compared to water.

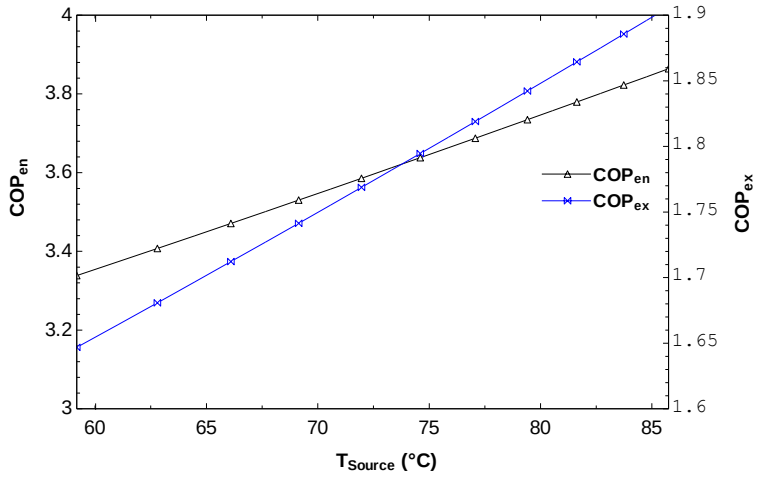

Figure 6.18 Influence of source temperature on the energetic and exergetic COPs.

The effect of pressure variation at source is shown in Figure 6.19. The variation is very similar the effect of source temperature, both energetic COP and exergetic COP increases with increase in evaporation pressure. The System 2 working fluids are cyclohexane and biphenyl. The efficient functioning of cascaded system requires the determination of ideal temperature for the condenser-evaporator, called as intermediate temperature.

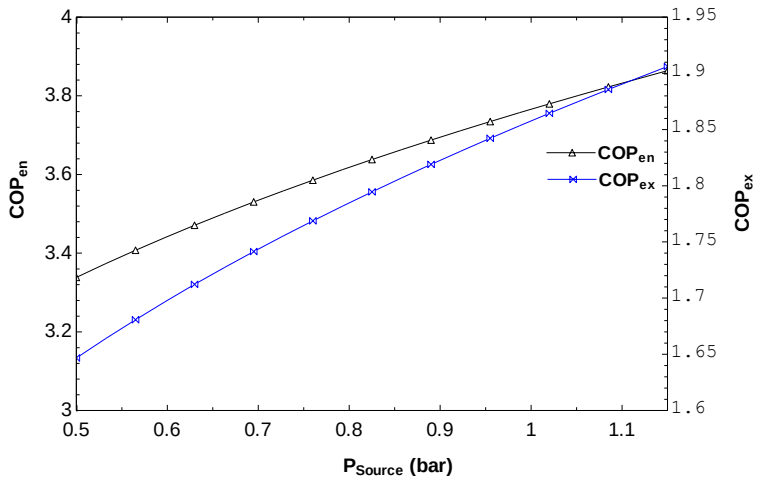

Figure 6.19 Influence of evaporation pressure on energetic and exergetic COPs.

For System 2 the intermediate temperature cannot be increased beyond 260 °C, as the critical temperature of cyclohexane is 280.65 °C (Lide 2006). The suitable intermediate temperature is determined around 245 °C. Figure 6.16 illustrates the influence of evaporation temperature of biphenyl on the energetic and exergetic COPs of the overall system. The intermediate temperature is varied from 224 °C to 256 °C, it is found that the energetic and exergetic COPs of the overall system increase from 3.47 to 3.76 and 1.73 to 1.85 respectively.

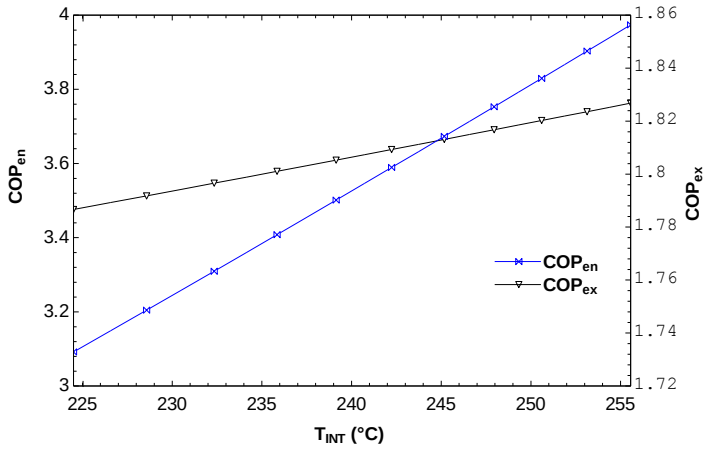

Figure 6.20 Influence of intermediate temperature on energetic and exergetic COPs.

Figure 6.20 indicates the effect of corresponding intermediate pressures on the performance of system. The intermediate pressure varied from 0.5 bar to 1.03 bar, and it is observed that the energetic and exergetic COPs of the overall system increase with increase in operating evaporator pressure.

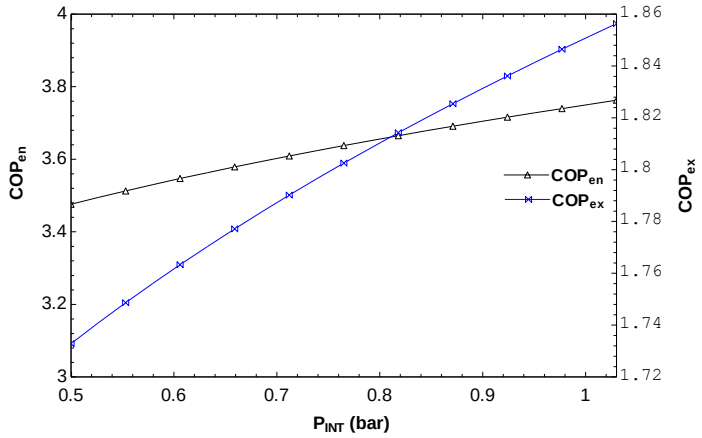

Figure 6.21 Influence of intermediate pressure on energetic and exergetic COPs.

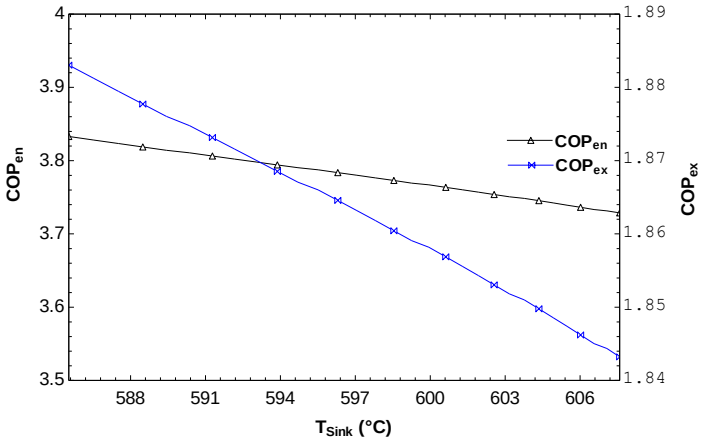

Figure 6.22 Influence of sink temperature on energetic and exergetic COPs.

The influence of sink temperature on system performance is shown in Figure 6.22. Both COPs decrease with increase in maximum temperature. The temperature variation included in the parametric study in the range of 585-607 °C, it is observed that the energetic and exergetic COPs of the overall system decreases by 2.87% and 2.13% respectively. This is attributed to the fact that the high temperature corresponds to high pressure, in other words the increase in sink temperatures increase the required compressor work, which affects the performance of system negatively.

The limiting maximum temperature for the present system is 600 °C. This value based on recommendations of past studies (Angelino and Invernizzi, 1993, Basco et al. 2003, Yildiz and Kazimi, 2006) which states that complex organic fluids are safe to use up to 100 °C more than their critical points. The critical temperature of biphenyl is 499.85 °C.

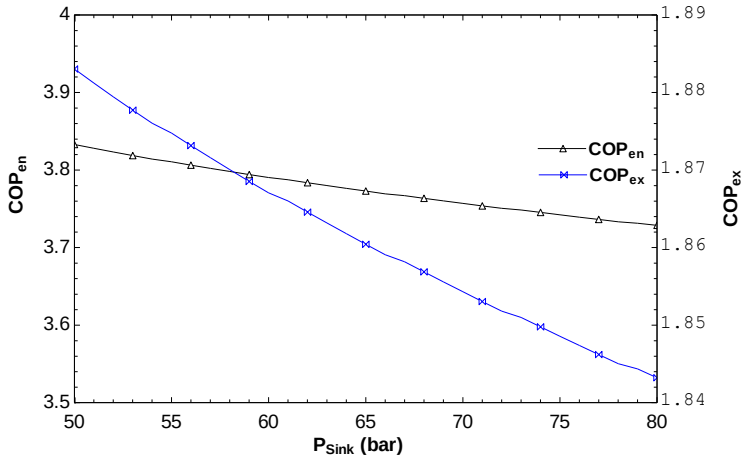

Figure 6.23 Influence of sink pressure on energetic and exergetic COPs.

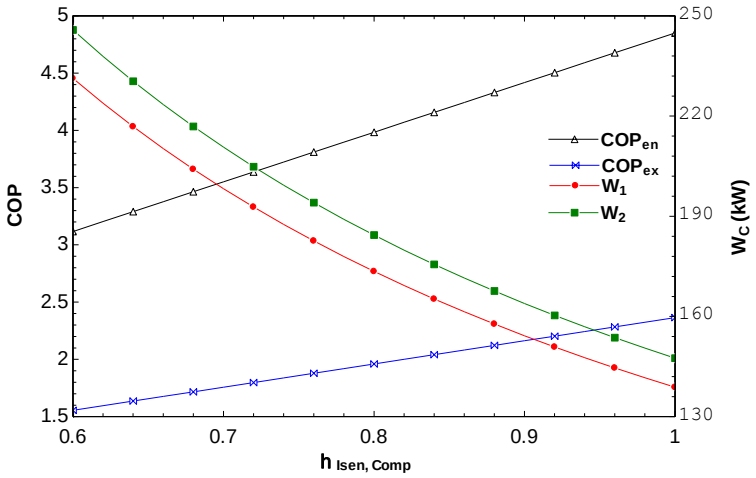

Figure 6.24 Influence of isentropic efficiency on the performance of System 2.

The Figure 6.23 presents the effect of sink pressures on the performance, where the energetic and exergetic COPs of the overall system decrease with increase in sink pressures. The range of pressure variation analyzed for the present study is 50-80 bar, which allows the liquid compression to achieve minimum required delivery temperature of 550 °C.

The influence of compressor isentropic efficiency on the performance of the system is shown in Figure 6.24. The parametric study is performed for a range of 0.6-1, it is varied simultaneously for each compressor, to assess the effect on the energetic and exergetic COPs of the overall system. The Figure 6.24 shows that with increase in isentropic

efficiency energetic COP increases from 3.11 to 4.85 and exergetic COP increases from 1.55 to 2.36. The higher efficiencies reduce the total work input required for the same compression ratio and positively affect the performance of system. The work required by each compressor is also plotted, in Figure 6.24, for the same range of isentropic efficiency. It is observed that the work required for both compressors drops by 40%.

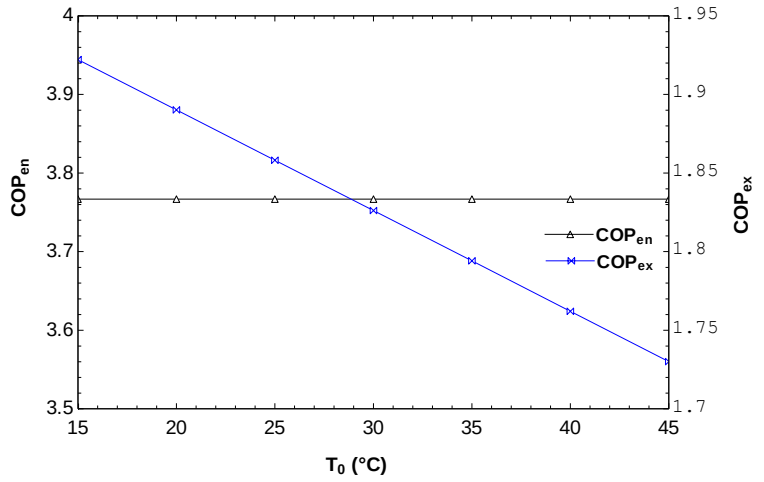

Figure 6. 25 Influence of ambient temperature on the energetic and exergetic COP of System 2.

Figure 6.25 shows the influence of ambient temperature on the overall energetic and exergetic COP of system.

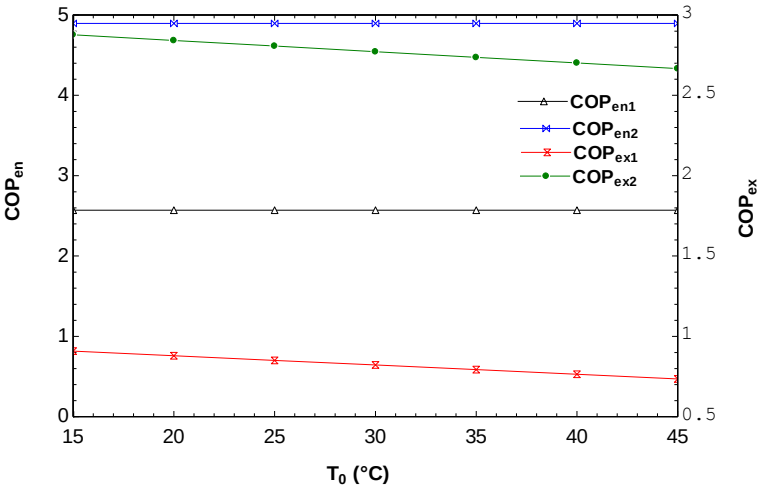

Figure 6.26 Influence of ambient temperature on the energetic and exergetic COPs of the topping and bottoming cycles of System 2.

The energetic COP does not vary with change in ambient temperature, whereas the exergetic COP of the system decrease by 10% when ambient temperature is changed from 15 °C to 45 °C. The variation of energetic and exergetic COPs of the topping and bottoming cycles with ambient temperature is shown in Figure 6.26. The energetic COP remains unchanged over the range of 15-45 °C, whereas the exergetic COP of bottoming cycle and topping cycle reduced by 19.05% and 7.3 % respectively. This analysis of energetic and exergetic COPs clearly indicates that, the exergetic performance analysis gives better information, about the influence on system performance when external conditions vary.

The bottoming cycle heat is delivered at relatively lower temperature as compared to topping cycle, due to which the exergetic performance of bottoming cycle is affected more than topping cycle.

6.3 System 3 Results

6.3.1 Energy and Exergy Analysis results of System 3

The analysis of System 3 is presented in this section. The table 6.3 tabulates the inputs and calculated thermodynamic data of the streams in System 3 for base case.

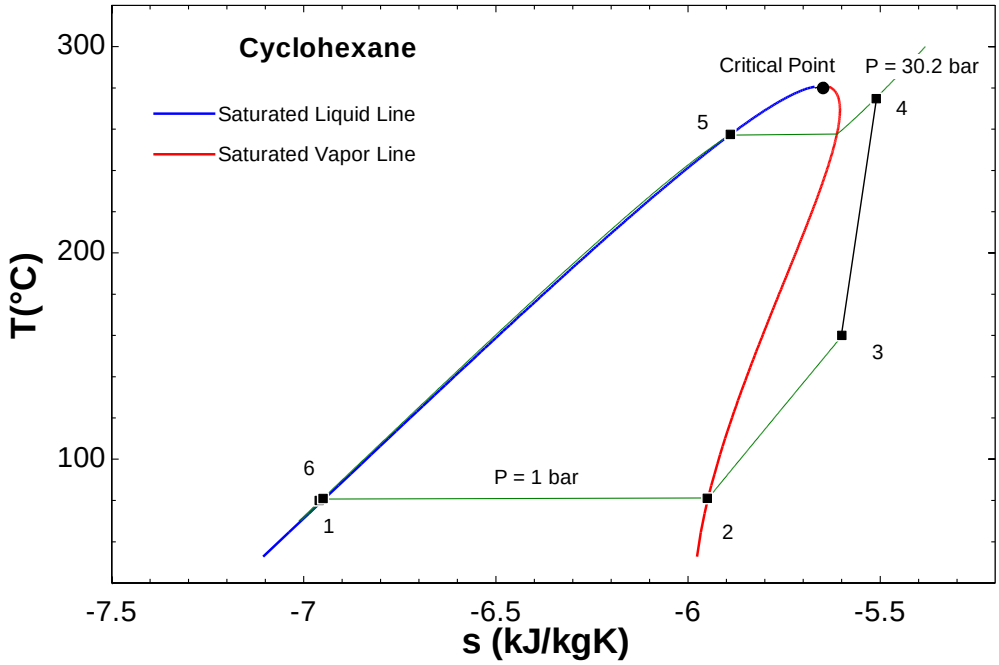

Figure 6.27 The T-s diagram of the bottoming cycle of System 3 (working fluid is Cyclohexane)

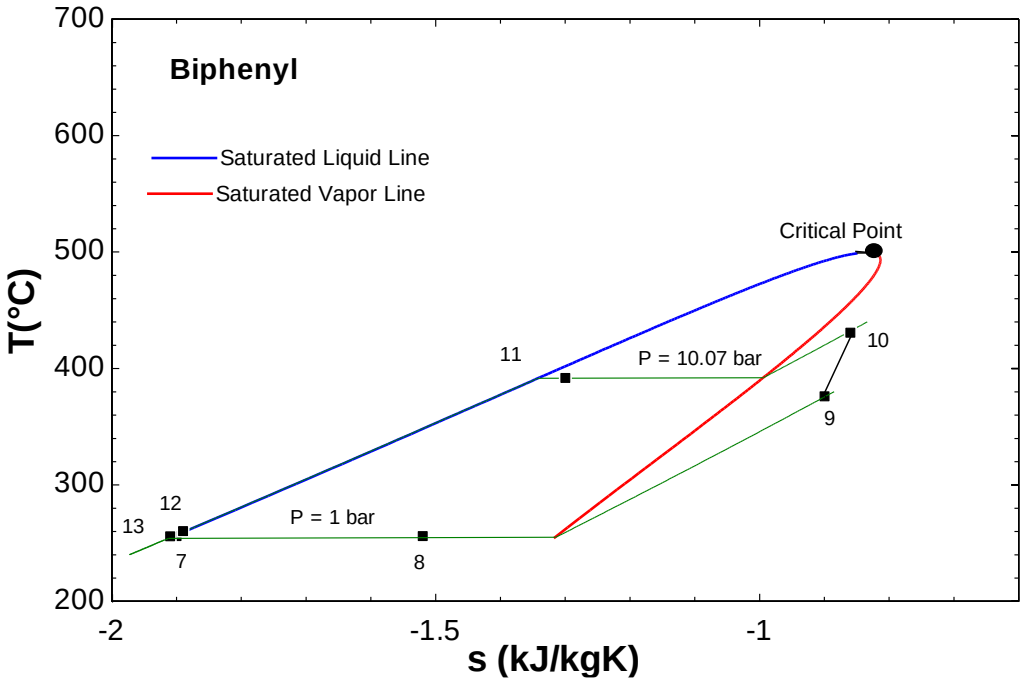

Figure 6.28 The T-s diagram of the intermediate cycle of System 3 (working fluid is Biphenyl)

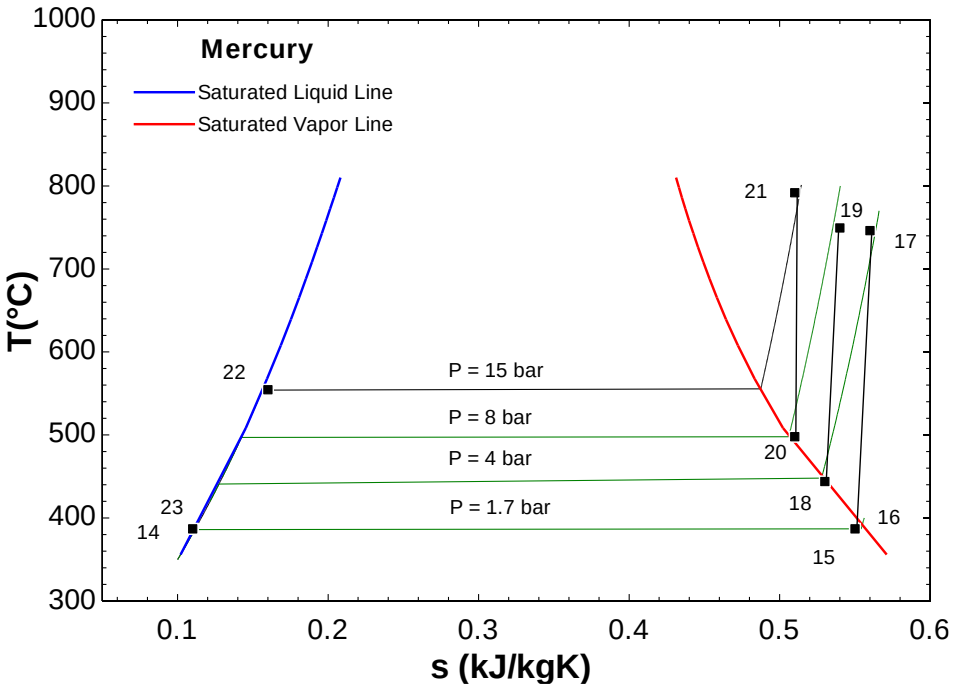

Figure 6.29 The T-s diagram of the topping cycle of System 3 (working fluid is Mercury)

The System 3 is a cascaded system, which utilises cyclohexane in bottoming cycle and biphenyl in the intermediate and mercury in the topping cycle.

Table 6.3 Input and calculated thermodynamic data of System 3.

State Point	Mole Flow Rate (kmol/s)	Mass Flow Rate (kg/s)	Temperature (°C)	Pressure (bar)	Specific Enthalpy (kJ/kg)	Specific Entropy (kJ/kgK)	Specific Exergy (kJ/kg)
1	0.0119	1	81.01	1	-1389.2	-5.95	64.8
2	0.0119	1	160	1	-1251.6	-5.6	98.22
3	0.0119	1	274.72	30.2	-1066.5	-5.51	257.73
4	0.0119	1	257.44	30.2	-1267.1	-5.89	169.37
5	0.0119	1	80	30.2	-1742.5	-6.96	12.18
6	0.0119	1	81	1	-1742.5	-6.95	8.93
7	0.0065	1	256	1.04	1181.23	-1.9	116.35
8	0.0065	1	256	1.04	1381.83	-1.52	203.93
9	0.0065	1	376	1.04	1736.63	-0.9	372.61
10	0.0065	1	430.75	10.07	1837.85	-0.86	463.03
11	0.0065	1	391.93	10.07	1546.22	-1.3	301.01
12	0.0065	1	260.33	10.07	1191.43	-1.89	121.45
13	0.0065	1	255.79	10.07	1181.23	-1.91	116.98
14	0.005	1	386.93	1.7	51.17	0.11	18.28
15	0.005	1	386.93	1.7	342.8	0.55	178.18
16	0.005	1	386.93	1.7	343.19	0.55	178.4
17	0.005	1	746.13	4	380.41	0.56	212.77
18	0.005	1	443.84	4	349.09	0.53	192.31
19	0.005	1	749.28	8	380.74	0.54	221.56
20	0.005	1	497.81	8	354.68	0.51	204.23
21	0.005	1	791.68	15	385.13	0.51	232.47
22	0.005	1	554.38	15	86.72	0.16	40.5
23	0.005	1	387	15	51.19	0.11	18.29

The heat delivered by source at 81.3 °C and at a corresponding pressure of 1.0014 bar. The system sink delivers heat at an elevated temperature of 792°C and condenser pressure is 15 bar. The energetic and exergetic COPs of the overall system values 2.125 and 0.9901

respectively. The net work input for System 3 is 385 kW. The intermediate temperature and pressure of topping cycle fluid is 387°C and 1.7 bar for mercury-biphenyl interaction.

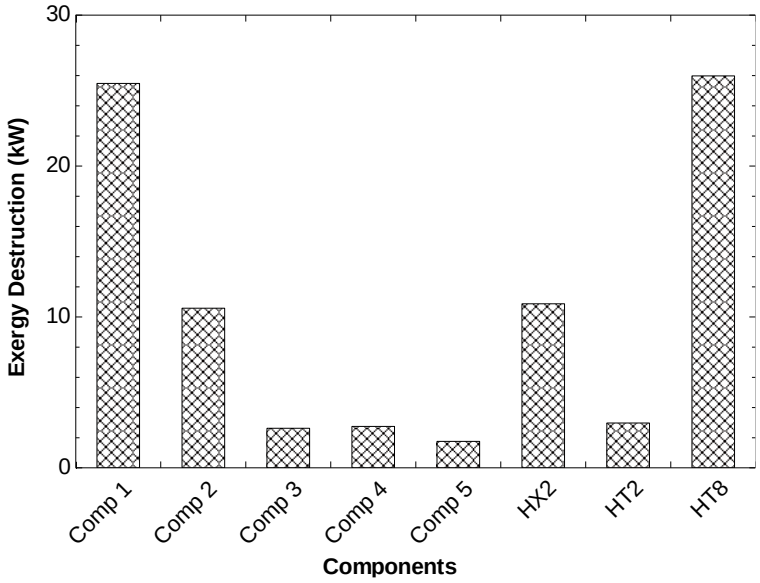

Figure 6.30 Exergy destruction rates of components of System 3.

The operating temperature and pressures of the evaporator for cyclohexane-biphenyl interaction is 256°C and 1.04 bar. The Figure 6.30 shows the rate exergy destruction of the selected components. It is observed that the exergy destruction rate is highest for heater 8 followed by compressor 1.

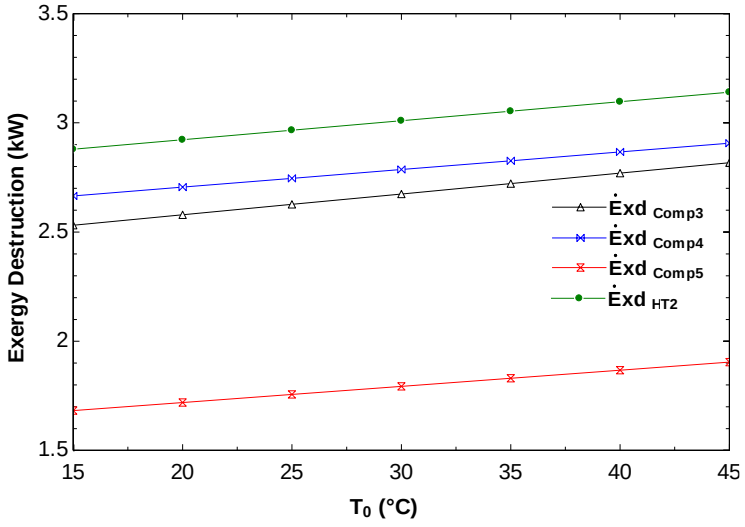

Figure 6.31 Effect of ambient temperature on the rate of exergy destruction of selected components of System 3.

The exergy destruction rate of compressor 2 and heat exchanger 2 are also significant. The system performance is highly dependent upon these key units and parametric studies shown in Figure 6.31 and 6.32 shows the effect of ambient temperature on the exergy destruction of these components.

As the ambient temperature is varied from 15 °C to 45 °C, the exergy destruction rate for all the components increases. It is observed that over the range of 30 °C the exergy destruction rate of these components increases in the range of 9.07% to 13.21%. The change in exergy destruction is highest for compressor 5 and lowest for heater 2.

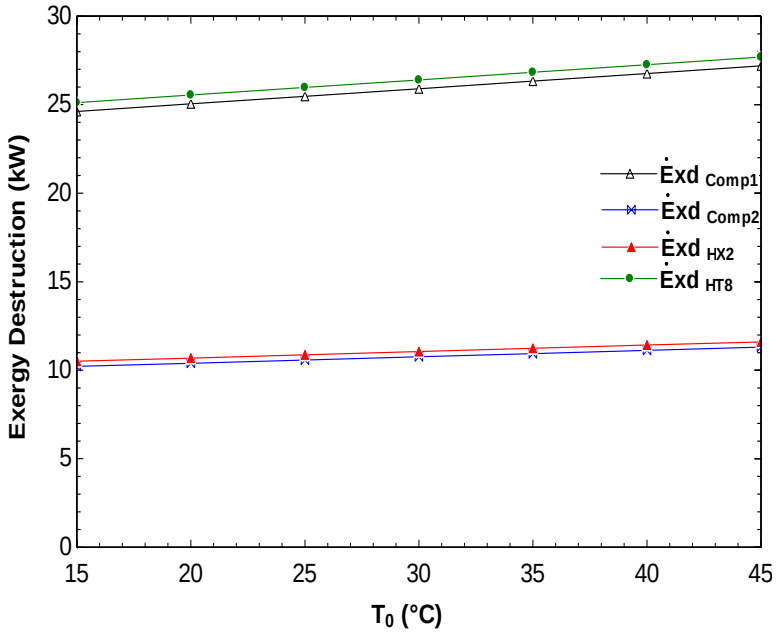

Figure 6.32 Effect of ambient temperature on the rate of exergy destruction of selected components of system.

Figure 6.33 shows the influence of source temperature on the energetic and exergetic COP of the system. The analysis is performed for the variation of source temperature from 59 °C to 81 °C, it is observed that the energetic COP increases by 7.05 % whereas the exergetic COP decreases merely by 0.2%. The decrease in energetic COP of overall system is attributed to the fact that higher source temperature increases the specific volume of fluid at compressor inlet and increases work done by the compressor 1 operating at same pressure ratio.

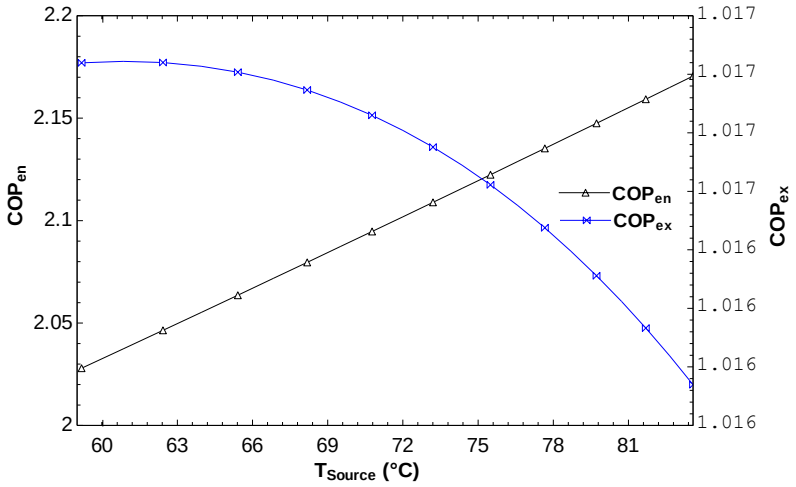

Figure 6.33 Influence of source temperature on the energetic and exergetic COPs.

The increase in exergetic COP of overall is due to the fact the increased inlet exergy counters the work-increased work required and improves the overall exergetic performance of the system, though for the System 3 this improvement is not very significant. The effect of evaporator pressure variation at point of heat intake is shown in Figure 6.34. The variation is very similar the effect of source temperature, the energetic COP decreases and exergetic COP decreases with increase in evaporation pressure.

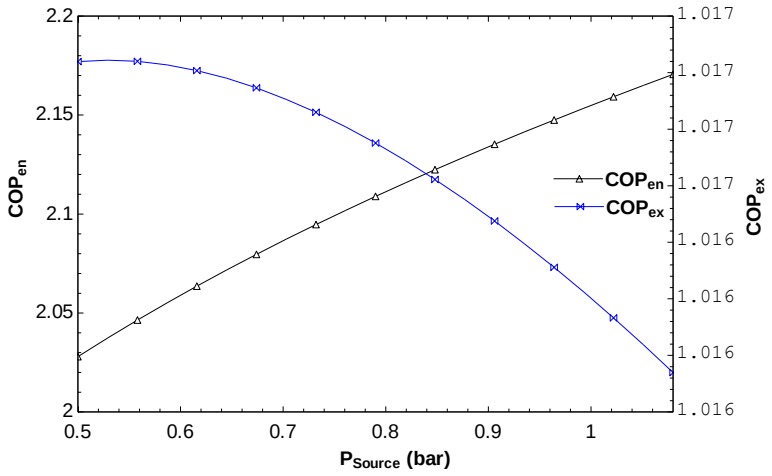

Figure 6.34 Influence of evaporation pressure on energetic and exergetic COPs.

System 3 utilise three working fluids operating in closed vapor compression cycles to achieve the required temperature elevation. This system has two intermediate stages, in lower stage cyclohexane-biphenyl heat interaction takes place, in the higher stage the interaction occurs between biphenyl and mercury. The intermediate temperature for both stages is determined. This temperature is based on the working fluid properties, the

intermediate temperature for lower stage is determined around 255 °C and for higher stage is determined around 387 °C.

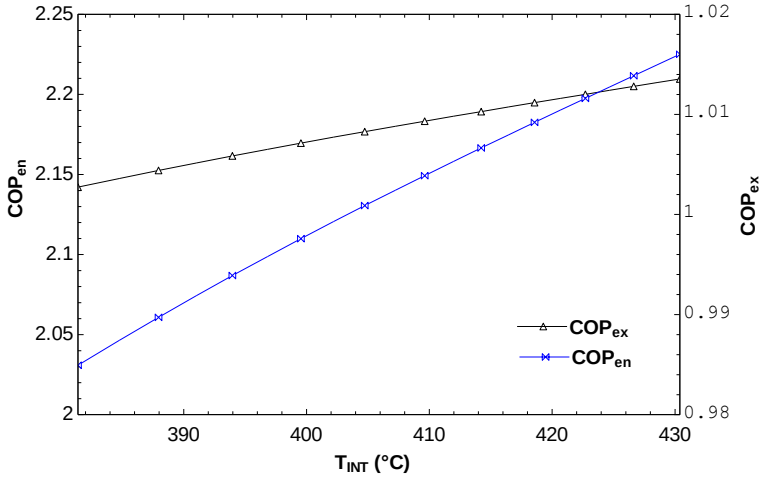

Figure 6.35 Influence of intermediate temperature on energetic and exergetic COPs.

Figure 6.35 illustrates the influence of evaporation temperature of mercury (higher stage intermediate temperature) on the energetic and exergetic COPs of the overall system. The energetic and exergetic COPs of the overall system increases by 2.5% and 2.62% over the range of 381.38-430.39 °C.

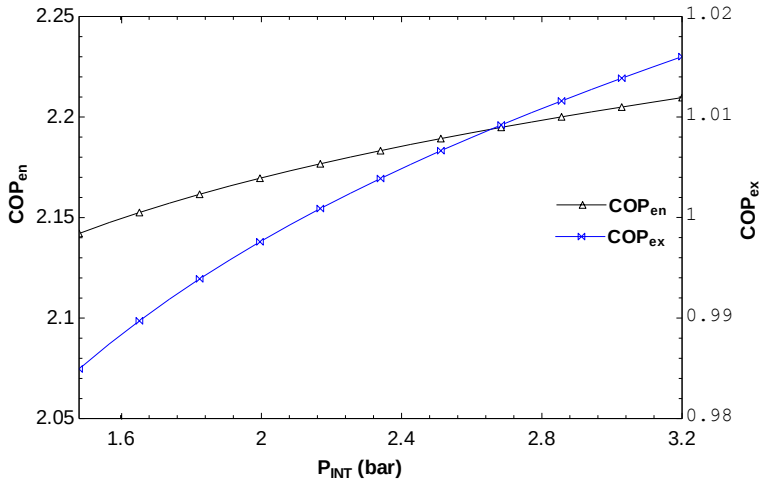

Figure 6.36 Influence of intermediate pressure on energetic and exergetic COPs.

Figure 6.36 indicates the effect of corresponding intermediate pressures on the performance of system. The energetic and exergetic COPs of the overall system increases with increase in operating evaporator pressure of higher intermediate.

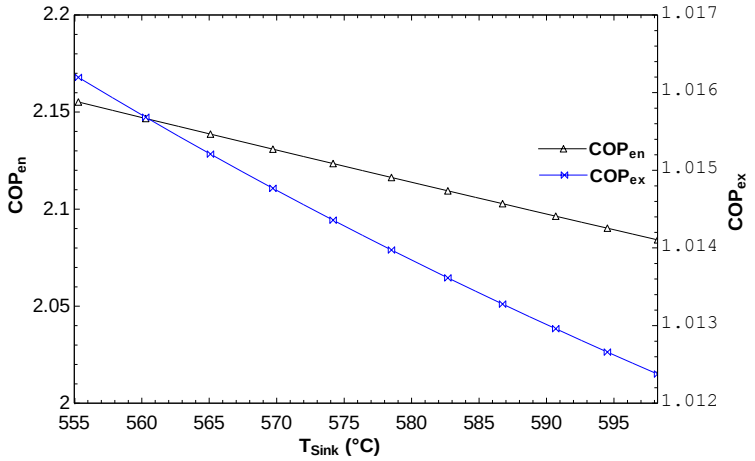

Figure 6.37 Influence of sink temperature on energetic and exergetic COPs.

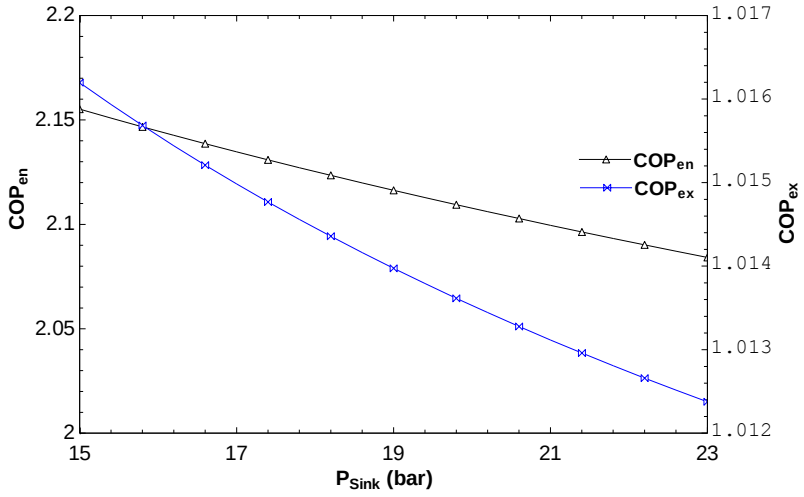

Figure 6. 38 Influence of sink pressure on energetic and exergetic COPs.

The sink temperature and pressure effects on the performance of System 3 are shown in Figure 6.37 and Figure 6.38. The sink temperature corresponds to the saturation temperature corresponds to the maximum cycle pressure obtained at the exit of compressor 5.The energetic COP and exergetic COP decreases by 3.29% and 0.4%. The higher sink temperature at the exit of compressor corresponds to higher pressure, thus needs more work input and reduce the COP. It is observed that effect is not significant for exergetic COP, it is attributed to higher temperature increase both work required and exergy of fluid delivered. The influence of compressor isentropic efficiency on the performance of the system is shown in Figure 6.39.

The increase in isentropic efficiency positively affects the performance of system. The energetic COP and exergetic COP increases from 2.04 to 2.28 and 0.96 to 1.07 for a range of 0.6-1. The performance is improved because the higher efficiencies reduce the work required for the same compression ratio.

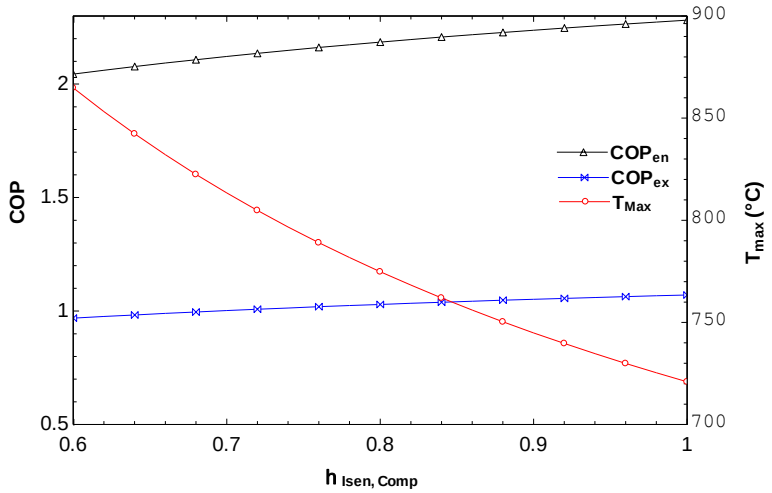

Figure 6.39 Influence of isentropic efficiency on the performance of System 3

The Figure 6.39 also shows the sink temperature variation with isentropic efficiency for the same range, it is observed that sink temperature decreases from 864 °C to 720 °C. The better isentropic efficiencies also improves the performance by reducing the intercooling energy loses.

The effect of ambient temperature on the overall energetic and exergetic COPs is shown in Figure 6.40. It is observed that the energetic COP does not change with ambient temperature, however the exergetic COP is reduced by 11.1 % over a range of 15-45 °C.

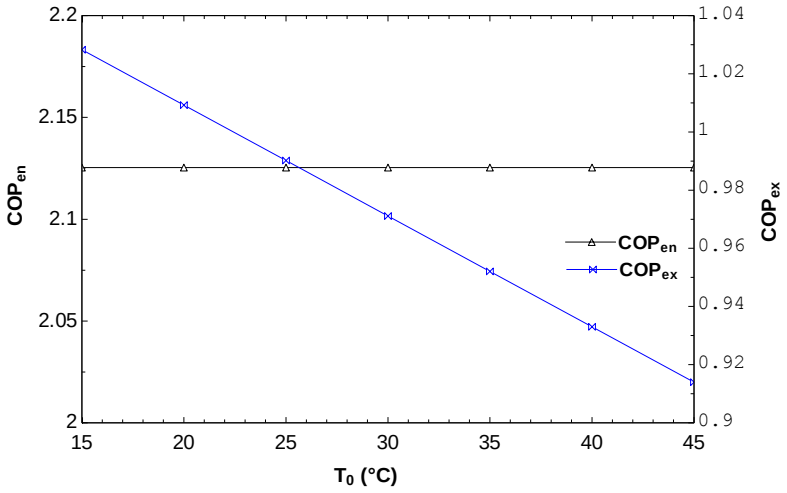

Figure 6.40 Influence of ambient temperature on the energetic and exergetic COPs of System 3.

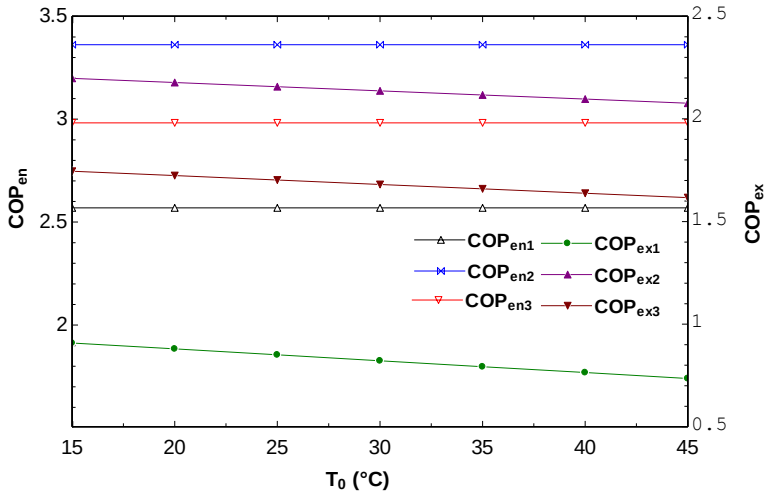

Figure 6.41 Influence of ambient temperature on the energetic and exergetic COPs of the topping and bottoming cycles of System 3.

The effect of ambient temperature on the performance of individual cycles of System 3 is shown in Figure 6.41. The energetic COPs remain unchanged while the exergetic COPs of bottoming, intermediate and topping cycle decreases by 19.05%, 7.38 and 5.52%. The difference in variation of energetic COP and exergetic COP is due to the fact that, the quantity of heat delivered by system does not change with ambient temperature while its work potential is reduced by increase in ambient temperature. The significant difference in the variation of COPs of individual cycles is due to difference in the temperature of heat delivery, for higher delivery temperature the effect is lesser.

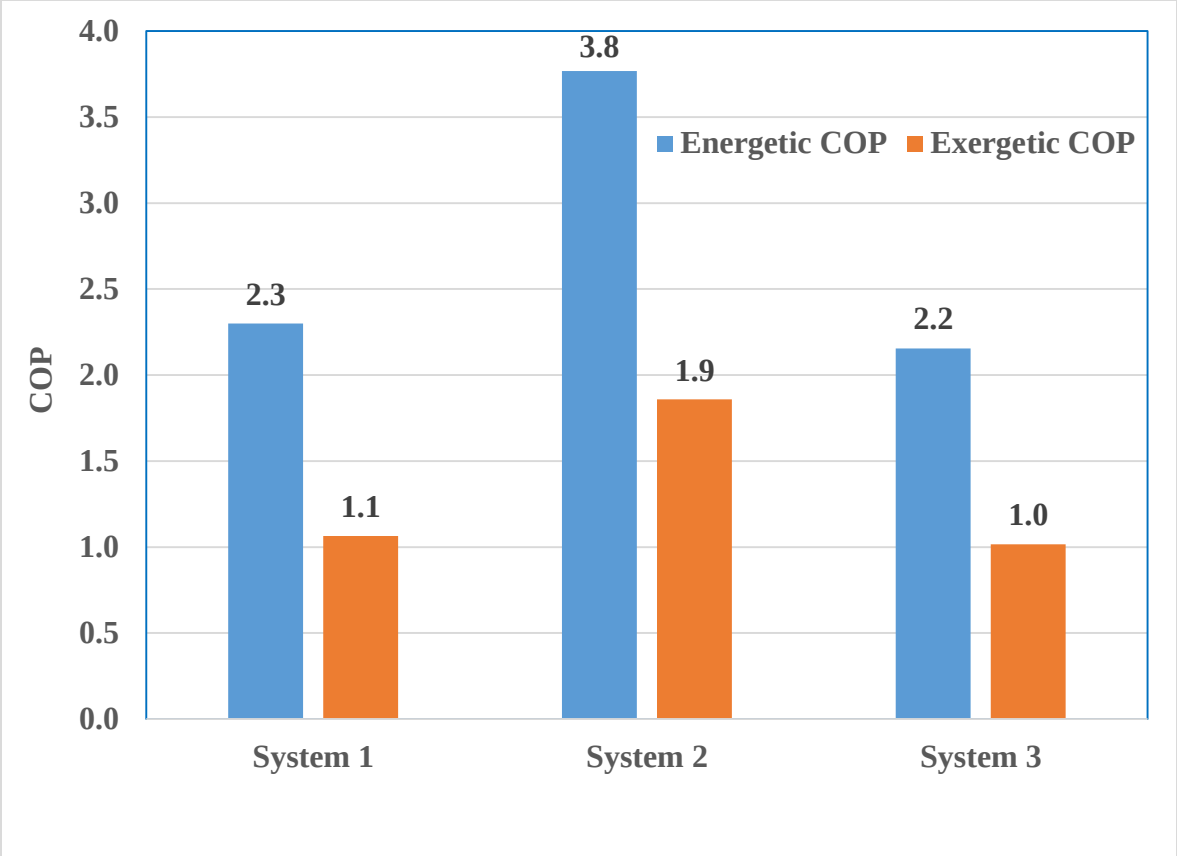

Figure 6.42 Energetic and exergetic COPs of systems 1, 2 and 3.

The comparison of energetic and exergetic COPs is shown in Figure 6.42. The Systems are compared for same source temperature of 81 °C and compressor efficiency values of 0.75. The maximum temperature achieved by System 1 and System 2 is 600°C and System 3 is 792°C. The energetic COP values of System 1, 2 and 3 are 2.3, 3.8 and 2.2 respectively. The exergetic values of COP values of System 1, 2 and 3 are 1.1, 1.9 and 1.0 respectively. The relative analysis shows that among System 1 and System 2 the performance of System 2 is better for same operating conditions. The COP of system 3 is lesser as compared to System 1 and 2 because the temperature lift achieved is much higher than these systems.

Chapter 7: Conclusions and Recommendations

This study presents three high temperature vapor compression heat pumps, with cascaded cycles. The heat is upgraded from 80 °C to 600 °C. The system performance is studied in terms of energetic and exergetic COPs. The parametric studies also conducted to analyse the effect of various operating parameters e.g. ambient temperature, sink and source temperatures, isentropic efficiencies. The working fluids, operating in these cycles are water, cyclohexane, biphenyl and mercury, selected from literature. The thermodynamic modeling is done based on accurate equations of state chosen from the literature, and simulations are performed using the ASPEN PLUS software. System 1 and System 2 operate with two cycles and their topping cycle works in supercritical condition. System 3 operates three cycles, while operating in sub critical conditions.

7.1 Conclusions

The following conclusions can also be drawn from this study:

- The energetic and exergetic COP values obtained are in the range of 2.08 to 4.86 and 1.01 to 2.36, depending upon the cycle and temperature levels.
- The System 2 (energetic and exergetic COPs are 3.8 and 1.9 respectively) outperforms System 1 (energetic and exergetic COPs are 2.2 and 1.0 respectively) both energetically and exergetically, while operating under same conditions of source temperature 81°C and sink temperature 600 °C. The System 3 achieves maximum cycle temperature of 792 °C while operating under moderate pressure ratios.
- The overall energetic performance of System 2 and 3 improves with increase source temperature, whereas System 1 exhibits a slight decline with increase in source temperature.
- The overall exergetic performance of System 1 and 2 improves with increase source temperature, whereas System 3 exhibits a slight decline with increase in source temperature.
- Compressor 1 and compressor 2 of System 1 exhibit the highest exergy destruction rates of 75.7 kW and 72.9 kW respectively.
- The System 3 uses three cascaded cycles, operates with cyclohexane, biphenyl and mercury in bottoming, intermediate and topping cycle. The use of mercury allows

System 3 achieves the highest sink temperature of 792 °C while operating at relatively lower pressures of 15 bar in topping cycle.

- The rate of exergetic destruction of components is adversely affected by increase in ambient temperatures.
- The isentropic efficiencies substantially improves the system performance, this effect is larger for system operating with more compressors. For System 3 the effect is highest, the energetic COP and exergetic COP increases from 2.04 to 2.28 and 0.96 to 1.07 for a range of 0.6-1.
- The higher sink temperatures require more work need to convert into heat, which reduce the coefficient of performance of the systems.
- The analysis of the effect of ambient temperature on COPs identifies the limitation energetic COP analysis, as it shows no effect on performance, while exergetic COP decreases with increase in temperature. This is because exergetic COP analysis accounts both First law and Second Law of thermodynamics and reflects the quality of heat delivered. For System 3 It is observed that the energetic COP does not change with ambient temperature, however the exergetic COP is reduced by 11.1 % over a range of 15-45 °C.
- The high-temperature heat pump systems, proposed in the thesis that upgrade low quality heat recovered in industry or utilities, provides a promising alternative to fossil fuels and hence leads to sustainability.

7.2 Recommendations

The high temperature mechanical heat pumps for heat upgrade applications are investigated in study forms the basis for further investigation and build more comprehensive and robust systems. The study has been conducted from thermodynamic analysis point of view and presents the performance in terms of coefficients of performance. The following recommendations can be made based on the outcomes of this study:

- The heat pump systems using retrograde organic fluids (cyclohexane and biphenyl) performed better because the compression work required is relatively lesser. More such retrograde fluids suitable for high temperature applications should be researched.

- Including the costs of individual components should enhance the performance analysis, an exergoeconomic analysis will provide more comprehensive results and better understanding of systems.
- To determine the optimum operating conditions a single or multi objective optimization should be performed.
- The integration of these systems with nuclear reactors for thermochemical splitting of water should be studied and optimised.
- The analysis of lab scale experimental unit should be used to validate the results obtained from simulations.
- The System 1 and 2 operates on moderate temperature and pressure limits. The working fluids and engineering equipments are commonly available. The lab scale model results and a mature heat pump technology should pave the development of industrial scale systems.
- Further research should extend the identification of working fluids, system development based on their thermophysical properties and thermodynamic analysis of these systems.

References

Abanades, S., P. Charvin, G. Flamant and P. Neveu (2006). "Screening of water-splitting thermochemical cycles potentially attractive for hydrogen production by concentrated solar energy." Energy 31(14): 2805-2822.

Angelino, G. and C. Invernizzi (1993). "Cyclic methylsiloxanes as working fluids for space power cycles." Journal of Solar Energy Engineering 115(3): 130-137.

Angelino, G. and C. Invernizzi (1996). "Potential performance of real gas Stirling cycle heat pumps." International Journal of Refrigeration 19(6): 390-399.

Austin, B. T. and K. Sumathy (2011). "Transcritical carbon dioxide heat pump systems: A review." Renewable and Sustainable Energy Reviews 15(8): 4013-4029.

Basco, J., M. Lewis and M. Serban (2004). "Hydrogen production at <550°c using a low temperature thermochemical cycle." Nuclear Production of Hydrogen: 145–156.

Bejan, A. (2002). "Fundamentals of exergy analysis, entropy generation minimization, and the generation of flow architecture." International Journal of Energy Research 26(7): 0-43.

Bejan, A., G. Tsatsaronis and M. Moran (1996). Thermal design and optimization. John Wiley & Sons, Inc.

Biberacher, M. and S. Gadocha (2012). Global energy scenarios, analysis of thematic emphasis, main drivers and communication strategies, Europian Fusion Development Agreement

BP SRWE (2015). BP statistical review of world energy (BP SRWE) June 2015, 64th edition. London, Centre for Energy Economics Research and Policy.

Brown, J. S., R. Brignoli and T. Quine (2015). "Parametric investigation of working fluids for organic Rankine cycle applications." Applied Thermal Engineering 90: 64-74.

Bruckner, S., S. Liu, L. Miro, M. Radspieler, L. F.Cabeza and E. Lavemann (2015). "Industrial waste heat recovery technologies: An economic analysis of heat transformation technologies." Applied Energy 151: 157-167.

Calderazzi, L. and P. C. di Paliano (1997). "Thermal stability of R-134a, R-141b, R-1311, R-7146, R-125 associated with stainless steel as a containing material." International Journal of Refrigeration 20(6): 381-389.

Chan, C. W., J. Ling-Chin and A. P. Roskilly (2013). "Reprint of "A review of chemical heat pumps, thermodynamic cycles and thermal energy storage technologies for low grade heat utilisation"." Applied Thermal Engineering 53(2): 160-176.

Chen, H., D. Y. Goswami, M. M. Rahman and E. K. Stefanakos (2011). "A supercritical Rankine cycle using zeotropic mixture working fluids for the conversion of low-grade heat into power." Energy 36(1): 549-555.

Chen, H., D. Y. Goswami and E. K. Stefanakos (2010). "A review of thermodynamic cycles and working fluids for the conversion of low-grade heat." Renewable and Sustainable Energy Reviews 14(9): 3059-3067.

Cho, H. (2015). "Comparative study on the performance and exergy efficiency of a solar hybrid heat pump using R22 and R744." Energy 93: 1267-1276.

Chua, K. J., S. K. Chou and W. M. Yang (2010). "Advances in heat pump systems: A review." Applied Energy 87(12): 3611-3624.

Chukwu, C. (2008). Process analysis and Aspen plus simulation of nuclear-based hydrogen production with copper-chlorine cycle. MASc Thesis, University of Ontario Institute of Technology.

Colonna, P., N. R. Nannan and A. Guardone (2008). "Multiparameter equations of state for siloxanes: $[(CH_3)_3\text{-}Si\text{-}O_{1/2}]_2\text{-}[O\text{-}Si\text{-}(CH_3)_2]i=1,\ldots,3$, and $[O\text{-}Si\text{-}(CH_3)_2]_6$." Fluid Phase Equilibria 263(2): 115-130.

Colonna, P., N. R. Nannan, A. Guardone and E. W. Lemmon (2006). "Multiparameter equations of state for selected siloxanes." Fluid Phase Equilibria 244(2): 193-211.

De Boer, R., W. G. Haije and J. B. J. Veldhuis (2002). "Determination of structural, thermodynamic and phase properties in the $Na_2S–H_2O$ system for application in a chemical heat pump." Thermochimica Acta 395(1–2): 3-19.

Dincer, I. (2012). "Green methods for hydrogen production." International Journal of Hydrogen Energy 37(2): 1954-1971.

Dincer, I. and M. A. Rosen (2012). Exergy: energy, environment and sustainable development. Newnes.

Fernández, F. J., M. M. Prieto and I. Suárez (2011). "Thermodynamic analysis of high-temperature regenerative organic Rankine cycles using siloxanes as working fluids." Energy 36(8): 5239-5249.

Ferreira, C. A. I., C. Zamfirescu and D. Zaytsev (2006). "Twin screw oil-free wet compressor for compression–absorption cycle." International Journal of Refrigeration 29(4): 556-565.

Forman, C., I. K. Muritala, R. Pardermann and B. Meyer (2016). "Estimating the global waste heat potential." Renewable and Sustainable Energy Reviews 57: 1568–1579.

Garrido, J. M., H. Quinteros-Lama, A. Mejía, J. Wisniak and H. Segura (2012). "A rigorous approach for predicting the slope and curvature of the temperature–entropy saturation boundary of pure fluids." Energy 45(1): 888-899.

Göktun, S. N. (1995). "Selection of working fluids for high-temperature heat pumps." Energy 20(7): 623-625.

Grimes, C. A., O. K. Varghese and S. Ranjan (2008). Light, water, hydrogen: the solar generation of hydrogen by water photoelectrolysis. New York, Springer.

IEA (2015). "World Energy Outlook 2015, Factsheet global energy trends to 2040." France, International Energy Agency.

Itard, L. C. M. (1995). "Wet compression versus dry compression in heat pumps working with pure refrigerants or non-azeotropic mixtures." International Journal of Refrigeration 18(7): 495-504.

Kato, Y. and Y. Yoshizawa (2001). "Application of a chemical heat pump to a cogeneration system." International Journal of Energy Research 25(2): 129-140.

Kim, M.-H., J. Pettersen and C. W. Bullard (2004). "Fundamental process and system design issues in CO_2 vapor compression systems." Progress in Energy and Combustion Science 30(2): 119-174.

Kim, T. G., Y. K. Yeo and H. K. Song (1992). "Chemical heat pump based on dehydrogenation and hydrogenation of i-propanol and acetone." International Journal of Energy Research 16(9): 897-916.

Kosmadakis, G., D. Manolakos, S. Kyritsis and G. Papadakis (2009). "Comparative thermodynamic study of refrigerants to select the best for use in the high-temperature stage of a two-stage organic Rankine cycle for RO desalination." Desalination 243(1–3): 74-94.

Lai, N. A., M. Wendland and J. Fischer (2011). "Working fluids for high-temperature organic Rankine cycles." Energy 36(1): 199-211.

Li, D. X., S.S. Zhang and G.H. Wang (2015). "Selection of organic Rankine cycle working fluids in the low-temperature waste heat utilization." Journal of Hydrodynamics 27(3): 458-464.

Liao, S. M., T. S. Zhao and A. Jakobsen (2000). "A correlation of optimal heat rejection pressures in transcritical carbon dioxide cycles." Applied Thermal Engineering 20(9): 831-841.

Lide, D. R. (2006). CRC handbook of chemistry and physics. Florida, CRC, Boca Raton.

Luickx, P. J., L. M. Helsen and W. D. D'haeseleer (2008). "Influence of massive heat-pump introduction on the electricity-generation mix and the GHG effect: Comparison between Belgium, France, Germany and The Netherlands." Renewable and Sustainable Energy Reviews 12(8): 2140-2158.

Ma, Y., Z. Liu and H. Tian (2013). "A review of transcritical carbon dioxide heat pump and refrigeration cycles." Energy 55: 156-172.

Marchetti, C. (2006). "Long-term global vision of nuclear-produced hydrogen." International Journal of Nuclear Hydrogen Production and Applications 1(1): 13-19.

Olivier, J. G. J., G. Janssens-Maenhout, M. Muntean and J. A. H. W. Peters (2015). Trends in global CO_2 emissions: 2015 Report. Netherlands, PBL Netherlands Environmental Assessment Agency.

Orhan, M. F., I. Dincer and M. A. Rosen (2008). "Energy and exergy assessments of the hydrogen production step of a copper–chlorine thermochemical water splitting cycle driven by nuclear-based heat." International Journal of Hydrogen Energy 33(22): 6456-6466.

Orhan, M. F., I. Dincer and M. A. Rosen (2008). "Thermodynamic analysis of the copper production step in a copper–chlorine cycle for hydrogen production." Thermochimica Acta 480(1–2): 22-29.

Orhan, M. F. (2011). Analysis, design and optimization of nuclear-based hydrogen production with copper-chlorine thermochemical cycles. PhD Thesis, University of Ontario Institute of Technology.

Pan, G. and Z. Li (2006). "Investigation on incomplete condensation of non-azeotropic working fluids in high temperature heat pumps." Energy Conversion and Management 47(13-14): 1884-1893.

Peng, D.Y. and D. B. Robinson (1976). "A New Two-Constant Equation of State." Industrial & Engineering Chemistry Fundamentals 15(1): 59-64.

Quoilin, S. and V. Lemort (2009). Technological and economical survey of organic Rankine cycle systems. 5th Europian Conference, Economics and Management of Energy in Industry. Portugal.

Robinson, D. M. and E. A. Groll (1998). "Efficiencies of transcritical CO_2 cycles with and without an expansion turbine. International Journal of Refrigeration 21(7): 577-589.

Rosen, M. A. (2008). Towards energy sustainability: a quest of global proportions. Forum on Public Policy.

Rowley, R. L., W. V. Wilding, J. L. Oscarson, Y. Yang, N. A. Zundel, T. E. Daubert and R. P. Danner (2004). DIPPR data compilation of pure chemical properties. New York, Taylor & Francis.

Sarkar, J., S. Bhattacharyya and M. R. Gopal (2005). "Transcritical CO_2 heat pump systems: exergy analysis including heat transfer and fluid flow effects." Energy Conversion and Management 46(13-14): 2053-2067.

Schuster, A., S. Karellas and R. Aumann (2010). "Efficiency optimization potential in supercritical organic Rankine cycles." Energy 35(2): 1033-1039.

Shu, G., X. Li, H. Tian, X. Liang, H. Wei and X. Wang (2014). "Alkanes as working fluids for high-temperature exhaust heat recovery of diesel engine using organic Rankine cycle." Applied Energy 119: 204-217.

Sugawara, S., T. Sato and T. Minamiyama (1962). "On the Equation of State of Mercury Vapor." Bulletin of JSME 5(20): 711-718.

Van der Stelt, T. P., N. R. Nannan and P. Colonna (2012). "The iPRSV equation of state." Fluid Phase Equilibria 330: 24-35.

Wall, G. (1986). "Thermoeconomic optimization of a heat pump system." Energy 11(10): 957-967.

Wagner, W. and A. Pruß (2002). "The IAPWS Formulation 1995 for the Thermodynamic Properties of Ordinary Water Substance for General and Scientific Use." Journal of Physical and Chemical Reference Data 31(2): 387-535.

Wang, E. H., H. G. Zhang, B. Y. Fan, M. G. Ouyang, Y. Zhao and Q. H. Mu (2011). "Study of working fluid selection of organic Rankine cycle (ORC) for engine waste heat recovery." Energy 36(5): 3406-3418.

WEC (2015). World energy issues monitor, energy price volatility: the new normal, United Kingdom, World Energy Council.

Yildiz, B. and M. S. Kazimi (2006). "Efficiency of hydrogen production systems using alternative nuclear energy technologies." International Journal of Hydrogen Energy 31(1): 77-92.

Zamfirescu, C. and I. Dincer (2009). "Performance investigation of high-temperature heat pumps with various BZT working fluids." Thermochimica Acta 488(1–2): 66-77.

Zamfirescu, C., I. Dincer and G. Naterer (2009). "Performance evaluation of organic and titanium based working fluids for high-temperature heat pumps." Thermochimica Acta 496(1–2): 18-25.

Zamfirescu, C., G. F. Naterer and I. Dincer (2010). "Upgrading of waste heat for combined power and hydrogen production with nuclear reactors." Journal of Engineering for Gas Turbines and Power 132(10): 102911-102911.